R. & M. No. 2976
(16,464)
A.R.C. Technical Report

MINISTRY OF SUPPLY

AERONAUTICAL RESEARCH COUNCIL
REPORTS AND MEMORANDA

Model Testing Technique Employed in the R.A.E. Seaplane Tank

By

T. B. Owen, M.A., A. G. Kurn and A. G. Smith, B.Sc., D.I.C.

LONDON: HER MAJESTY'S STATIONERY OFFICE
1955
PRICE SIXTEEN SHILLINGS NET

Model Testing Technique Employed in the R.A.E. Seaplane Tank

By

T. B. OWEN, M.A., A. G. KURN and A. G. SMITH, B.Sc., D.I.C.

COMMUNICATED BY THE PRINCIPAL DIRECTOR OF SCIENTIFIC RESEARCH (AIR), MINISTRY OF SUPPLY

Reports and Memoranda No. 2976*

September, 1953

Summary.—A description is given of the various techniques evolved in recent years to provide model data as a basis for predicting the full-scale behaviour of a seaplane.

The seaplane tank and associated equipment is described in detail, together with the routine methods of operation. The factors affecting the choice of model scale are discussed and the methods of model construction described. A description is given of a typical test programme on a new design to determine the longitudinal and lateral stability on the water, spray and rough water behaviour and water drag. This description is illustrated with typical results for a modern conventional hull of length : beam ratio of about 7. Finally, the design factors affecting the longitudinal stability and spray formation are discussed in Appendices.

1. *Introduction.*—Considerable progress has been made in the last decade in improving the techniques of predicting the full-scale performance of seaplanes by the use of scale models in the Royal Aircraft Establishment Seaplane Tank. The basic flow conditions on the hull bottoms have also been investigated.

While some of the new apparatus and techniques have been briefly referred to in reports issued during this period, a considerable amount was still unreported. This report collects together in some detail, the various methods and apparatus now available for the model testing of seaplane designs and describes the various tests made during a typical investigation to determine the spray, stability and water resistance of a seaplane during take-off and landing.

The tests made are of two general types,

(*a*) stability and spray tests which are made on a powered dynamic model free to pitch and heave and, for directional stability tests, also to roll and yaw,

(*b*) force measurements made on solid models to determine the water resistance of the hull and the rise and resistance characteristics of the wing-tip floats.

These two types of tests are discussed in section 4 and Appendices I and II, following a general description of the apparatus in section 2 and model making in section 3.

* R.A.E. Report Aero. 2505, received 11th January, 1954.

2. *Description of Apparatus.*—2.1. *General.*—The Royal Aircraft Establishment Seaplane Tank is 635 ft long, 9 ft wide and 4 ft 6 in. deep, with docks 11 ft long and 3 ft wide at eithe rend. A section showing the construction is given in Fig. 1. The length of track is 658 ft from buffer to buffer and the carriage brakes are automatically applied 252 ft from the east end buffers (running direction being towards the east end). Allowing for clearance at the west end, there is about 360 ft left for acceleration and the steady speed part of the run. Acceleration is automatic on pressing a button and pre-set steady speeds from 4 ft/sec to 40 ft/sec are obtainable. With the normal acceleration the lengths of steady run vary from about 345 ft at 4 ft/sec to 200 ft at 40 ft/sec, with corresponding times of 86 sec and 5 sec respectively. The acceleration can, however, be decreased from its normal value of about $0 \cdot 16g$ to a mean value of about $0 \cdot 12g$* when a speed of 40 ft/sec is reached after a run of about 240 ft.

A curved profile beach is installed at either end of the tank in front of the docks and has a centre-section which can be lowered to allow models to pass in and out of the dock. There is also a series of beaches down the south side of the tank, extending for about 350 ft to correspond to the acceleration and steady-speed part of run. These beaches consist of 17 flat plates 10 ft long by 1 ft wide, half submerged in the water at an angle of 7 deg which, with the end beaches, damp out the disturbances set up by the model. The interval between runs to allow the water to settle should be about 10 minutes, though it can be reduced to 7 or 8 minutes for stability tests, if required. An improvement in the steadiness of balance readings may be obtained by increasing the interval to 12 or 15 minutes, especially with large or heavily loaded models.

The velocity of propagation of long waves in the tank is 12 ft/sec. The running of the carriage, especially with large models or with the air-screen (section 2.3) tends to pile up the water at one end during the run, and start an oscillation of the water known as a ' surge ' or ' seiche '[1]. The period of the oscillation is equal to the time for a long wave to travel from one end of the tank to the other and back again, *i.e.*, 106 sec. For this reason, it is advisable to keep fairly accurately at a time interval which does not reinforce the oscillation, *e.g.*, 10 minutes $= 5 \cdot 7$ periods and 15 minutes $= 8 \cdot 5$ periods are suitable and convenient intervals. As might be expected, running at 12 ft/sec is especially liable to cause a surge. If there are several runs to be made at this speed, it is advisable to make these the last runs of the day. The surge affects only draft readings to any appreciable extent and the above precautions may be neglected for dynamic model tests. If, however, a surge of more than about $\pm 0 \cdot 1$ in. amplitude is allowed to build up, it will not have died out by next morning. This makes it impossible to set accurately a draft datum for resistance model tests.

Wave Maker.—A wavemaker is installed in the Seaplane Tank, which can produce steady wave trains up to about 6 in. in height. Waves shorter than about 20 : 1 length/height ratio† tend to be unstable and break up as they travel along the tank, but waves of a greater length/height ratio than 30 : 1 can be produced satisfactorily and will travel for the length of the tank with little deterioration. The wavemaker consists of a simple paddle hinged $26 \cdot 6$ in. below the water surface and is oscillated about a mean vertical position by a crank and connecting rod. Figs. 2 and 3 give the wavemaker calibration in terms of the semi-stroke and period of the crank for most combinations of wavelength and height required in practice. Further details of the wavemaker and formulae for extending the calibration to other wavelengths and heights are given in Ref. 1.

It is essential that, when the wavemaker is in operation, the centre portions of the end beaches should be raised, to avoid reflections and to prevent water splashing over the ends of the docks. Also, the side beaches must be hinged up clear of the water surface to avoid interference with the waves.

---

* This corresponds roughly to the mean acceleration of a flying boat during take-off at normal all-up weight and is sometimes used for simulated take-off runs (section 4·23).

† By convention the length of a wave is taken as the distance from crest to crest, or trough to trough, and height is from trough to crest.

Air and Water Conditioning.—The air in the tank building is thermostatically controlled to about 59 deg F in cold weather but may rise to 70 deg F or 75 deg F during the day in hot weather. The water temperature is, however, unlikely to vary more than between 59 deg F and 62 deg F and for the majority of calculations the properties of fresh water at 60 deg F may be assumed. Fresh water is used for convenience of supply (the tank holds 157,000 gallons) and also to reduce corrosion difficulties. The only significant difference between the properties of salt and fresh water is in the densities, which differ by about 3 per cent, and this can easily be allowed for. All sunlight is excluded from the building and no precautions in the way of chemicals or livestock are required to prevent weeds or any other forms of life appearing in the water. The water surface is, however, skimmed weekly to remove the inevitable surface layer of dust and oil which accumulates.

Carriages.—There are two similar carriages of light alloy construction with a total weight of about 4 tons each. Each carriage is driven by four 35 h.p. electric motors and current is picked up from a set of conductor wires on the north wall (Fig. 1). Electrical interlocking permits only one carriage to run at one time and then only if the other is right up to the buffers at the appropriate end. Running is from west to east for either carriage. The carriage speed is set prior to a run by adjusting a pair of variable rheostats calibrated directly in ft/sec. The actual carriage speed obtained will normally be within 1 or 2 per cent of the nominal value and each carriage has an indicator which can be read to 0·1 ft/sec, and for which the calibration is checked at intervals. For calibrating these indicators and also for the accurate measurement of low speeds, when required, each carriage carries a recording drum geared to the carriage wheels, on which a pair of traces can be recorded. One trace records 10-ft intervals picked up by a cam from a series of rollers at this interval along the track, and the other 1- or $\frac{1}{2}$-sec intervals from a chronometer on the carriage. Measurement of these traces will give the speed to within 0·5 per cent.

Carriage No. 1 is equipped for testing dynamic models and Carriage No. 2 for force and moment measurements. The apparatus on each is described separately below.

2.2. *No. 1 Carriage Equipment.*—The cross-section of the carriage is appreciable compared with the building cross-section (Fig. 1) and there is a backward flow of air in the vicinity of the carriage as it travels down the tank, the relative velocity of the air under the carriage being about 1·4 times the carriage speed. This is not satisfactory for dynamic model testing. It was found, however, that the air forward of about 5 ft ahead of the carriage was practically unaffected by the carriage. Accordingly, the model is mounted with its c.g. about 8 ft ahead of the carriage. The rig for normal longitudinal stability and spray tests is shown in Fig. 4.

The towing arms are two light $1\frac{1}{4}$-in. outside diameter Dural tubes mounted on a wooden cross-beam in such a way that the lateral spacing can be adjusted to accommodate models of from 3 ft to 7 ft span. The beam is attached to a linkage (Fig. 5) which constrains the forward ends of the arms to move approximately vertically, the longitudinal variation being about 0·1 in. for 1-ft vertical movement compared with about 0·8 in. for a simple pivot.

On powered dynamic models a supply of compressed air is required either to drive the aircraft propellers by means of compressed-air turbines[2] or, on jet aircraft[3], to provide jet thrust directly. An electric motor on the carriage drives a compressor which will supply up to 90 cubic ft of free air per minute at pressures up to 20 lb/sq in. The blower output is connected to the rear ends of the arms through flexible rubber pipes. At the forward ends of the arms it is necessary to turn the airflow through 90 deg, at the same time allowing the model to move freely about the pivot point. A labyrinth packed hollow trunnion was developed for this purpose[2], and can be seen in Fig. 4. The trunnion on the starboard wing tip also carries a small pulley connecting to an indicator, just forward of the carriage, from which the aircraft attitude can be read. All pivots in the system are on ball-races and the arms themselves are counterbalanced, so the model is quite free to pivot in attitude and rise and fall in heave, while being constrained in yaw, roll and lateral movement. The arms, etc., though not contributing any vertical static load to the model, do effectively increase the inertia in the vertical plane by about 1·2 lb.

A light braced beam projects forward from the carriage about 5 ft above the water (Fig. 4) and carries two pulleys near its forward end. Two cords from the model, spaced about 11 in. forward and aft of the pivot, run up over the pulleys and back to a pair of handles. The operator on the carriage holding a handle in each hand normally allows the cords to be slack so as not to affect the model, but is able to raise the model out of the water or restrain it if a dangerous oscillation occurs. Except during the actual test run, the model is held clear of the water.

For calibration of the model propeller or jet thrust, the links CD in Fig. 5 are removed, leaving the model, arms and cross-beam free to move fore and aft. The beam is then connected by a pair of light struts to a balance under the carriage. An air-screen must be mounted on the carriage to shield the cross-beam from the slipstream for these tests. The balance can alternatively be used to measure the model lift by replacing the two control cords by fine wires which are led back over pulleys from the model to the balance.

Another rig, designed for directional stability tests, is shown in Fig. 6. A light tubular frame, free to rise and fall vertically, is connected to the model through a universal joint. The frame is counter-balanced and the air supply is led in horizontally through a flexible rubber pipe near the top on the port side (Fig. 6) so that no load is applied to the model. The inertia in the vertical direction is, however, increased by about 14 lb and, since the model weight is normally only 10 to 15 lb, the dynamic behaviour will be considerably affected. Only steady conditions can therefore be tested.

The universal joint is shown in Fig. 7. The platform near the bottom is bolted to the model and connection made to the tubular frame by a single nut at the top. There is a single ball-race in the platform permitting 360 deg rotation in yaw. Two sets of ball-races coupled by a ring provide $\pm$ 10 deg rotation in roll and pitch. The three axes of rotation meet at a point and there are two portions of concentric spheres about this point. The lower and outer partial sphere is attached to the platform, the upper and inner one to the short pipe connecting to the tubular frame. This pair of partial spheres operates with about 0·002 in. clearance so that, while there is no sliding friction, the air leakage is small—less than 2 per cent of the total flow. The outlet pipe below the platform splits into two, at the same time passing through an adjustable valve which regulates the proportion of the air passing into each exit. This valve permits accurate equalisation of the thrust from the port and starboard units so that there is no resultant torque in yaw due to the jet or propeller thrust. The installation of the unit in the model is discussed later in section 3·2, under model construction.

Cameras and floodlamps are available for photography. Sufficient power is available on the carriage to provide up to 3,000 W for the floodlamps and the blower motor, enabling ciné photographs of model behaviour in waves to be made at speeds up to 100 frames per second. A high-speed electronic flash unit is also available as required.

2.3. *No. 2 Carriage Equipment.*—The air velocity under the carriage as originally used was found to be about 40 per cent greater than the carriage speed[4] and a simple system of flaps was developed to reduce the ratio to 1·0. This was fairly successful but, though the mean velocity was correct, there was a considerable velocity gradient which produced a forward thrust on the model. There was another disadvantage in that the flap setting required varied with carriage speed. Following the decision to contruct an improved drag balance, a complete ' wind tunnel ' was fitted to the carriage to overcome these difficulties. This wind tunnel is shown in Fig. 8. It consists of three sides of a rectangular duct 80 in. wide by 30 in. high, with the walls finishing 1 in. clear of the water surface. The duct extends about 4 ft 6 in. ahead of the carriage to ensure smooth entry flow and a series of three louvres is fitted at the rear to control the flow. It was found that, with the louvres set to cut off 29·5 per cent of the exit area, an air velocity in the vicinity of the model was obtained which was within 1 per cent of the carriage speed over the normal speed range. The louvres have been locked in this position. Fig. 9 shows the velocity distribution at 30 ft/sec and it is apparent that there is a slight outward leakage of air under the sides of the duct, but this does not become important till well behind the model position.

The front of the duct roof is hinged as shown in Fig. 8, so that the leading edge can be lowered to within 1 in. of the water surface. In the lowered position a ' pocket ' of air is carried along with the carriage so that the model is effectively in still air and the only forces are due to the water.

A photograph of the balance, designed largely by the late Mr. W. D. Tye of Tank Staff, is shown in Fig. 10, and the operation is shown diagrammatically in Fig. 11. A light alloy casting is bolted down on to a ring frame on the carriage and a second casting is suspended from the first on a pair of links. The rear link is of very rigid construction and, besides carrying some of the weight of the lower casting, also prevents any lateral movement or twist. The front link is quite light and only serves to carry part of the vertical load. The links and castings are connected by light spring steel strips which act as frictionless pivots, and on these the bottom casting can swing fore and aft 0·018 in. between stops. A pair of coil springs locate the position of the bottom casting and their strength is such that the full deflection requires about 1·8 lb drag load. An inductance pick-up is used to convert the balance movement into deflection of an a.c. ammeter which can be calibrated directly in pounds of drag force. A weight changer unit is incorporated at the rear of the balance and enables the drag range to be extended in 1-lb steps up to 15 lb, plus the 1·8 lb spring deflection.

Two screwed rods 16 in. long project up from the rear link and each carries a pair of 18·7-lb weights which can be locked at any vertical height. These weights are adjusted to counterbalance the inertia of the model and lower half of the balance so that the carriage acceleration and deceleration do not produce violent movements of the drag balance. A variable oil-dashpot is fitted to steady the drag readings.

The connection to the model is by a 2-in. steel tube which can move vertically in two sets of rollers in the lower casting but is prevented from rotating by a short arm with a pair of guide rollers. The tube is faired where it projects into the airflow and a fixed fairing in which the faired tube moves with 0·05 in. clearance extends 8·25 in. down from the duct roof. This can be seen in Fig. 12, which shows a model in position on the balance.

The model is free to rotate in pitch about a pivot at the bottom of the strut and is restrained by a pair of wires which run up vertically from 15-in. radius arms on the model. The wires are coupled to light chains (Fig. 11) which run over a pair of pulleys, A and D, on a shaft, B. The shaft, B, is free to rotate in ball-races in an arm which is pivoted in pitch on frictionless spring steel pivots. The wheel, A, is locked to the shaft, B, which also carries a pointer, C. The wheel, D, can be locked to the shaft by a friction clutch and the model attitude can be adjusted by loosening the clutch and moving the pulleys differentially. A scale is marked on wheel D, calibrated in degrees so that, once the scale datum has been set to correspond to the model datum, the model attitude can be read off or set directly.

With the wheel D locked to the shaft, the pitching moment is transmitted directly from the model to the top pivoted arm. The arm is constrained by springs, the total deflection covering a range from −4 lb ft to +4 lb ft pitching moment. An inductance pick-up and a.c. meter similar to that used on the drag balance is fitted and can be calibrated directly against pitching moment. A 6-lb rider sliding on the top of the beam is used to extend the range of measurement. A variable damping dashpot is also fitted.

On top of the centre tube of the balance a plate $16\frac{1}{2}$ in. × $3\frac{1}{2}$ in. is fitted, on which standard slotted weights can be placed. A pair of light chains spaced $16\frac{3}{8}$ in. apart at the ends of the plate are led up and over a pair of pulleys, Z and Z′, to another similar plate, Y, which is freely suspended. There is a scale on the pulley, Z, calibrated in inches movement of the chain. This scale moves past a fixed pointer, V, so that, once the scale datum is adjusted to correspond to the model draft datum, the model draft can be read off directly from the scale. The vertical travel of the tube is 10·7 in. and three struts are available giving ranges of movement of the pivot at the bottom of the strut above the water of 0·3 to 11 in., 6·3 to 17 in. and 12·3 to 23 in. The weight of the model with the tube and fairing, etc. (usually about 60 lb) is counterbalanced,

partly by weights on the scale-pans suspended from the chains over the pulleys, A and C (usually 15 lb on each) and the remainder by weights on the plate, Y. The model can thus be accurately balanced and the load on water to be carried, applied as weights on the plate, X.

The lower half of the balance can be rotated through 90 deg about the axis of the centre tube and can then be used to measure side-force instead of drag.

A large dial tachometer is coupled to the carriage wheels and calibrated directly in ft/sec. The tachometer calibration is checked at intervals and the instrument appears to be consistent to within the accuracy of reading, 0·1 ft/sec. A speed recorder drum similar to that on No. 1 Carriage is also fitted.

An air-bottle, of 4·2 cubic ft capacity on the carriage, can be charged from a stationary compressor at the west end of the tank building. The outlet is taken through a reducing valve and compressed air is then available on the carriage at any pressure below 150 lb/sq in.

3. *Model Design.*—3.1. *Dynamic Model for Longitudinal Stability Tests.—Dynamic Similarity.*—The model tests must satisfy the following standard conditions of dynamic model testing, *i.e.*, that:

(*a*) the ratio of the model density to that of its surrounding fluid be the same as full scale

(*b*) the corresponding speed on the model be directly proportional to the square root of the scale*

(*c*) the centre of gravity be the same as full scale

(*d*) the pitching radius of gyration be directly proportional to the scale.

Since there are two fluids present in seaplane testing, water and air, and since in the Royal Aircraft Establishment Seaplane Tank the ratio of the water density to that of the air cannot be altered, condition (*a*) is satisfied only for identical densities, model and full-scale. The model weight is therefore reduced proportionally to the cube of the scale chosen and the tests strictly represent fresh water operation at approximately sea level.

Model Size.—Condition (*b*) normally determines the model scale as the design model take-off speed at the anticipated overload condition should be about 36 ft/sec. This leaves a little in reserve for the inevitable further increase in weight during the development of a new design. The model span can then be calculated and, provided it does not exceed 88 in., the scale is satisfactory, as the model can be accommodated in the tank. If the span comes to between 88 in. and 96 in., it is better to crop the tips to 88 in. and regain the area by increasing the tip chord than to reduce the hull size. If, however, the estimated span is greater than 96 in., it is better to reduce the scale, to bring the span to below 96 in., and then crop the tips as above. In some cases the model size required to cover the whole speed range up to take-off may be too small for convenience and a larger model is also made. The larger model is then used for examining the low-speed behaviour and the smaller one used to fill in the high-speed characteristics. The larger model will in practice cover the majority of the speed range, *e.g.*, even if the larger model is twice the scale and eight times the weight of the smaller model, the larger model will cover 0·7 of the speed range of the smaller one.

Model Weight and Inertia.—The models are usually designed to be about 20 per cent lighter than the minimum weight to be tested, so that the remainder of the weight, usually in the form of small pieces of lead and Plasticine, can be distributed inside the model to bring the centre of gravity to the correct position (condition (*c*)) and at the same time bring the radius of gyration nearer to its scale value (condition (*d*)). The models tend to be tail-heavy in spite of omitting the fin and rudder and hollowing out the tailplane, and the majority of the ballast is usually required to bring the centre of gravity forward. The radius of gyration can then be found by

* Froude's law for obtaining the correct waveforms and wave-drag is automatically satisfied by this rule.

swinging the model about a suitable point. If it is too small, the remainder of the ballast can be distributed fore and aft to increase the radius of gyration, taking care not to alter the c.g. position. If the radius of gyration is too large, it can be reduced only by lightening the model, preferably as far from the c.g. as possible. In practice the model radius of gyration still tends to be a little high when the model has been lightened as far as is consistent with sufficient strength. If the radius of gyration is not more than 5 per cent too high, it is usually considered to be acceptable*.

Slipstream Representation.—Propeller slipstream has a considerable effect on the stability and spray behaviour and it is important that it should be accurately represented on project designs. The motors used for driving the propellers must be very light and must be capable of accurate speed control. Electric motors are unsuitable at the Royal Aircraft Establishment Tank scale due to their low power/weight ratio and need of protection from wetting. Petrol or 'diesel' engines are not very reliable, apart from the fumes and fire danger. A series of compressed-air turbines has therefore been designed which has proved to be completely satisfactory in use. The design, construction, installation and performance of these turbines has been described very fully in Ref. 2. A survey of the main details of the turbines is given in Table 1.

The propellers are made to the scale diameter and are required to produce the same thrust coefficient as full-scale and at the same advance ratio, *i.e.*, the same scale slipstream velocity distribution. This means that the propeller speed is increased as the square root of the scale and the power required reduced as the scale to the power 3·5. This power requirement is only true if the propeller efficiencies are the same model and full-scale, and about 20 per cent should be added to allow for the loss in efficiency of the model fixed-pitch propeller if the full-scale propeller is of variable pitch. A suitable turbine and reduction ratio can then be selected using the calibrations of Ref. 2. Since the model propeller is of fixed pitch and is required to supply the scale thrust up to take-off speed without appreciable increase in r.p.m., a high blade angle (50 to 55 deg at 0·7 radius) is required, so that the blades are stalled throughout the speed range. Using the curves of Ref. 5, the solidity required to give the scale thrust can then be found. The propellers of the aircraft shown in Figs. 15 and 16 were designed on this principle and on calibration the measured speeds of 5,400 r.p.m. static and 5,300 r.p.m. at 36 ft/sec compared favourably with the design speed of 5,500 r.p.m.

Wing Lift Characteristics.—A present-day trend in flap design is to use single-slotted trailing-edge flaps of about 20 per cent chord with some rearward movement on deflection. The lift increments obtained with such flaps at low Reynolds numbers are quite unrepresentative and a split flap at the same angle and with the trailing edge in the same position gives a very similar full-scale lift increment while being less liable to scale effect[6]. Model flaps are accordingly made as triangular section strips attached to the wing lower surface as shown in Fig. 17. This method is satisfactory for normal flaps but, if the aircraft is fitted with a special high-lift flap system, this should be correctly represented.

At the low Reynolds number of the model tests, the wing commences to stall at a much lower angle than full-scale and leading-edge slats are normally fitted over the portions of the wing not covered by propeller slipstream. A simple design evolved by the staff of the Hamburg Testing Tank is shown in Fig. 17. The slat is beaten out of 24*g* light alloy sheet on a hardwood former to the shape of the wing leading edge, and positioned as shown.

3.1.1. *Model construction.*—For lightness the models are constructed almost entirely of balsa wood. Balsa is available in densities varying from about 4 lb/cubic ft to 10 lb/cubic ft. To ensure reaching the lower model weights, 5 to 6 lb/cubic ft wood is normally used. Cedar, which weighs about 10 to 12 lb/cubic ft, is used for strengthening-members and propellers. Thin

* The inertia of the model in the vertical plane is already about 10 per cent too high due to the inertia of the towing arms, etc., and it is a moot point whether the resulting dynamic behaviour is more representative with the moment of inertia correct, or also increased by 10 per cent.

spruce ply is used to strengthen joints, and structural members are made up using balsa sandwiched between two layers of $\frac{1}{32}$-in. spruce ply. A resin glue, 'Beetle Cement', has been found to be completely waterproof and is used throughout. The inside of the model is treated with five coats of shellac and one of varnish. The outside receives five coats of shellac and two of varnish, being rubbed down with fine glass-paper between each coat. After the final rubbing-down it is polished with a wax polish.

As an illustration, the construction of a multi-engined flying-boat model of about 7-ft span and 10-lb weight is described below. In order to save weight the fin, rudder and wing-tip floats are omitted, since the model is constrained in yaw and roll and these items cannot affect the behaviour. The model is constructed in three parts:

(*a*) hull

(*b*) wing with motor installation

(*c*) tailplane and elevators.

(*a*) *Hull.*—A pair of plywood templates are cut out to the form of the side elevation cross-section at the centre-line and also a series of sheet metal templates marked out from the offset table showing the external cross-section at a number of longitudinal stations, usually 30 to 40. Before these latter are cut out an internal shape is also marked on each, leaving a wall thickness of about $\frac{3}{8}$ in. The internal shape need not follow the external contour exactly, in particular it is advisable to have a radius in the corner corresponding to the chine line. For a model intended for a development series of tests, it is also advisable to increase the thickness to $\frac{1}{2}$ or $\frac{5}{8}$ in. near the chine and in the step region to allow for modifications to the planing bottom. The internal and external templates are cut out, and port and starboard halves of the hull started separately.

Two blocks of balsa wood are made up, with dimensions rather greater than the length, height and maximum half-breadth of the hull, and the inside hollowed out to the internal templates. Two bulkheads are then made up to fit one just forward and one just aft of the wing and connected by a pair of longitudinal beams, the tops of which are shaped to the profile of the wing undersurface. The bulkheads are usually cut away to a 'figure eight' shape to save weight and also to provide some access to the inside of the hull when complete. The beams and bulkheads are made up of a sandwich of balsa between plywood. The beams also include four cedar blocks running from top to bottom of the beams to take four rods securing the wing to the hull.

The bulkhead and beams are glued together and then into one half of the hull, the whole of the inside of the hull treated with shellac and the two halves glued together. The hull is then cut on a bandsaw till it approaches the side-elevation and plan-form shapes and then cut down accurately to the wooden templates to give the centre-line shape. Each side is then taken down to the correct shape using the metal templates. The portion of the hull over the wing and between the two bulkheads is then cut away level with the wing under surface and shaped to the wing upper surface so that it fits with the wing in place. Two mahogany inserts are glued in on the top centre-line about 11 in. forward and 11 in. aft of the c.g. position to take the screw-eyes for the two control cords.

(*b*) *Wing with Motor Installation.*—Fig. 13 shows a typical wing construction for a four-engined aircraft with independent motors.

The wing is made up of leading-edge and trailing-edge spars of balsa joined by balsa ribs. The spars are partly hollowed internally and the ribs are pierced by a number of holes for lightness. If weight permits, $\frac{1}{10}$-in. balsa sheeting is used for covering the wing but $\frac{1}{16}$ in. can be used if necessary with rather closer rib spacing, as shown in Fig. 16. The two inner ribs are made of cedar and spaced at the same

distance apart as the two beams in the hull, so that four screwed rods can be passed down through the ribs and beams to secure the wing to the hull. The nacelle construction is shown in Fig. 14. It is built up of a hollow balsa shell attached to the leading-edge spar, with a plywood or cedar bulkhead for holding the motor. The propellers shown are of mahogany set into built-up plywood bosses, but cedar has been found to be sufficiently strong and considerably lighter. A motor installation of a different type is shown in Fig. 16, where a single turbine in each wing drives the propellers through shafts and gearing. Wing construction is as before, except that the front spar has been strengthened by the addition of a cedar and plywood sandwich to ensure rigidity of the motor unit. The propellers are of cedar and, in this case, the nacelles are simple balsa fairings (Fig. 15).

The air connections in the wings are by fabric tubes for the straight run, with $\frac{3}{4}$-in. outside diameter 18*g* aluminium tube for the joins and corners. At the wing tip an airtight box is made up, as shown in Fig. 16, consisting of a sandwich of cedar, or possibly balsa if the weight is strictly limited, between plywood. The towing attachments are fitted exactly on the c.g. axis of the model, and different c.g. positions can be covered by making up a set of cover plates with the attachments in different positions. Each attachment is secured to the cover plate by two 10 BA bolts only, to act as a weak link and protect the towing arms from damage in case of an accident to the model.

Between the two centre ribs a pair of detachable clips are fitted to hold a $\frac{1}{4}$-in. Duralumin tube, which is also located on the c.g. axis. This is used in balancing the models. The model weight can be altered without altering the c.g. position, by adding or removing circular lead weights to or from the tube.

The wing flaps are made up as triangular section balsa strips and attached by screws to the underside of the trailing-edge spar. A set of flaps to represent different flap settings is made up and the rearward face can be hollowed out, if desired, at the higher angles. The leading-edge slats are attached to the wing leading edge through a number of thin plywood brackets, as shown in Fig. 17. The wing trailing edge is strengthened by varnishing on a strip of Nylon fabric about 1 in. wide, folded round on the top and bottom surfaces of the trailing-edge spar.

(*c*) *Tailplane and Elevators.*—The tailplane (Fig. 14) is constructed, like the wing, with a leading-edge spar and rear spar connected by ribs and covered with $\frac{1}{10}$-in. balsa sheeting. Movable elevators, usually of solid balsa, are fitted to cover the full range of elevator movement expected full-scale. Each elevator is adjusted by means of a pair of quadrants, one on the tailplane drilled at 10-deg intervals, and one on the elevator drilled at 8-deg intervals. By selecting suitable pairs of holes, the elevators can then be set at 2-deg intervals and locked by means of an 8 BA bolt and nut.

On assembly the model is checked approximately for weight, c.g. and radius of gyration. The joins between the wing and hull and tailplane and hull are then carefully filled in with wax, to ensure that they are waterproof.

3.2. *Dynamic Model for Directional Stability Tests.*—Directional stability tests are made as a qualitative check following the evolution of a longitudinally stable and seaworthy hull form, and the model is usually a modification to the longitudinal stability model described in the previous section. The modifications required are as follows.

(*a*) The wing-tip air boxes and tubes are removed and the pivot unit (section 2.2) installed in the wing centre-section, as shown in Fig. 15, with the pivot at the scale c.g. position. The proper wing-tip shape can then be used if the span does not exceed 96 in.

(*b*) A fin and adjustable air rudder are added, which are constructed in a similar manner to the tailplane and elevators.

(*c*) An adjustable water rudder is added if this is to be fitted full-scale.

(*d*) Two rings are fitted in each wing tip to take the check strings for roll and the guiding reins (Fig. 16).

(*e*) Wing-tip floats are added (Fig. 16) which are normally made of solid balsa and are shaped up to templates in the same way as the outside of the hull. It is difficult to keep the chines sufficiently sharp and it is usual to insert a strip of very thin sheet metal along the chine line, leaving about 0·01 in. protruding as shown in Fig. 16. The float shown in Fig. 16 is of the retractable type and the two attachment rods represent the two struts of the attachment mechanism. The two rods are shown with a ' waist ' in them, and it is possible if desired to make the struts fail at the scale side loads after rotating through the correct angle and moving the scale distance sideways, by suitable choice of the diameter, length and lengthwise position of the waist.

3.3. *Model for Force and Moment Measurements.*—At low speeds the tests have to be made according to Froude's Law to obtain the correct wavemaking drag and buoyancy forces. This means that the model loading is reduced as the cube of the scale and tests made at speeds reduced as the square root of the scale, as for dynamic model tests. The limitation on model size to represent speeds right up to take-off does not apply, as the higher speeds are covered by a generalised method of testing described in a later section. The model can therefore be made as large as possible to reduce the scale effect corrections and improve the accuracy of reading at small draft values. It is difficult to handle a model with a loading greater than about 25 lb and in practice the model scale is usually chosen so that, when representing the maximum anticipated full-scale weight, the model load is 20 to 25 lb. Providing the model is less than 4 ft 6 in. in length, there is no interference from the side walls or bottom, but there is a small but unimportant depth effect at low speeds if the length is between 4 ft 6 in. and 9 ft. Both the depth and side-wall interference become important at low speeds if the model length exceeds 9 ft, and this should be considered as a limiting factor on the size.

As shown in Fig. 11, the attachment of the model to the balance is by a pair of $\frac{5}{16}$-in. bolts to a board with two radius arms carrying wires leading up to the balance. The bolts are 9 in. forward and 9 in. aft of the pivot point along the centre-line. The bottom of the board is 1·50 in. below the pivot point. It is usual to make the model solid up to a level 1·50 in. below the scale c.g. position and parallel to the keel, making the upper half as light fairings as shown in Fig. 12. The lower half of the model is normally constructed of planks glued together vertically to form the necessary width. Apart from the difficulty of obtaining a single piece of wood of the required size, the built-up hull is less liable to warp.

The central glued joint also forms a convenient and indestructible centre-line for marking-off purposes. Yellow pine is normally used for the lower part of the hull and should be of about 12 per cent moisture content, and in any case less than 15 per cent to avoid warping, etc. Mahogany is also a suitable wood, and can have about 15 per cent moisture content, but in any case less than 20 per cent.

The lower half of the hull is shaped up to templates in the same way as the dynamic model hull, but the only hollowing is a small cut-out for the forward radius arm of the balance attachment. The planing bottom and the sides for about an inch above the chines, are given a black ' Phenorock ' finish as shown in Fig. 12. The wood is first filled with an ordinary wood filler and rubbed down. Five or six coats of the ' Phenorock ' are then applied and rubbed well down with wet abrasive paper between each coat. This gives a very hard semi-glassy finish and a sharp chine line can be obtained by rubbing down towards the edge both on the bottom and on the side. The remainder of the lower half of the hull is finished in the usual way with five coats of shellac and two of clear varnish.

The upper half of the hull is usually made in three sections (Fig. 12). Fairly dense balsa is a convenient wood for shaping and is used for the nose and tail sections, which are shaped up to templates in the usual way. The centre portion has to be hollow and about 32 in. long to fit

over the balance attachment, and also has three clearance holes for the balance strut and the two pitching-moment wires. If the cross-section is constant the centre portion can conveniently be made of thin plywood bent over about four bulkheads, but if the shape is more complicated it may be necessary to shape it up in hardwood and hollow it out as required. The model shown in Fig. 12 uses the former type. In this case it was necessary to fit a pair of small blisters on the sides due to the pivot fittings protruding through the sides of the model. The parts are waterproofed in the usual way with five coats of shellac and two of varnish.

4. *Model Test Techniques.*—4.1. *Calibration of Dynamic Models for Air Lift and Thrust.*—The dynamic model is first calibrated for air lift and thrust. For these results the model is ballasted internally with about 15 to 20 lb of lead to ensure that the suspension wires still remain taut in the maximum lift condition. The model is suspended with the rig described in section 2.2, so that the towing arms are horizontal and it is set at an attitude which is a compromise between those for no lift and for the thrust line horizontal. The net thrust, or drag, is then measured over a range of speeds at various compressed-air supply pressures and also with the propellers replaced with spinner caps only. The variation of propeller thrust with supply pressure at each speed can then be found by adding the model drag with no propellers to the measured net thrust, and correcting for the increased drag of the parts in the slipstream and for apparent thrust produced by the flexible pipe connections straightening under pressure. The variation with speed of the supply pressure required to produce the required scale thrust can then be deduced. The propeller speeds are then measured at one or two carriage speeds to check :

(*a*) that the design r.p.m. are being approximately attained

(*b*) that on a multi-unit aircraft there are no large differences in speed between the units.

If these conditions are satisfied, the model lift is measured over the speed and attitude range, with and without the propellers running, with the model just clear of the water surface. For aircraft which have a large proportion of the wing area in the propeller slipstream there is no real check on the results obtained, as the standard method of estimating the wing lift with slipstream[7] is not accurate at high values of thrust coefficient, and wind-tunnel results usually overlap the take-off range only for about the last 10 per cent. It is therefore advisable to make the lift calibration as accurately as possible and to cover an adequate range of conditions, in order to provide sufficient data for use in making take-off estimates.

In the case of jet aircraft, however, or when representing landing with power off, a fairly accurate full-scale lift estimate is usually available, and it may be possible to get better agreement between the model and full-scale lift curves by adjusting the slat leading-edge[3]. It can be seen from Fig. 18 that the slat, while increasing the lift at high angles, reduces the lift at low angles with a cross-over at about 6 deg in the example shown. The whole lift increment effect can be shifted quite simply by adjusting the slat leading-edge angle. On the model from which the results of Fig. 18 were obtained, the leading-edge angle has been increased by about 2 deg by reducing the curvature just behind the leading edge, as the standard setting (Fig. 17) was producing a severe loss of lift at 4 deg attitude.

When satisfactory agreement has been obtained, the model, when re-balanced to correct c.g. position and ballasted to the correct weight, is then ready for the stability tests.

4.2. *Longitudinal Stability, Trim and Spray Tests.*—With the use of the rig described in section 2.2, the dynamic model, ballasted to the appropriate weight and c.g. position, is towed from the c.g. axis so that it is free to pitch and heave. With the appropriate slipstream or jet stream, the model running attitude, draft, spray and stability correspond to full-scale[15], apart from the effect of other scale factors, mainly secondary.

The exploration of longitudinal stability is made at a series of steady speeds over the speed range[15]. Full-scale, the aircraft accelerates in take-offs and decelerates in landings up to the order of $0{\cdot}2g$, the actual values varying with available thrust, wing and hull design, attitude

and water roughness. The major effect of such acceleration is to reduce the time available for any possible event to happen, this time being determined by the operating conditions. It is the practice, in the Royal Aircraft Establishment Tank, to determine the basic hull characteristics without acceleration or waves present and, where necessary, particularly in a project design development, to add a few with acceleration with and without the presence of waves[3, 9]. These tests are done on the controlled dynamic model in the towing tank, but it is considered better to test where possible with free-flight models. The worst possible deterioration of performance in full-scale sea conditions is measured by determining the effect of disturbances to the running attitude of the model on its stability[15].

The procedure during a typical steady-speed test run is as follows :

(*a*) the model is lowered on to the water in the planing range as the carriage reaches its steady speed, taking care to avoid giving the model any initial disturbance

(*b*) the steady running angle is read and any spray interference noted

(*c*) if any oscillation develops spontaneously, the steady or greatest amplitude is noted. If no oscillation develops, the rear cord is jerked to give the model an impulsive nose-down disturbance of about 6 deg, or sufficient to reduce the keel attitude to zero, whichever is the smaller. The actual disturbance given and the pitching amplitude of any resulting oscillation are noted.

4.2.1. *Longitudinal stability and trim results in calm water.*—Fig. 19 shows a typical stability and trim diagram for one weight at one flap setting, c.g. position and slipstream condition and Fig. 20 an important effect of all-up weight. The usual procedure is to run through the elevator-central curve at 4 ft/sec intervals (model-scale), followed by the elevators-fully-up curve and fill in points at intermediate elevator angles and speeds. A suitable number of points are obtained to draw in the position of the stability limit relative to the trim curves. A few runs at positive elevator setting may be necessary at mid-planing speeds to complete the diagram. The symbols used are explained in the key on Fig. 19.

The motion is considered to be unstable if the total amplitude in pitch exceeds 2 deg. It is emphasised that the oscillation need not be divergent and in the majority of cases will not be so. The figure of 2 deg was arrived at after correlating full-scale records with pilots' opinions as to undesirable oscillations. It is subject to change with experience[15]. The choice of a more severe limit of 1 deg will not normally affect the stability limits appreciably. It is usual to draw in the limits obtained with a severe nose-down disturbance as being the worst possible case. At any one test condition, however, it is often possible to determine a series of limits depending on the amplitude of the applied disturbance.

An analysis of porpoising instability, model and full-scale, is given in Ref. 15, but for convenience some of the results which may be found in any one series of model tests are briefly recapitulated in Appendix I.

It must also be strongly emphasised that this analysis is based on evidence accumulated for hulls of length/beam ratio up to 7 and beam loadings up to $C_{\Delta 0} = 1{\cdot}0$. The effect of using much higher length/beam ratios and beam loadings and, in particular, very long afterbodies must be considered as well and general trends are reviewed in Ref. 11.

4.2.2. *Spray behaviour in calm water.*—Figs. 25a and 25b show a typical spray formation at low speed taken with two different exposure times. The photographs were taken with an F.24 camera synchronised for flash, using

(*a*) an electronic flash of about 1/3000 sec

(*b*) a flash-bulb of about 1/30 sec duration.

The electronic flash 'freezes' all water motion and produces a photograph showing innumerable drops of water suspended in space with no indication of their origin or direction of travel, while the flash-bulb with its much longer duration 'integrates' the spray drops into a sheet which

clearly shows the spray boundaries and direction of motion. The difference in the two photographs may not be very apparent in the final reproduction but it is very marked in direct prints, more particularly in the rear views where the spray has had more time to separate into drops. Long exposures (flash-bulbs) are therefore considered more suitable for photographs under steady conditions, whilst the short exposure (electronic flash) is reserved for analyses of unsteady behaviour.

Fig. 26 shows diagrammatically the spray formation from a vee-bottom planing surface, such as a flying-boat forebody and a description is given in Appendix II to help interpret test development and should be read in conjunction with Figs. 25b and 26.

4.2.3. *Tests in waves.*—The model can only be run directly into a steady wave train, which is a very severe case, but such tests do give a qualitative impression of the deterioration in behaviour to be expected in rough water. The tests usually consist of:

(i) a number of steady speeds in the taxying speed range

(ii) accelerated runs to take-off and decelerated runs from touch-down. The waves are selected to have about two heights and three lengths.

For take-off runs the aircraft is trimmed to take-off smoothly with no appreciable change in attitude on leaving the water, and in practice only a few degrees variation in elevator angle is possible. At each elevator setting the carriage speed is set to about 1 ft/sec higher than the unstick speed and the reduced acceleration of about $0 \cdot 12g$ is used.

For simulated landings the model is trimmed to give practical touch-down attitudes, and at each elevator setting the carriage speed is set at slightly below the flying speed of the model, so that a reasonable rate of descent is obtained. The model is held well above the water till the carriage has reached its steady speed, and then released to glide gently down to the water. As the model touches down, the carriage brakes are applied.

The taxying tests indicate whether the bow and forebody design is satisfactory, so that excessive spray is not thrown over the cabin or into the propeller discs or air intakes in rough water. The landing and take-off runs, though the accelerations and decelerations are not strictly correct, do indicate whether any mid-planing instability present is sufficient for large amplitude oscillations to build up in the time taken to pass through the critical speed range, and how rapidly any oscillations die out once the critical speed is passed. The time scale on the model is reduced proportionately to the square root of the model scale, which makes observation difficult but, by using a high-speed ciné camera running at a suitable increased speed, the film, on projection at the standard 24 frames/sec, will give the full-scale time scale. This gives a much better impression of the behaviour and enables more detailed observation of the spray to be made.

It is possible to analyse the aircraft motion in some detail by phographing the pair of pointers indicating the model draft and attitude with a ciné camera. In this case about 30 to 40 frames/sec are sufficient. Fig. 31 shows typical records during a steady-speed run. A series of tests[19] have been made using one wave height and varying the wave length, at a steady speed of $0 \cdot 7$ of the take-off velocity, to determine whether there was any particularly severe resonance at some wave lengths. Fig. 32 shows a typical variation of pitch and heave amplitudes with wave length and Fig. 33 the variation of the ratio of maximum to mean amplitude, which is a measure of the irregularity of the motion. From these it is apparent that, while there is a resonant pick-up for a wave length equal to about four times the hull length, with corresponding harmonics at shorter wave lengths, the largest oscillations and highest vertical accelerations may occur in the irregular off-resonance wave lengths.

The accuracy of this method is not high (particularly in obtaining vertical accelerations), and some form of accelerometer would be required for, say, a quantitative evaluation of the relief in vertical accleration to be obtained by an increase of length/beam ratio or an increase in forebody deadrise. Some degree of longitudinal freedom for the model would also be advisable to allow for resistance relief by deceleration in waves.

4.3. *Directional Stability on a Complete Dynamic Model.*—With the rig described earlier (section 2.2) the model is towed from a universal joint at the c.g. and is free to pitch, heave, yaw and roll. One operator holds the usual two strings to lift the model out of the water when not running and to restrain the model in case of emergency, but these are normally held slack during a test run. A second operator holds a pair of reins from the wing tips (Fig. 6) and pulls the model slowly round through a range of angles of yaw, feeling the direction and magnitude of the yawing moment at any angle. The operator reads the angle of yaw, by means of a sight, off a scale on the model tailplane. A typical test result at one speed might read ' Just stable $\pm$ 5 deg then violently unstable '.

Although a fully representative dynamic model is used, the lack of freedom in lateral movement and the increased vertical inertia due to the towing attachment prevents oscillatory motions being correct. The tests are therefore confined to steady-speed runs over a range of speeds and elevator angles at each condition of weight, c.g. position and flap setting, the yawing moment variation being noted over what is effectively a series of steady angles of yaw during the run.

Since it is not possible to obtain the running attitude without considerable elaboration of the apparatus, the elevator angle can conveniently be used in plotting the results instead of the running attitude. Figs. 34 and 35 show two methods of presenting the results. Fig. 34 is effectively the normal longitudinal stability diagram, showing the positions of the longitudinal stability limits relative to the elevator angles, and with the directional stability limits added. The directional stability over, say +3 deg to −3 deg of yaw is taken in this case. Alternatively, the stability variation with angle of yaw over the speed range can be shown, as in Fig. 35, for any chosen elevator setting. This method of plotting is probably better than that shown in Fig. 34 for showing up the effect of modifications. Fig. 35 shows the effect of adding a skeg* to one aircraft.

The effectiveness of the water or air rudder can be found by determining the angle of yaw or neutral point produced by a range of fixed rudder angles. It would, of course, be possible to measure the yawing moments by connecting the reins to some type of balance, but it is doubtful whether the results have more than qualitative value due to the large scale effect on this type of test.

Flying boats are normally directionally unstable for low forward speed, but improvement in pre-hump speed directional stability, except for the very low speeds, can be obtained in two fairly simple ways. One method is to add a skeg as mentioned above. In general the size of skeg required to produce a considerable improvement is quite small, say 0·5 sq ft on an aircraft of 100,000 lb all-up weight. The pre-hump and hump speed directional instability is generally due to the water flow sticking to the afterbody sides above the chines, and a series of small breaker steps in the region where this is occurring has been found very effective in eliminating the instability, except at very low speeds. These steps can be quite shallow, say 0·5 in. high full-scale, and should be arranged at about 45 deg in side elevation (Fig. 36) to enable the air to flow down behind them.

4.4. *Force and Moment Measurements.*—4.4.1. *Drag and pitching moments.*—4.4.1.1. *Method of test.—Choice of force parameters.*—Fig. 37 shows typical attitude-speed curves and Fig. 38 typical load on water against speed curves during take-off. The curves are given for two weights and two flap settings at one weight, and are at a fixed elevator angle. As can be seen, the number of test points required to cover a combination of weights, flap angles and elevator angles becomes prohibitive if each condition is tested individually. However, it has been found possible to plot the results in terms of coefficients so eliminating some of the variables and find the drag

* A skeg is a small vertical fin projecting down from near the rear step and usually consists of a flat plate of triangular shape in side elevation (Fig. 36).

and pitching moment at any particular load, speed and attitude by interpolation[17, 20]. The coefficients and symbols in general use are :

Keel attitude	α_K		
Drag	R	Drag coefficient	$C_R = R/wb^3$
Load on water	Δ	Load coefficient	$C_\Delta = \Delta/wb^3$
Speed	V	Speed coefficient*	$C_V = V/\sqrt{(gb)}$
Pitching moment	M	Pitching moment coefficient	$C_M = M/wb^4$
Draft	d	Draft coefficient	$= d/b$

where b is the beam of the aircraft—usually the maximum width of the forebody planing bottom, though the width of the planing bottom at the step has been advocated,

and w is the density of water.

Any consistent series of units can be used.

It has been found experimentally that, above a value of C_V of about 2, the drag, load and pitching-moment coefficients at a given attitude are independent of Froude effects. The corresponding speed is probably higher for higher length/beam and C_Δ values. Examination of the flow pattern on the planing bottom and of the theoretical forces show that this is due to the gravitational effects on the wetted area shape and the buoyancy force diminishing very rapidly with speed, till above a C_V of about 2 they can be neglected. The filling in of the wake behind the forebody is still, of course, a function of gravity and hence varies in shape with the speed, so that the results will only coalesce if the afterbody is clear of the wake. However, the afterbody is normally clear of the wake for all speeds above the hump speed, except at very high attitudes. Practically the whole of the speed and attitude range above the hump speed—usually known as the planing range—can therefore be covered on the basis that C_Δ, C_R and C_M are functions of d/b and α_K only, and are independent of Froude number defined by C_V, providing it is greater than about 2.

Consider a simplified planing bottom of a prismatic form with a straight step (Fig. 26). The wetted area inside the stagnation line, from which the lift is derived, is of a triangular shape as long as the stagnation line is inside the chines at the step. The apex angle of the triangle varies with attitude, but at any given attitude the apex angle remains constant with varying draft, and the keel wetted length varies linearly with draft. The wetted area is therefore proportional to (draft)^2 at constant attitude. The C_L at constant attitude depends on the aspect ratio of the wetted area but, if the stagnation line is within the chines, the wetted area is of constant aspect ratio at a fixed attitude and so C_L is also constant. The dynamic lift at a constant attitude is therefore proportional to wd^2V^2 or in terms of coefficients,

$$C_\Delta \propto (d/b)^2 \, C_V^2$$

or

$$C_\Delta^{1/2}/C_V \propto d/b.$$

In practice, both in making take-off estimates and also in making the tests with a free-to-rise type of balance, as installed in the Royal Aircraft Establishment Seaplane Tank, it is actually C_Δ, C_V and α_K which are known or set and the draft, drag and pitching moment measured[21]. It is therefore more convenient to treat $(C_\Delta^{1/2}/C_V)$ and α_K as the independent variables and d/b, C_R and C_M as the dependent variables.

* The speed coefficient is sometimes referred to as Froude number due to its similarity to the Froude number $V/\sqrt{(gl)}$ used in ship testing, where l = length of ship.

For most of the planing region the stagnation line is within the chines and, although on an actual hull the relationship between $C_\Delta^{1/2}/C_V$ and d/b may no longer be linear, due to curvature of the planing bottom and/or step plan-form, the use of $C_\Delta^{1/2}/C_V$ as the independent variable is still equally valid. This will, however, need reconsideration for highly loaded high length/beam ratio hulls.

Test condition in planing speed range.—Since the results in terms of coefficients are independent of C_V, as discussed earlier, it is usual to cover the planing range by a series of tests at one speed, varying the load on water at a number of attitude values—usually 4 deg, 6 deg, 8 deg and 10 deg suffice, though a few points at 2 deg and 12 deg may sometimes be necessary. 28 ft/sec is a convenient speed, with the normal size of model, as it makes possible loads which neither become too large to handle at high values of $C_\Delta^{1/2}/C_V$ nor too small to affect the accuracy unduly at low values.

The reason for using one speed rather than two or more is that the drag, and to a small extent the draft and pitching moment, vary with Reynolds number because of movement of position of the transition of the boundary layer. Until a technique is evolved for fixing the transition where required, the rapid changes of drag with Reynolds number preclude the use of different speeds.

Test conditions in displacement speed range.—At the lower speeds it is necessary to test the model at the correct value of C_V to obtain the correct flow pattern round the hull. In this region, however, the effect of elevator angle, flap angle and weight on the aircraft attitude is comparatively small up to the hump speed (Fig. 37) and only a fairly limited range of angles need be covered at each speed. In practice, in order to join up with the planing region curves, it is usual to test at three of the standard attitudes, such as 2 deg, 4 deg and 6 deg or 6 deg, 8 deg and 10 deg, at each of about ten values of C_V, the attitude range at each speed being determined from the results of tests on a complete dynamic model. Similarly, with the use of the calculated reduction of C_Δ with speed, as shown in Fig. 38, the load range to be tested at each speed can also be determined. Usually about four or five loads are necessary such as, say, values of C_Δ of 1·3, 1·2, 1·1, 1·0 and 0·9 at a C_V of 0·5, dropping to values of 1·0, 0·9, 0·8, 0·7 and 0·6 at a C_V of 2·5. It is useful to have at least one load running through the speed range for assistance in drawing the curves.

The number of experimental points to cover ten speeds, five loads and three angles is 150. Since up to eight readings can be taken in one run at 4 ft/sec, falling to two at 20 ft/sec, less than forty runs are required to obtain these. At speeds below the hump speed, pitching moment has only a small effect on the hull attitude and hence on the drag.

Since the aerodynamic pitching moment is small, reasonably accurate drag values can be obtained by towing the hull free to trim. This requires the hull to be balanced roughly about the centre of gravity, and it is usual to apply a moment equal to the propeller or jet thrust moment. The balance is designed to allow free-to-trim testing by simply withdrawing a pin holding the wheel D to the shaft B (Fig. 11). The model attitude is then indicated by the pointer C against a scale on the wheel D. Comparisons of the drag obtained on the solid hull, tested both free-to-trim and also fixed at attitudes determined from tests on a complete dynamic model, show that the differences in drag are not likely to exceed 5 per cent. The method is therefore useful for a preliminary examination of the hull drag at speeds below the hump speed, and it is the only way if dynamic model tests have not been made. It has the advantage of reducing the number of test points required to one-third, so that the whole range up to the hump speed can be covered in about fifteen runs.

Tests in airflow and no airflow.—The tests can be made either in airflow or screened, so that either the air and water forces on the hull are measured, or the water forces alone. The second method, though at first sight the simpler, has two disadvantages. One is that the flow round the afterbody, particularly at higher speeds, is altered by the absence of airflow; the second is

that the water surface is disturbed rather badly by the screen at speeds below 16 ft/sec, as described later. For normal tests, the models are therefore tested in airflow, and the air forces on the hull, suspended just clear of the surface, are subtracted from the total forces to give nominal water forces. These are not the true water forces, as the air forces on the hull just clear of the surface are not the same as the air forces when the hull is partly submerged, but these nominal water forces are what are required for take-off estimates[21]. If, however, the true water forces are required, it is necessary to make the tests screened, and if possible use only speeds greater than 16 ft/sec.

The procedure in measuring the air forces on a hull is as follows. The rear pitching moment wire is removed, and an attachment is inserted at the bottom of the strut whereby the model attitude can be adjusted while the model is suspended from the front wire only. The scale pan hanging from pulley D (Fig. 11) is secured to a fixed point and weight applied to the scale pan on A till the pitching-moment arm is ' floating '. The pitching-moment dynamometer can then be calibrated directly in terms of lift on the model. The model drag can be measured on the balance directly in the usual way. It is necessary to measure the air lift and drag over the attitude range expected at all speeds to be used as the air forces are not even approximately proportional to the square of the speed on account of the very low Reynolds number. The model is usually suspended with its step about 0·2 in. clear of the water for these tests, and a note is made of the draft indicator reading in each case.

4.4.1.2. *Corrections to measured readings.*—The corrections to be applied to the measured quantities and the probable accuracies are as follows:

(*a*) *Draft.* The tank rails have been aligned to the water surface to within $\pm$ 0·002 in. with the use of the optical instrument described in Ref. 22, and the wheels ground up in position to $\pm$ 0·001 in. on diameter, so the readable accuracy of 0·01 in. on draft should not be influenced by variations of carriage height.

The water, however, is affected by the aerodynamic pressure field of the carriage and a depression or series of waves is formed under the carriage. The draft correction to allow for this surface deflection has been measured, with the technique described in Ref. 23, over the carriage speed range both screened and with correct airflow, and should be within 0·005 in. The overall accuracy on draft should therefore be $\pm$ 0·01 in. Fig. 39 shows the water surface deflection with airflow and Fig. 40 that in the screened condition 1·5 in. behind the balance strut centre-line, corresponding to the normal step position of a model. For both conditions above 12 ft/sec, they can be regarded as applicable up to 2 ft forward or aft of this position. Below 12 ft/sec in the screened condition a wave system is set up, originating at the high air pressure line at the front of the screen, which is illustrated in Fig. 40. A semi-empirical curve has been fitted to these points on the basis of which the water surface profile can be calculated. For convenience of calculation, Fig. 41 gives, plotted against carriage speed:

(i) the theoretical wave length

(ii) the wave semi-amplitude in inches

(iii) the distance of the wave origin ahead of balance strut centre-line.

(*b*) *Attitude.* A general accuracy of $\pm$ 0·1 deg is attainable without applying any corrections during normal tests, excluding the screened speed range below 12 ft/sec, where the water surface inclination has to be calculated from the surface profile described above. If a higher accuracy is required, corrections have to be made as follows :

(i) *Water surface inclination.* The data of Ref. 23 suggest that inclinations of the water surface up to 0·05 deg may occur during screened tests above 12 ft/sec, but that in airflow the inclination should be negligible at all speeds.

(ii) *Position of pitching-moment balance arm.* The pitching-moment balance arm (Fig. 11) rocks through about $\pm$ 0·1 deg between its stops. To minimise this movement it is customary to use the rider to keep the pitching moment measured by the movement of the arm to a fairly small value. If greater accuracy is sought, the angular movement of the arm can be plotted directly against the pitching-moment indicator reading, and the correction read off from the indicator reading for each test.

(iii) *Stretch of the pitching-moment wires.* The model is connected to the pitching-moment arm by a pair of 18-gauge steel wires about 5 ft 6 in. long. There is therefore some relative change in angle between the model and the balance arm, which is roughly proportional to the total pitching moment. The deflection is approximately 0·01 deg for 1 lb/ft pitching moment, but a complete curve of angle correction against total pitching moment can easily be produced in any particular case, and the correction applied.

(*c*) *Load on water.* In the rise system there are twelve ball-races and four chains carrying loads of 30 to 40 lb, so that there is a fair amount of static friction present. However, when properly adjusted and lubricated the system should just move with 0·1 lb out of balance load. Despite this static friction it is possible to counterbalance the model to about $\pm$ 0·02 lb, by inspecting the rate of movement of the system in either direction with an out of balance load of about 0·15 lb applied alternately at X and Y (Fig. 11).

No air lift correction is necessary during screened tests. For tests in airflow the air lift is either subtracted from the total load on water applied, or alternatively weights equivalent to the air lift are applied separately to the weight arm X (Fig. 11). The air lift is usually applied to the nearest 0·05 lb and the vibration of the carriage is assumed to allow the system to balance out to about $\pm$ 0·05 lb. To maintain this accuracy it is necessary to check the counterbalancing at intervals, to make sure that no water has collected inside the model and that excessive spray is not wetting the strut and upper half of the model.

(*d*) *Drag.* In the airflow condition there are two sources of drag correction, first the drag of the unshielded streamlined strut supporting the model (Fig. 12), second the effect of the airflow round the upper part of the drag balance including the weight bar X and the inertia counterbalance weights (Fig. 11). Fig. 42 shows the variation with speed of the drag per inch length of strut exposed to the air stream, and Fig. 43 the drag of the upper half of the balance.

It is not normally necessary to separate out these two components, as the measured model air drag already includes the balance drag and part of the strut drag. Knowing the draft reading at which the air drag was measured, the drag at any other draft can be found simply by adding on the drag of the extra part of strut exposed.

In the screened condition the only correction is for the effect of airflow over the top part of the drag balance. The correction unfortunately shows some variation with the number of weights on the weight bar X (Fig. 11), and also with the height of X and the vertical position of the inertia-counterbalance weights. A single curve of drag correction against speed is therefore not sufficiently accurate and it is necessary, after setting the inertia-counterbalance weights, to remove the model and measure the drag correction over the anticipated verrical range with various weights on the weight bar. A typical curve at one setting is shown in Fig. 43. If a reasonable interval, say 15 minutes is allowed between runs, repeat readings on the drag indicator can be read fairly easily to the nearest half division on the scale, corresponding to a drag accuracy of $\pm$ 0·01 lb.

(*e*) *Carriage speed.* The carriage-speed indicator (section 2.3) is calibrated directly in ft/sec and can be read fairly easily to the nearest 0·05 ft/sec above about 6 ft/sec. The scatter in producing the correction curve shown in Fig. 44* suggested there was no measurable error in consistency of the instrument reading, so that the corrected speed is probably within $\pm$ 0·03 ft/sec. Below 6 ft/sec the speed can conveniently be measured by timing a 100-ft interval with a stop watch. If the accuracy obtained by the above methods is not considered sufficient, the speed can be measured from the recorder drum and the speed obtained to better than $\pm$ 0·5 per cent, up to 30 ft/sec. Above this speed the records become rather difficult to interpret.

(*f*) *Pitching moment.* The pitching moment is corrected only for the effect of airflow over the top part of the balance. The correction† is given in Figs. 45 and 46 for the screened and airflow conditions for the normal range of carriage speeds. The pitching-moment indicator can normally be read to the nearest half division and the corresponding accuracy in pitching moment is probably $\pm$ 0·05 lb/ft.

4.4.1.3. *Presentations of results.*—The quantities R/Δ, d/b and $M/\Delta b$ are plotted against $C_\Delta{}^{1/2}/C_V$ for each attitude. One difficulty of using $C_\Delta{}^{1/2}/C_V$, as abscissa is that its value becomes infinite at zero forward speed and, to overcome this, the reciprocal $C_V/C_\Delta{}^{1/2}$ is used for the low speed range. A method of plotting the results has been devised[20] to enable continuous curves to be drawn over the whole open range as shown in Figs. 47, 48 and 49. By choosing a suitable scale such that 1·0 unit of $C_V/C_\Delta{}^{1/2}$ is equal to 0·05 units of $C_\Delta{}^{1/2}/C_V$, a continuous scale can be obtained running from $C_V/C_\Delta{}^{1/2} = 0$ to 4 with an overlap of from $C_V/C_\Delta{}^{1/2} = 4$ and $C_\Delta{}^{1/2}/C_V = 0{\cdot}25$ to $C_V/C_\Delta{}^{1/2} = 5$ and $C_\Delta{}^{1/2}/C_V = 0{\cdot}20$ and then down to $C_\Delta{}^{1/2}/C_V = 0$. The reversal range can of course be altered to any other position such as 5 and 0·2 to 10 and 0·1 by adjusting the relative scales, but that shown has been found suitable for the usual model test range for hull forms of length/beam of about 7.

The above method of plotting is quite useful for comparing two hull designs, but if the results are wanted for use in take-off estimates a more convenient way of plotting the results is:

(*a*) in the low-speed range to plot drag against attitude at each speed used, interpolating lines of constant load on water

(*b*) in the planing region to plot R/Δ against α_K, interpolating lines of constant $C_\Delta{}^{1/2}/C_V$.

4.4.2. *Side force and yawing moments.*—The No. 2 carriage balance has so far not been used for measuring side force or yawing moments, and the corrections have not been measured. For side force there will be no correction for the balance strut in the airflow, as this is not yawed with the model. It is anticipated that there will be a small correction for the airflow over the top half of the balance, dependent only on the carriage speed, which may vary with the vertical position of the inertia balance weights or the weight bar.

No yawing-moment balance has been designed as difficulty has been found due to the large drag loads which occur when the model is yawed and the fact that the structure of the balance is not designed to resist the large yawing moments likely to occur (it is believed that scale effects lead to very large yawing moment on models relative to the full-scale case).

It has not so far been considered justified to build the necessary attachments for the small range of angles over which they are likely to be usable, especially in view of the uncertain scale effects which will affect the results.

---

* The calibration shown was made in April 1950 and should be checked at intervals.

† This correction will be influenced by any alterations to the balance shielding and to some extent by the positions and number of persons on the carriage and requires checking occasionally.

4.5. *Wetted Area Measurements.*—The method proposed in Ref. 17 for examining the wetted-area and boundary-layer conditions on a hull bottom has been adapted, as described below, to give accurate measurements of the hull wetted areas throughout the take-off run. These are required to correct the model drag measurements to full-scale, to allow for the difference in Reynolds number.

The hull bottom is sprayed with a thin coating of a white substance which is only sparingly soluble in water. Hydroquinone diacetate has been found to be suitable for the Royal Aircraft Establishment Tank speed range and length of run. It is prepared as a 5 per cent solution in acetone and applied with a compressed-air spray gun. The acetone evaporates off almost immediately leaving a thin coating of the solute on the hull bottom. The procedure after coating the model bottom is as follows.

The model is replaced on the balance, taking care not to dip it in the water for longer than necessary and to avoid any agitation of the water. The carriage is run back to the west end of the tank and about five minutes allowed for the ripples in the water surface to damp out. The model attitude and load on water are then set, with the model still clear of the water, and the carriage started. As the carriage reaches its steady speed, the model is plunged rapidly in to its correct, or nearly correct, draft and then released. The model is assisted to find its steady running draft by damping out any oscillations as quickly as possible. The draft recorder reading is taken and, after the model has been in the water for about 200 ft, the hull is quickly raised clear of the water again. The carriage is then run to the east end dock and the model removed from the balance, care being taken not to dip it in the water more then necessary. The bottom is next dried with a compressed-air jet and the wetted areas can then be measured or photographed. The bottom is finally carefully cleaned and, after respraying, is ready for the next run.

A single reading requires quite a lot of effort and even with practice it is difficult to make runs at less than half-hour intervals, and then only for simple wetted area shapes requiring only a few lengths to be measured to define them. Fig. 50 shows the type of result that can be obtained. The stagnation line can be clearly seen and also the limit of the spray wetted area. The white spots are small pieces of Plasticine which had been put on to produce turbulent wakes, illustrating the direction of the flow (Fig. 26) and also whether or not the flow at that point was already turbulent.

For analysis and estimation of skin-friction drag a provisional general method has been evolved[21]. A wetted-area coefficient C_{S2} and a wetted-length coefficient l/b are first defined, Fig. 51. If

S_1 is the main wetted area inside the stagnation line

S_3 is the spray wetted area

ϕ is the angle between the stagnation line and keel in the plane of the wetted surface

$$S_2 = S_1 + S_3 \cos 2\phi,$$

$$\text{then } C_{S2} = S_2/2b^2;$$

where b is the hull beam, and C_{S2} is the equivalent drag area in the direction of the keel.

In S_1 and S_3 the mean wetted lengths are determined separately by $\Sigma l\delta s/\Sigma\delta s$ where l is measured in the direction of flow assumed to be parallel to the keel in S_1 and at angle 2ϕ to the keel in S_3. If $\bar{l}_1$ and $\bar{l}_3$ are the mean wetted lengths in S_1 and S_3 respectively, then

$$\frac{\bar{l}}{b} = \frac{\bar{l}_1 S_1 + \bar{l}_3 S_3 \cos 2\phi}{b(S_1 + S_3 \cos 2\phi)}$$

where $\bar{l}$ is the mean wetted length in the direction of the keel referred to S_2 as defined above.

The values of $C_{S\,2}$ and $\bar{l}/b$ can be worked out in this way for the whole of the planing region but for the low-speed range there is a similar additional wetted area on the afterbody of mean defined area S_4 and wetted length $\bar{l}_4$. Also at the deeper draught the planing bottom no longer approximates to a simple prism, owing to the turn-up at the bow and shape and upsweep of the afterbody. No exact treatment is possible with the shapes involved without very considerable complication, and the following approximate method is suggested as being of sufficient accuracy for use in estimating the scale-effect correction to the drag[21].

Suppose

$$S_2 = S_1 + S_3 \cos 2\phi + S_4 \cos \alpha_{kk},$$

where α_{kk} = angle between the forebody and afterbody keels. Then with less than half the afterbody length wetted, it is suggested that the mean value for the three areas should be used, *i.e.*,

$$\frac{\bar{l}}{b} = \frac{\bar{l}_1 S_1 + \bar{l}_3 S_3 \cos 2\phi + \bar{l}_4 S_4 \cos \alpha_{kk}}{b(S_1 + S_3 \cos 2\phi + S_4 \cos \alpha_{kk})}$$

In this condition it has been found that even with turbulent flow on the forebody bottom, laminar flow is obtained for conditions on the afterbody.

Figs. 52 to 55 show results obtained on a 7·2 length/beam ratio hull with a streamline planform step. Figs. 52 and 53 show the values of $C_{S\,2}$ and $\bar{l}/b$ for the low-speed range. Two discontinuities occur, the first when the flow breaks away from the main step, and the second when the afterbody lifts clear of the wake. The results were plotted in each case against d/b, C_V and $C_V/C_\Delta^{1/2}$ and the abscissae chosen are the ones which gave a reasonable collapse for this particular model.

Figs. 54 and 55 show the values of $C_{S\,2}$ and $\bar{l}/b$ for the planing region. A dotted line has been added showing the limit of the constant cross-section of the forebody. Inside this limit it is possible to calculate the theoretical wetted areas and mean wetted lengths fairly easily. This assumes no splash-forward and a splash-up factor of $\pi/2$ on the stagnation line in the beam direction. In practice there is usually some splash-forward and also a splash-up of rather more than $\pi/2$, particularly at high attitudes. This is most easily allowed for by applying a simple factor to the theoretical curves and only about two measured points at each attitude are required for this purpose as shown in Figs. 54 and 55.

5. *General Remarks.*—Considerable changes have been made in the last decade in the testing techniques using the Royal Aircraft Establishment Seaplane Tank, which may be summarised under the three following headings :

(*a*) to increase the accuracy of measurement

(*b*) to extend existing test techniques to wider or different parameter ranges

(*c*) to make possible an examination of the mechanism of the water flow over seaplane hulls.

These three headings are not dependent on each other but form convenient sub-divisions with which to analyse broadly the advances made in tank testing techniques. The techniques have developed and changed considerably and will probably continue to do so as new departures in the design of waterborne aircraft throw up either more detailed requirements on old problems or new problems to be examined. The basic aim in tank testing technique has been to try and anticipate the full-scale problems and to check the model-scale methods continually by comparison with full-scale.

Improvement in accuracy has been directed both to the testing of dynamic models for stability and of solid models for hydrodynamic forces, but the major changes have been made in connection with the latter. It has been found necessary to increase greatly the accuracy of measurement of draft, this parameter being, with attitude, the important one determining planing forces. To improve the accuracy of measurement, it has been found possible to level the rail surfaces relative

to the water surface to within 1 to 2 thousandths of an inch and grind the wheels circular with respect to their axles accurate to 1 thousandth of an inch. Examination of the water surface in the vicinity of the balance then showed considerable depression due to the presence of the pressure field created by the movement of the carriage along the tank. This has been partially reduced by designing the carriage as a wind tunnel with constant pressure field over the water, which was also required for accurate measurements of the drag of hulls in the presence of air flow, but it was still necessary to measure the actual water depressions under the carriage at various speeds so that correction to draft could be made.

The use of the wind-tunnel similarity to obtain uniform air speed conditions in the presence of models used for force measurements was made necessary on discovery of the important effects of airflow on the interference which could occur between the forebody water wake and the hull afterbody. Under earlier test conditions, there was very serious variation of velocity in the region of the model.

For tests under swell conditions, it has been possible to analyse the results so that a more rational understanding of the nature of the waves produced, and hence of their effect on stability, could be obtained.

Extensions of testing techniques to examine more closely the prevailing hydrodynamic problems and also the importance of new parameters have been partly covered in the brief conclusions on the accuracy required in the measurement of draft and waves.

Improvements in model making technique, in particular the problem of keeping down weight and obtaining a reasonably correct moment of inertia in pitch and better representation of slipstream, have made possible much closer model/full-scale correlation of attitudes, elevator power and stability in stability testing. Compressed-air driven turbine motors have been developed which successfully make possible the correct representation of high slipstream and can also be adapted to represent correct jet airflow.

There are still some outstanding problems on the correct model techniques to give the full-scale stability found in various degrees of water roughness and various types of swell. The present model disturbance techniques, *i.e.*, a 7 deg nose down disturbance in pitch, undoubtedly give the pessimistic answer corresponding to operation into an infinite range of swells full-scale but, as such, are very valuable.

A particularly useful technique is that successfully developed to qualitatively measure the stability in yaw and roll on dynamic models. This has made possible a quick and reasonably accurate design assessment for a model over the whole speed and attitude range and will give an immediate indication of whether trouble may occur and, by examination of the flow conditions existing, of possible cures.

Under the conditions of tank length and maximum top speed, it is still better to use the constant-speed run techniques rather than acceleration and deceleration techniques as used in American tanks where much greater lengths and speeds are available. It is also still considered best to use steady-run methods when tests of a research nature are being made. Force measurements are now made as far as possible by generalised technique which is proving not only more economical in time than the old techniques of testing each and every speed, load and trim case, but, because of its rational nature, is much more accurate and illuminating. For research purposes the tests are usually made in zero airflow, but for an actual hull design, tests in airflow are preferred. At approximately the hump speed and upwards, it has been found possible to collapse all force measurements on the basis of draft and attitude, hence the importance of accurate measurements with draft given earlier. Below the hump speed the effect of wave-making, *i.e.*, Froude number, still makes it necessary to test according to the dynamic similarity laws, but this is also done in as rational a way as possible to enable full extrapolation to be made as and when necessary.

Finally, techniques have been developed with which to examine the mechanism of water flow over seaplane hulls in the tank. This has been done to investigate further the differences still existing between model and full-scale on the resistance measurements in particular and also the interference between forebody water wakes and afterbody. A reasonably economical test procedure will give accurately the actual wetted surface and show both the directions of water flow and the extent of turbulent and laminar boundary layers on the hull bottom. The boundary-layer conditions have been shown to line up reasonably consistently with the Reynolds number of operation, given a standard finish, and possibly more usefully an approximate technique has been developed to ensure that the hull boundary layer is turbulent, so enabling full-scale extrapolation of skin-friction resistance to be made with reasonable accuracy.

In stability testing the possibility of recording attitude and heave characteristics have demonstrated quantitatively that there is in fact a minimum threshold disturbance below which the model will stabilise itself and above which it is unstable. This critical disturbance unfortunately varies from model to model and with speed, and further work is necessary for correlation with sea conditions full-scale.

Much of the development in technique, particularly on mechanism of water flow and stability testing, is basically applicable to any form of seaplane design, but the more specific tank tests have all been applied to hulls of the more conventional length/beam ratio and beam loading. Contemporary developments to make possible a choice of length/beam ratio by use of the forebody length rather than beam to increase loading will probably raise different critical design cases, *e.g.*, drag and stability at the hump speed and directional stability at all speeds, for which further extensions of the model techniques may well prove necessary.

REFERENCES

No.	Author	Title, etc.
1	C. H. E. Warren and W. D. Tye ..	Calibration of the wavemaker in the R.A.E. Towing Tank. R.A.E. Tech. Note Aero. 1764. A.R.C. 9770. March, 1946. (Unpublished.)
2	D. I. T. P. Llewellyn-Davies, W. D. Tye and D. C. MacPhail.	The design and installation of small compressed-air turbines for testing powered dynamic models in the R.A.E. Seaplane Tank. R. & M. 2620. April, 1947.
3	G. L. Fletcher	Tank tests on a jet-propelled boat-seaplane fighter (Saunders-Roe E6/44). R. & M. 2718. January, 1946.
4	K. M. Tomaszewski, S. Raymond and G. F. Chalmers.	The airflow under the towing carriages in the R.A.E. Seaplane Tank. C.P. 38. June, 1946.
5	C. N. H. Lock	*Handbook of Aeronautics*, Vol. III. Part II (Airscrews). Pitman and Sons, Ltd.
6	A. D. Young	The aerodynamic characteristics of flaps. R. & M. 2622. February, 1947.
7	R. Smelt and H. Davies	Estimation of increase in lift due to slipstream. R. & M. 1788. February, 1937.
8	A. G. Smith and H. G. White	A review of porpoising instability. R. & M. 2852. February, 1944.
9	A. G. Smith, D. F. Wright and T. B. Owen.	Towing tank tests on a large flying boat seaplane to specification 10/46, *Princess*. Part II. R. & M. 2834. November, 1950.
10	J. A. Hamilton and R. V. Gigg ..	The full-scale hydrodynamic performance of a large four-engined flying boat at overload in calm water and swell. R. & M. 2898. August, 1952.
11	A. G. Smith and J. E. Allen	Water and air performance of seaplane hulls as affected by fairing and fineness ratio. R. & M. 2896. August, 1950.
12	A. G. Smith	Water performance of a four-engined flying boat with step fairings of lengths 3, 6 and 9 times the step depth. R. & M. 2868. April, 1941.
13	J. A. Hamilton	A full-scale investigation into the hydrodynamic behaviour of a highly faired flying boat hull. R. & M. 2899. July, 1952.
14	K. M. Tomaszewski and A. G. Smith ..	Some aspects of the flow round planing seaplane hulls or floats and improvement in step and afterbody design. M.A.E.E. Tech. Memo. 5. A.R.C. 14,376. July, 1951.
15	K. M. Tomaszewski	Hydrodynamic design of seaplane floats. C.P. 15. November, 1946.
16	D. C. MacPhail and W. D. Tye	The waves close behind a planing hull. R.A.E. Report Aero. 1992. A.R.C. 8461. November, 1944. (Unpublished.)
17	G. E. Pringle and J. D. Main-Smith ..	Visualisation of the boundary-layer transition in water. R.A.E. Tech. Note Aero. 1688. A.R.C. 9151. September, 1945. (Unpublished.)
18	E. G. Stout	Development of high-speed water-based aircraft. *J. Ae. Sci.*, Vol. 17, pp. 457 to 480. August, 1950. A.R.C. 13,320.
19	T. B. Owen and D. F. Wright	Comparative model tests of the *Princess* and *Shetland* Flying Boats in waves. R.A.E. Tech. Note Aero. 2166. A.R.C. 15,496. May, 1952. (Unpublished.)
20	A. G. Smith	An analysis of planing forces on wedges and hulls and generalised methods of test. M.A.E.E. Report. (To be published.)
21	T. B. Owen and A. G. Kurn	Towing-tank tests to determine the water drag and pitching moments on the final hull form of a large flying boat seaplane. R.A.E. Tech. Note Aero. 2159. A.R.C. 15,178. April, 1952. (Unpublished.)
22	T. B. Owen	Track levelling in the R.A.E. Seaplane Tank. R.A.E. Report Aero. 2313. A.R.C. 12,630. March, 1949. (Unpublished.)
23	T. B. Owen	Draft corrections for water surface deflection under No. 1 Carriage of the R.A.E. Seaplane Tank. C.P. 67. March, 1950.

APPENDIX I

Longitudinal Instability Characteristics

Longitudinal instability can be divided up into four types, described for convenience by the regions in which they occur.

(*a*) *Lower Limit Instability.*—This occurs at low attitude at all speeds above the hump attitude speed and depends primarily on the combination of the forebody, wing and tail characteristics. It is initiated by hydrodynamic loads on the forebody, the afterbody being clear of the water all the time, except at the hump. It usually requires no disturbance to initiate it; as the trim is decreased at constant speed the instability appears initially as a gentle pitching motion of small amplitude. As the trim is decreased further the amplitude of the oscillation increases rapidly and at higher speeds can build up till the aircraft leaves the water during each cycle, re-landing with a heavy forebody impact. The lower dotted curve in Fig. 21 shows the 2-deg amplitude limit and how the attitude and draft are related in a steady oscillation.

At the higher planing speeds the aircraft can also be unstable at trims rather above the no-disturbance limit, when given a disturbance, and a second limit can be drawn as shown by the full curve in Fig. 21. The oscillations in these cases are of large amplitude with the aircraft leaving the water, as again illustrated in the lower diagram of Fig. 21.

Lower-limit instability is present on all flying boats and it is important that the normal trim curves should be above the limit by at least 1 deg to 2 deg at the hump speed and 2 deg to 3 deg at unstick and touchdown. The trim curves can be altered:

(i) by moving the main step*

(ii) by altering the wing to keel setting

(iii) by changing the forebody deadrise, but the forebody dimensions have usually been determined already from considerations of impact and spray.

(*b*) *Upper Limit Instability.*—At high trim angles, when the aircraft is running on both main and rear step, an unstable oscillation can occur which starts as a gentle rock as the trim is increased, the amplitude increasing with further increase in trim. The upper dotted curve in Fig. 21 shows the 2-deg total amplitude limit, and also one form of the draft attitude characteristics.

Upper limit instability is not normally important during take-off, but it is advisable to have the upper limit above the maximum attitude for landing, otherwise the aircraft may be thrown off the water below its stalling speed, with a subsequent heavy impact. This is most serious in sea swells.

The upper limit can be raised, if necessary, by an increase in the forebody to afterbody keel angle, 1 deg increase in the keel-to-keel angle producing about 1 deg increase in the upper limit. Weakening the rear step, *i.e.*, reducing the planing forces on it by increase of dead-rise angle and reduction of beam, is also effective in raising the upper limit and in damping oscillations in pitch.

Such weakening will, however, also increase the hump attitude and water drag.

(*c*) *Mid-planing Instability.*—This region is approximately that corresponding to the first half of the planing region between the attitude hump and take-off. Ordinary two-step, porpoising referred to above as upper limit instability will often extend to much lower attitudes in the presence of a disturbance, particularly when the hull is highly loaded. As shown in Fig. 20, the upper and lower limits of stability may join up at the beginning and end of this region. The severity and extent also depend a lot on the order of disturbance, as illustrated in Fig. 20.

* This at the same time changes the afterbody keel to keel angle and afterbody length.

For example, in Figs. 20, 21 and 22, a record of draught against attitude at constant speed shows how, in the middle of this region, instability is only obtained with a disturbance greater than 3 deg nose down.

This mid-planing instability probably results from an interaction of the afterbody with the wake of the forebody which is changing with attitude. If this interaction is in phase with the original oscillation and of sufficient magnitude to overcome the damping, a steady oscillation will result. The speed range over which this can happen on conventional flying boat forms, *i.e.*, length/beam ratio of the order of 7 : 1 and $C_{\Delta 0} = 1{\cdot}0$, is the mid-planing range from about $0{\cdot}5$ to $0{\cdot}7$ of the take-off velocity. This instability is more probable with the highly loaded high length/beam ratio hulls, but may be reduced by a different choice of afterbody design.

Whether or not the afterbody is in contact with the wake for a sufficient time in each cycle to maintain an oscillation is dependent mainly on the load on water. An increase in the load on water by increasing the all-up weight or by a reduction of wing lift produces a deterioration in stability.

The magnitude of the force produced on the afterbody is dependent on the plan-form shape and deadrise over the aft $0{\cdot}3$ of the afterbody. A gradual increase of deadrise up to say 60 deg at the rear step reduces the impact forces and increases the time to maximum draft, so producing a damping effect on the oscillation.

This mid-planing type of instability will only occur full-scale if there is sufficient disturbance in pitch to start it. Across long swells of the appropriate length, large-amplitude pitching oscillations can build up sufficiently to start this instability when present. The instability found is of the same order as model-scale.

(*d*) *Skipping Instability.*—This normally occurs in a 5- or 10-knot band immediately before unstick or after touchdown speeds (Fig. 19) and is associated with the intermittent attachment of the forebody wake to the afterbody bottom. It often takes the form of large changes in draft, the seaplane leaving the water combined with large changes of incidence, and was originally called bounce porpoising[15] in this country. It can be the result of:

(i) inefficient separation of the water flow at the main step, usually only present with too small a discontinuity of height or angle

(ii) inefficient ventilation* of the afterbody (the more common). Full-scale research conducted in this country on such instability which describes its form and the nature of the associated water flow is given in Refs. 12 and 13.

At sufficiently high speeds the draft decreases so that the forebody wake and spray blisters leave from inside the chine at the step and under the afterbody. This tends to close the gap between the wake and the afterbody chine immediately behind the step and restrict the afterbody ventilation, and can produce suctions under the afterbody which will lead to this skipping instability.

Skipping instability is not usually important during take-off in sheltered water conditions since it seldom occurs below a speed at which the aircraft can be held, but it must be eliminated for landing as the aircraft may be thrown off the water at a speed well below a stall, with a subsequent heavy impact out of control. Even on take-offs control may be lost in the presence of a long swell or if the afterbody interference is bad under flat calm conditions.

Skipping can usually be eliminated by raising and rounding the afterbody chines in the step region as described in Ref. 9, the addition of artificial ventilation, or by a simple increase in the afterbody clearance. The first two methods are preferable, as with care they can reduce the aerodynamic drag of the hull, while the last increases it.

---

* At planing speeds the afterbody clears the forebody wake with a fairly narrow air gap (Fig. 24). It is necessary that the air should flow freely round the step and chines and down into the space between the wake and the afterbody, otherwise aerodynamic suction will develop. This airflow is known as ' afterbody ventilation ' and may be supplemented by ducts exhausting through the step fairing.

APPENDIX II

Spray and Wake Formation

The water surface rises locally in the neighbourhood of the planing surface, so that the stagnation line does not coincide with the undisturbed water surface intersection with the planing surface (Fig. 26). A thin sheet of water is apparently reflected at the stagnation line, clings to the planing bottom as far as the chines, and then leaves tangentially to the planing surface in that region. This is usually referred to as ' forward spray '. The planing bottom leaves a wake in the water which, immediately behind the step, is of the same cross-section as the planing surface, but whose walls are higher than the undisturbed water surface. In between the wake and the forward spray, and originating from the point of intersection of the stagnation line with the chine, there is a second spray formation referred to as ' main blister spray ' or simply ' main spray '. The main spray originates as a semi-cone with its apex at the intersection of the stagnation line and the chine line, its edges joining up with the edges of the wake and forward spray. The path of the main and forward spray, once clear of the planing bottom, is dependent mainly on the effect of gravity though it is also affected to some extent by the airflow. In particular, the high propeller slipstream at low speeds can lift the main spray into the propeller disc in conditions where the spray is well below the disc when the power is off, and a completely false impression of the spray clearance would be obtained without the correct slipstream.

The two different types of spray should be distinguishable in Fig. 25, which corresponds to a fairly low water speed. Fig. 27 shows the change in shape and position of the spray pattern with aircraft speed. Fig. 28 shows a convenient way of illustrating the speed and attitude range over which the spray interference takes place. This is for one condition of slipstream, weight, flap position and c.g. only, and a separate diagram is required for each condition. If, however, a typical elevator angle is selected, the speed range in which spray interference takes place can be plotted against one of either weight, flap angle or c.g. position, keeping the other two constant. Fig. 29 shows a typical plot against weight.

The factors found to affect the spray height are as follows :

(*a*) *Side spray.* The side spray leaves the planing bottom tangentially and it can therefore be controlled by altering the deadrise locally at the chine. This is usually done by adding a radius to the planing bottom as in Fig. 30, which shows a typical forebody. A suitable figure for the radius is 40 per cent to 50 per cent of the local beam. It is advisable in general to make the deadrise at the chine 5 deg to 10 deg rather than 0 deg, as with less than 5 deg the spray tends to strike the water surface close to the hull and bounce up again. A small deadrise angle also means excessively high impact pressures when full chine immersion occurs in landings, *i.e.*, in heavy landings or with narrow beam hulls and floats.

(*b*) *Main spray.* At any speed the height of the main spray is dependent mainly on the pressure on the stagnation line. For a simple vee-bottomed planing surface this is approximately $\frac{1}{2}\varrho V^2 \sin^2 \phi$ (Fig. 26), where ϱ = water density, V = forward speed, ϕ = angle of stagnation line to keel measured in plane of the bottom surface. If θ = deadrise angle and γ = keel attitude, then ϕ is given by $\tan \phi = \frac{1}{2}\pi \tan \gamma / \sin \theta$.

The spray height above its point of origin can therefore be reduced by a decrease in attitude or an increase in deadrise. However, a decrease in attitude also causes the spray origin to move forward, which may actually reduce the spray clearance if the top of the spray blister was previously behind the part of the aircraft concerned. An excessive increase of deadrise causes the aircraft to sink deeper into the water and also the local water surface to rise higher so that the spray origin relative to the aircraft increases in height, and the final result may actually be a decrease in spray clearance. This may be avoided by increasing forebody length. It can be seen that it is very difficult to predict what any local modification will do to the spray clearance,

and the possible improvements are small anyway, the characteristics being determined basically by the forebody buoyancy and arm relative to the c.g.[11]. Alternatively external devices such as spray strips or lifting devices may be used.

The design of a typical contemporary forebody of about four beams length is illustrated in Fig. 30. The keel deadrise in the step region is a compromise between low angle for drag reasons and high angle for impact load considerations with a typical value of 25 deg for sheltered water operation (no swell). This deadrise is continued constant for about 1·5 beams forward of the step and then increases more or less linearly to 70 deg at the bow. A turn-down radius of about 0·4 of the local beam is superimposed everywhere with about 5 deg deadrise at the chine.

Ref. 18 suggests how this deadrise distribution should be modified for hulls of high length/beam ratio.

The propellers, flaps and tailplane are then positioned to clear the spray envelope or are strengthened to withstand the spray loads.

If it is necessary to reduce the main spray height appreciably for some reason, it can be done with spray strips, though at the expense of some increase in drag. Figs. 30A and 30B show two types of spray strips. In Fig. 30A, the strip projects down vertically from the chine and is very effective if the right length, a certain amount of confused spray still rising along the outside of the strip and at the rear, but there being no well-defined blister. The spray strip shown in Fig. 30B is less effective, simply deflecting the spray once it has left its point of origin at the chine. It is suggested that the spray strips need only be used over a fairly short length of the chine, as the spray suppression is usually required over a fairly narrow speed range and hence a short length of travel of the spray origin along the chine line. They could probably be made retractable.

The spray strip, or spray dam, as it is referred to [19], shown in Fig. 30C is basically the same as 30A and is confirmed to be very effective. It is used inside the chine and can also be used without a chine if required.

A method of afterbody design has also been evolved which was successful in eliminating all upper limit, mid-planing and skipping instability on a float seaplane. It consists of drawing out the wake shapes, using the data of Ref. 16, at several stations on the afterbody, for a range of speeds and attitudes in the planing range, and fitting the afterbody to the wake shape. The final form of float is shown in Fig. 23 and reported in Refs. 14 and 15.

In practice it was found that two keel attitudes, 6 deg and 10 deg, and three speeds

(*a*) just above the hump speed, 0·3 of the take-off velocity

(*b*) medium planing speed, 0·6 of the take-off velocity

(*c*) high planing speed, 0·9 of the take-off velocity

were sufficient to give the internal envelope of the wake shapes at each station. Fig. 24a shows the wake at one speed and attitude and Fig. 24b the internal envelopes of the wake shapes at two stations. To ensure good ventilation, a fully streamlined step was used and the chines rounded for the first third of the afterbody, Fig. 23. It is essential for stability that, when the wake does touch the afterbody, it should be at the keel before the chine, and the afterbody above the chine should always be clear of the wake.

Since the purpose of the afterbody is to control the static floating angle, and the attitude up to the hump speed, it is not possible to design the afterbody completely in this way. Some adjustment of the plan-form or keel to keel angle may be required to obtain suitable static or hump attitudes, or with high length/beam ratios, increase in afterbody length.

TABLE 1

Details of Compressed-Air Turbines

Turbine	Mk. 1	Mk. 2A	Mk. 2B	Mk. 3A	Mk. 3B
Type	Pelton wheel	contra-rotating unit Pelton wheel	Pelton wheel	4-stage axial flow	3-stage axial flow
Height (in.)	2·74	4·58	2·48	2·53	2·16
Breadth (in.)	2·22	2·76	2·22	2·16	2·16
Overall length (in.)	5·00	6·50	4·80	7·70	4·85
Weight* (lb)	0·44	0·91	0·33	0·72	0·31
Design r.p.m.	40,000	43,000	25,000	40,000	8,000
Reduction gear ratio as constructed	8·56 : 1	10·15 : 1	5·25 : 1	25·6 : 1	None
Maximum power (h.p.)	0·71	1·16	0·37	1·79	0·40
Air pressure at maximum power (lb/sq in.)	29·0	13·0	14·5	22·5	14·0
Air consumption at maximum power (cubic ft/minute of free air)	50·0	108·0	46·0	83·0	68·0
Maximum overall adiabatic efficiency (per cent)	20	22	16	37	17·5

* Includes weight of reduction gearing.

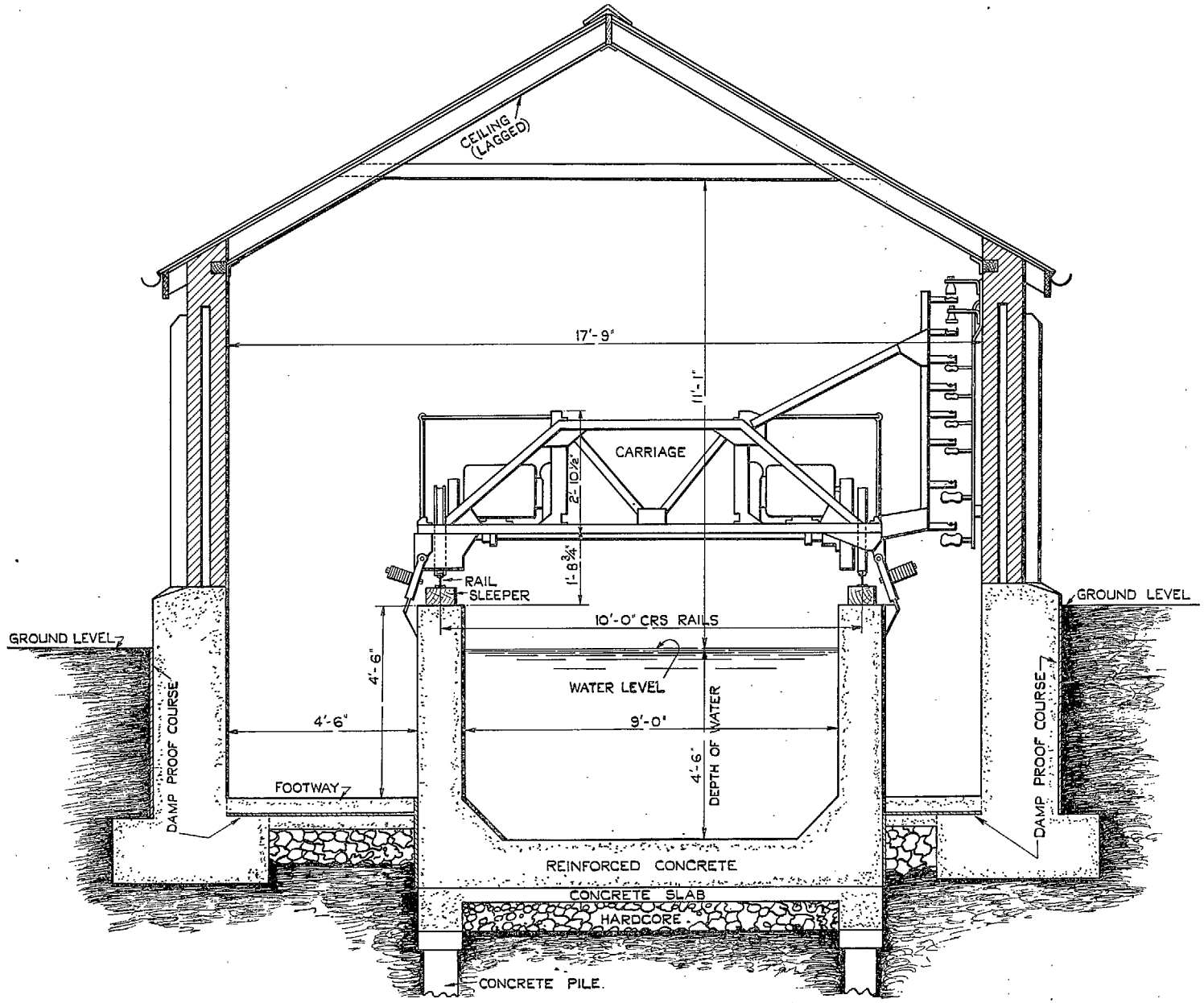

FIG. 1. Cross-section of R.A.E. Seaplane Tank (looking west).

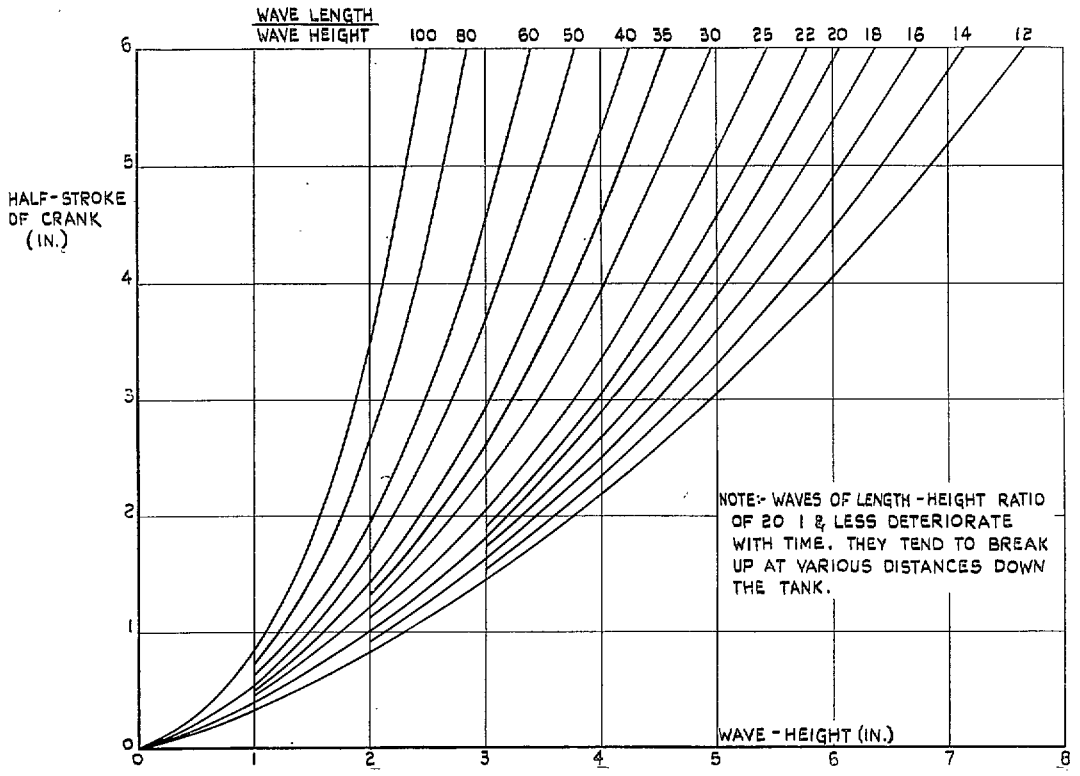

FIG. 2. Calibration of wavemaker. Chart to determine half-stroke of crank.

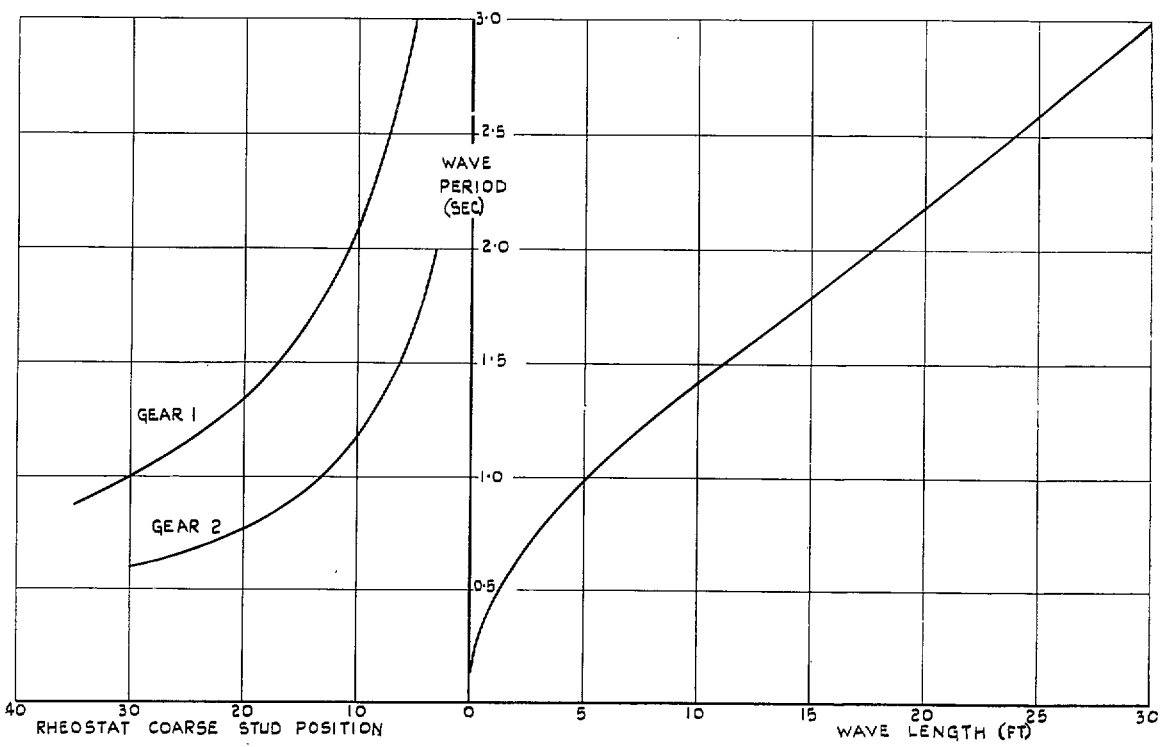

FIG. 3. Calibration of wavemaker. Chart to determine wave period and rheostat coarse-stud position.

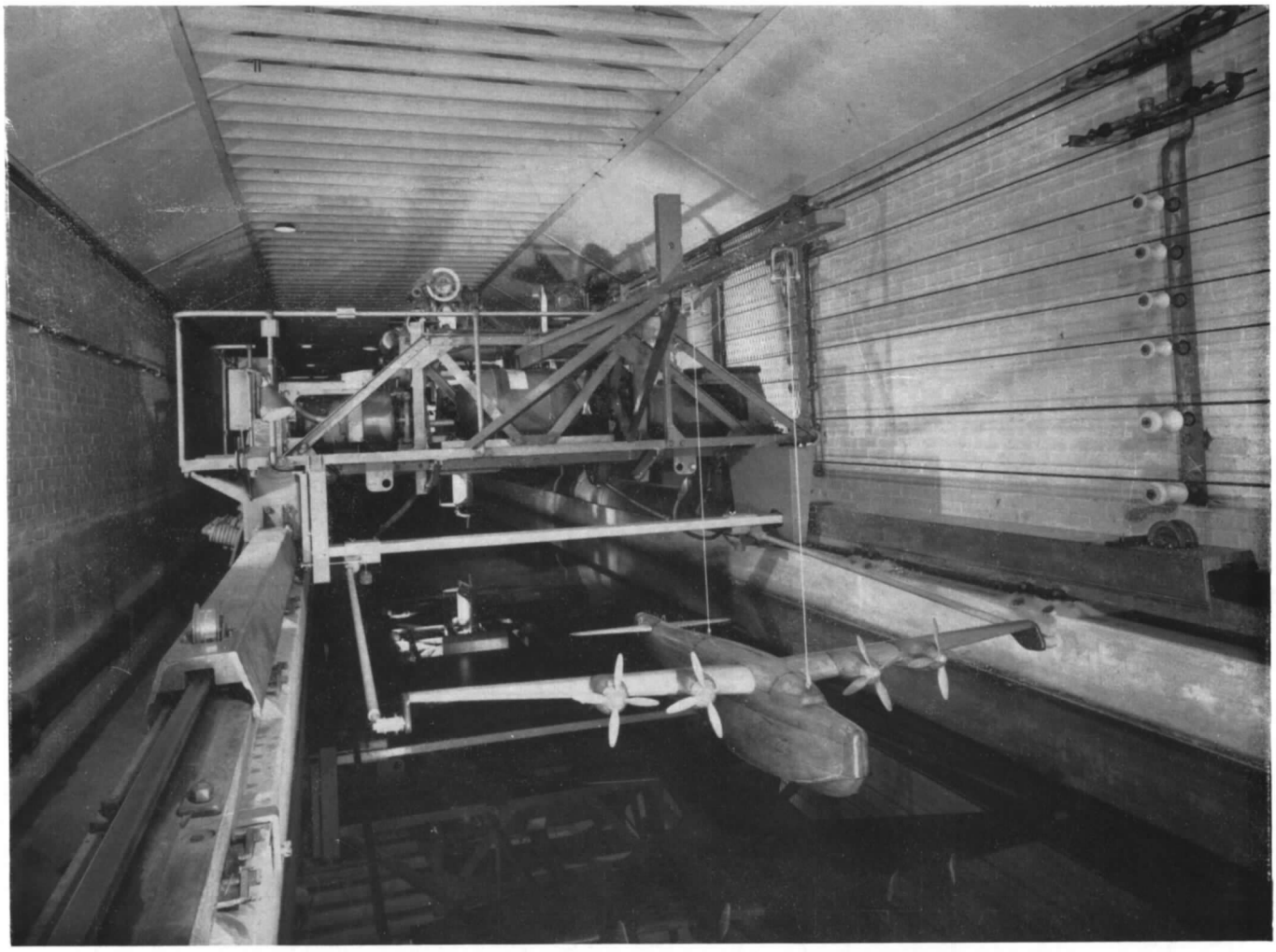

FIG. 4. Rig for dynamic model longitudinal stability, trim and spray tests (No. 1 Carriage).

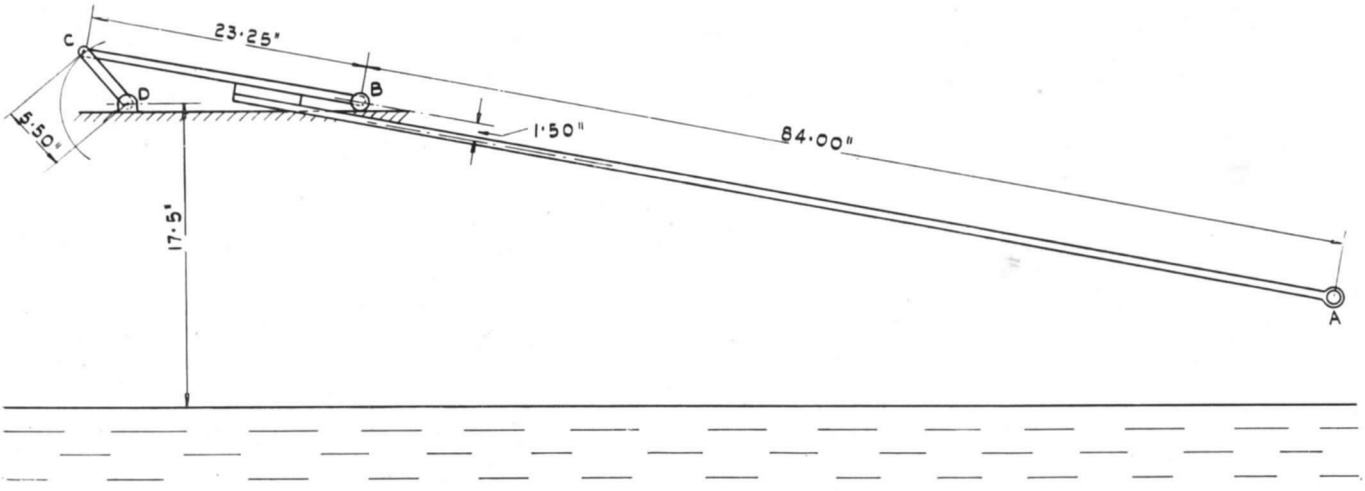

FIG. 5. Straight line linkage for towing arms.

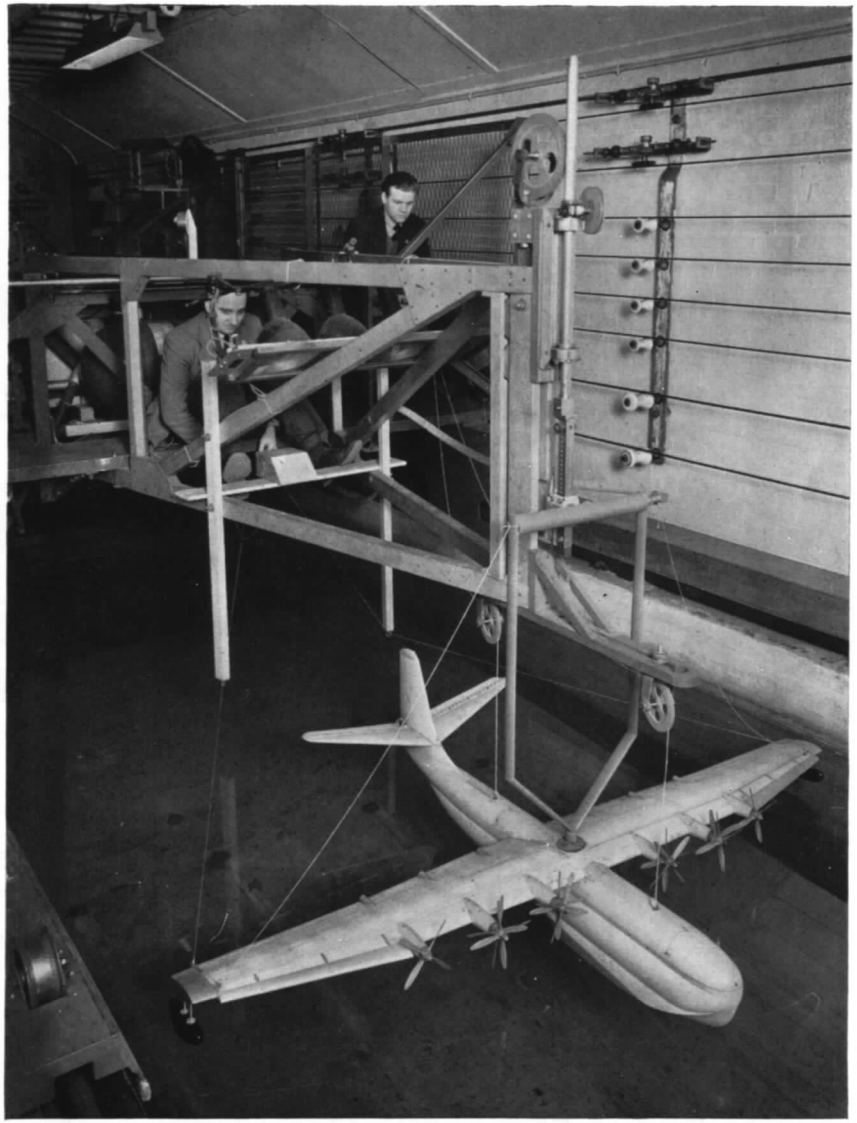

FIG. 6. Rig for directional stability tests (No. 1 Carriage).

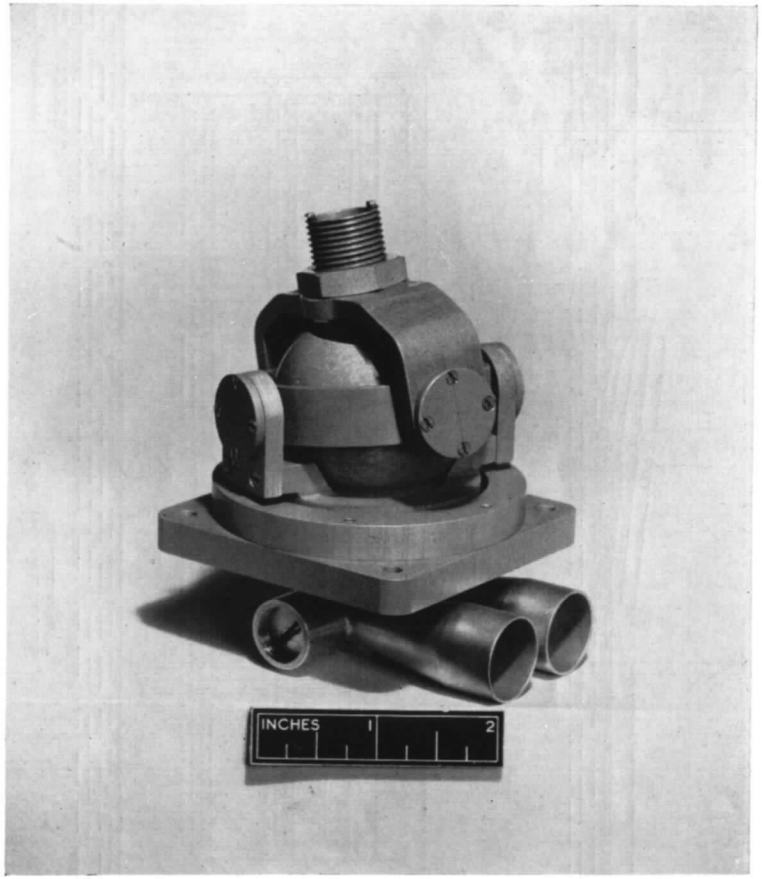

FIG. 7. Combined universal joint and air connection for directional stability tests.

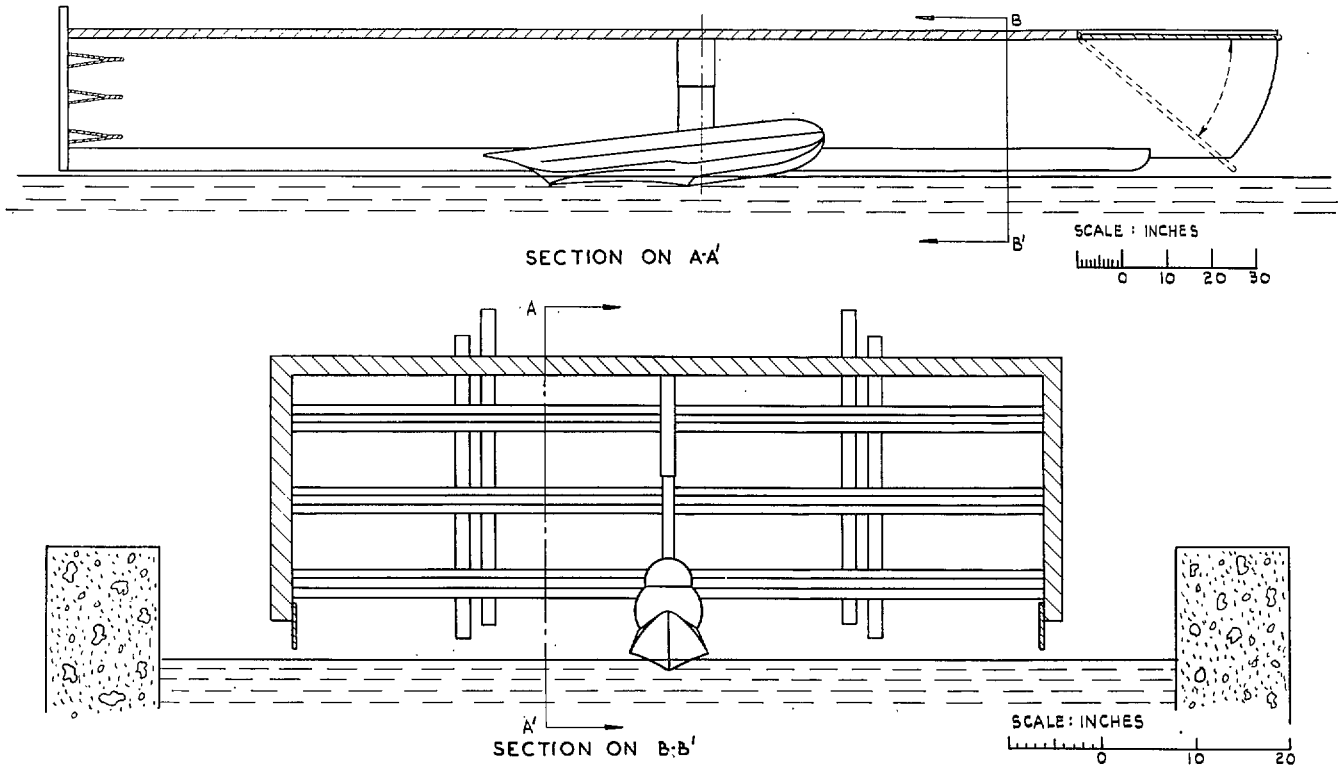

FIG. 8. ' Wind tunnel ' on No. 2 Carriage.

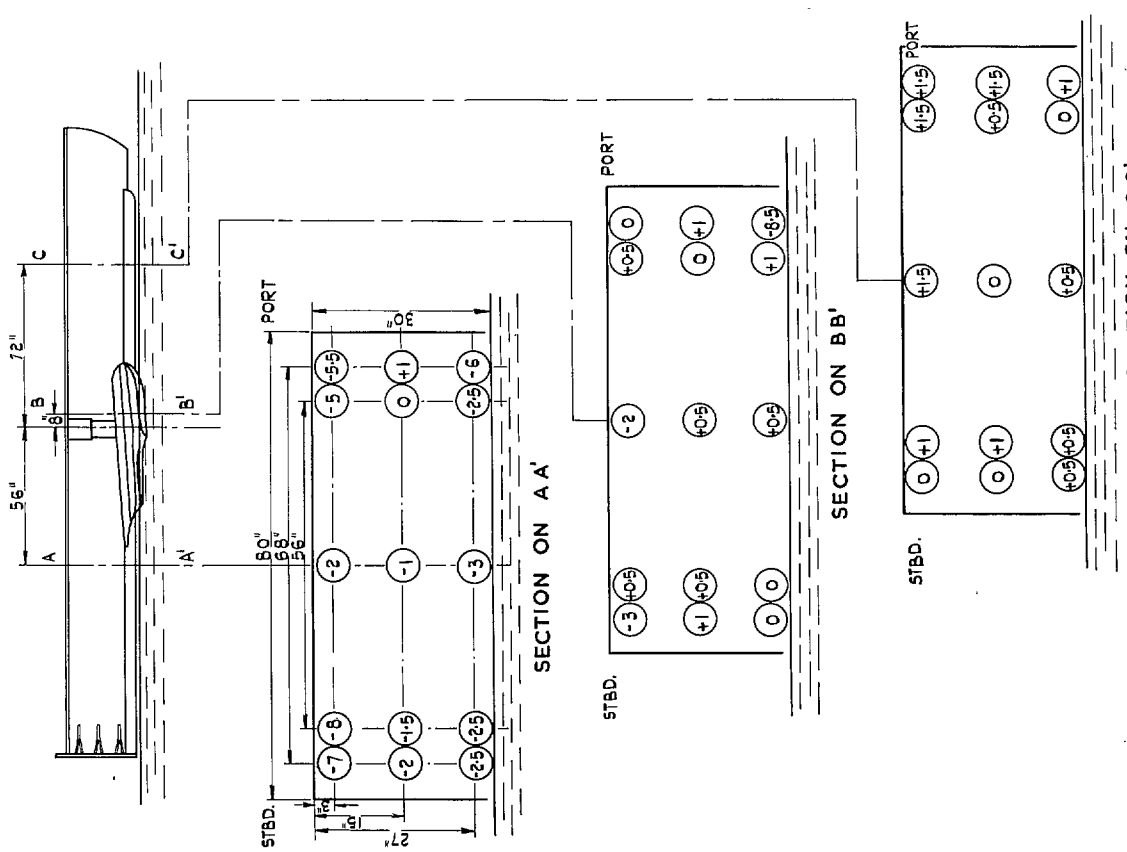

FIG. 9. Air velocity distribution in ' wind tunnel '. No. 2 Carriage. Figures in circles show velocity error at that point as a percentage of the carriage speed.

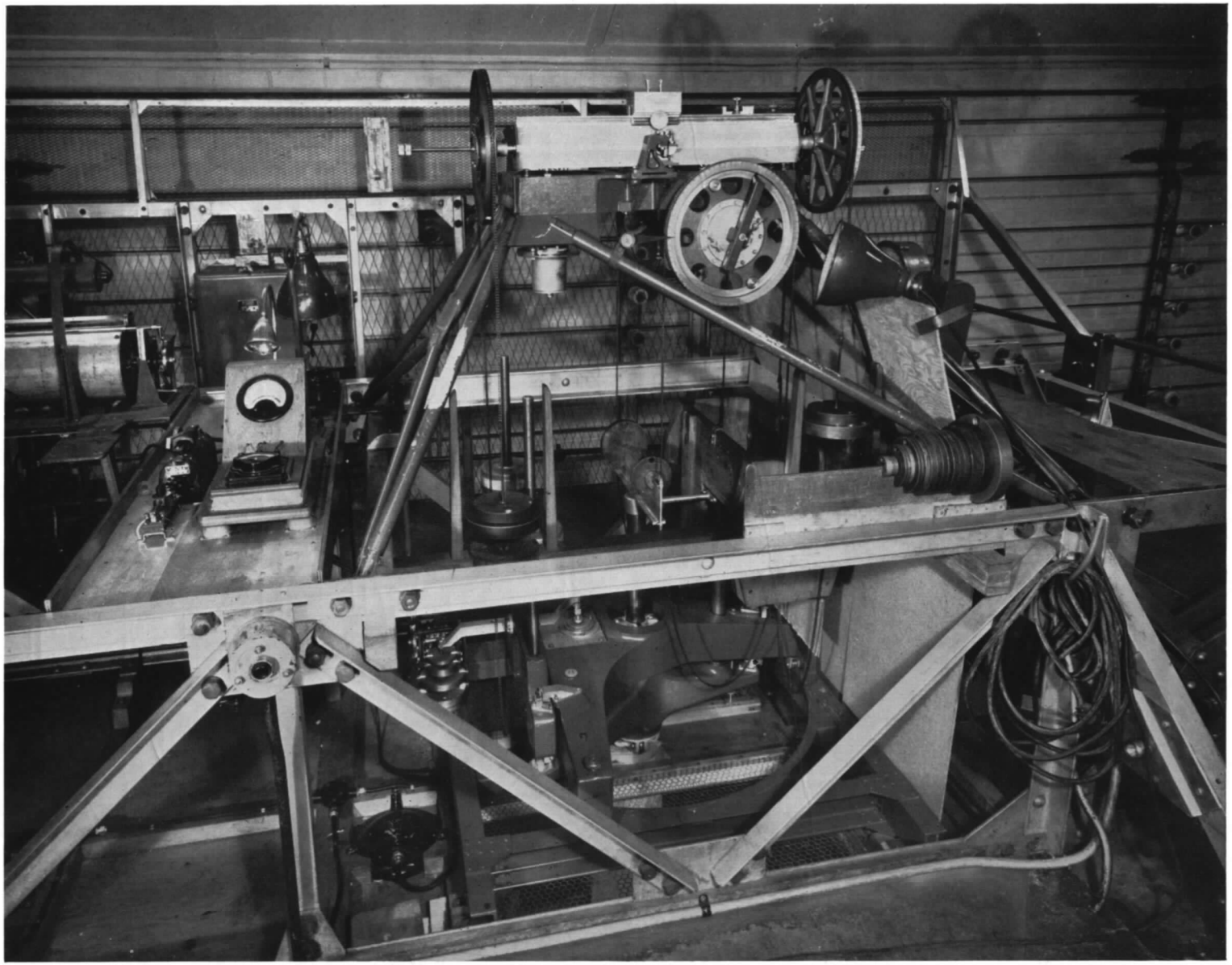

FIG. 10. Drag and pitching-moment balance, No. 2 Carriage.

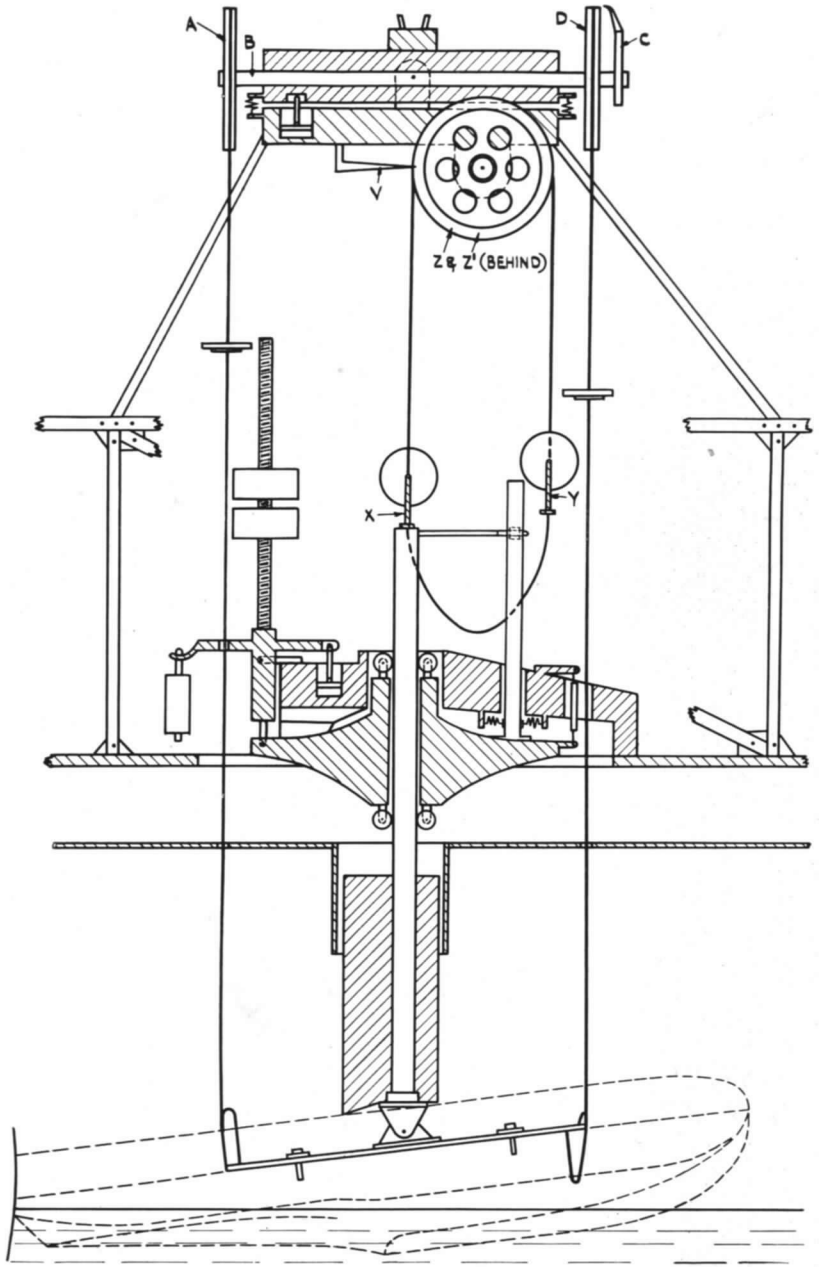

FIG. 11. Diagram of balance operation, No. 2 Carriage.

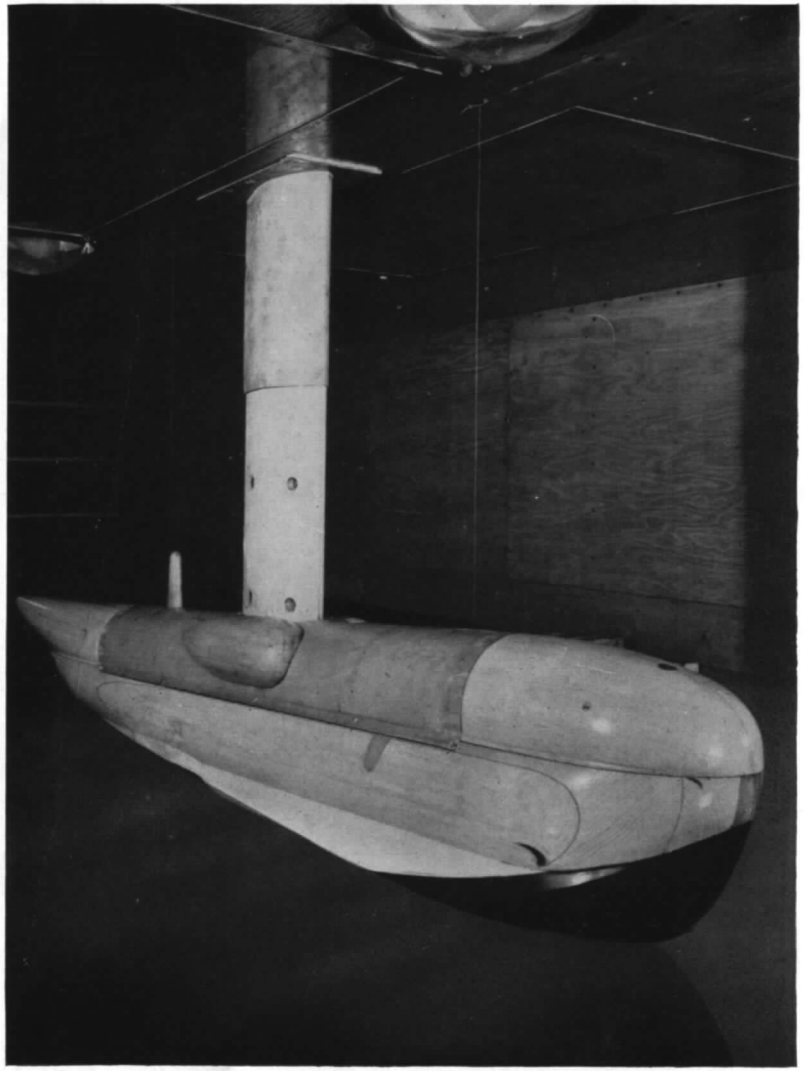

FIG. 12. Model on balance, No. 2 Carriage.

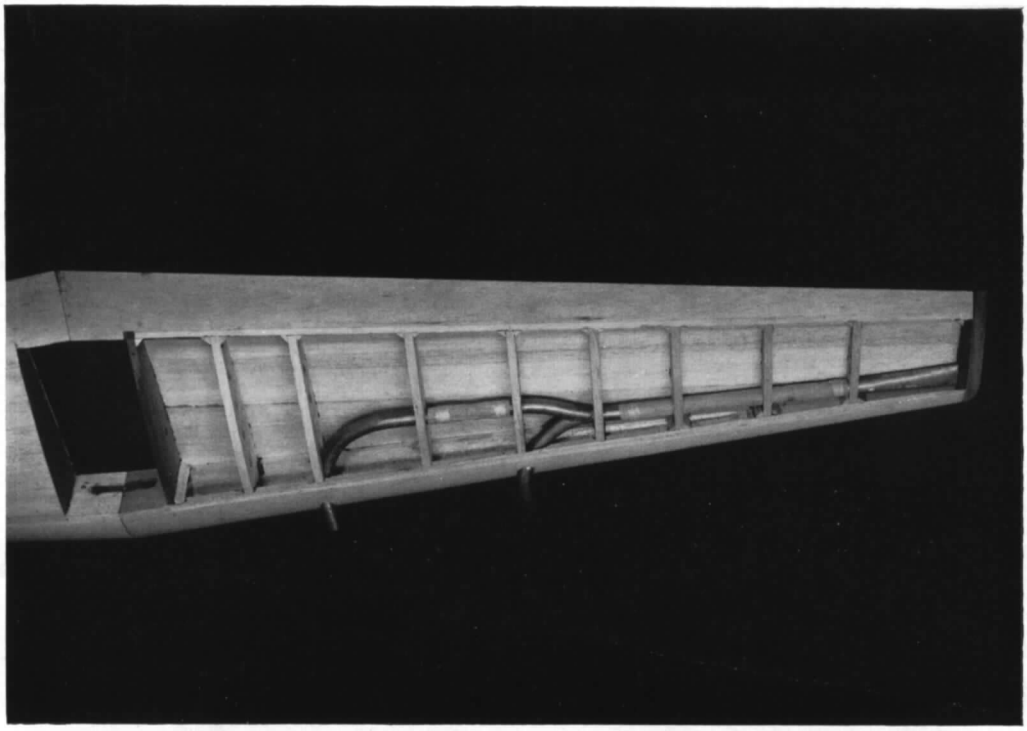

FIG. 13a.

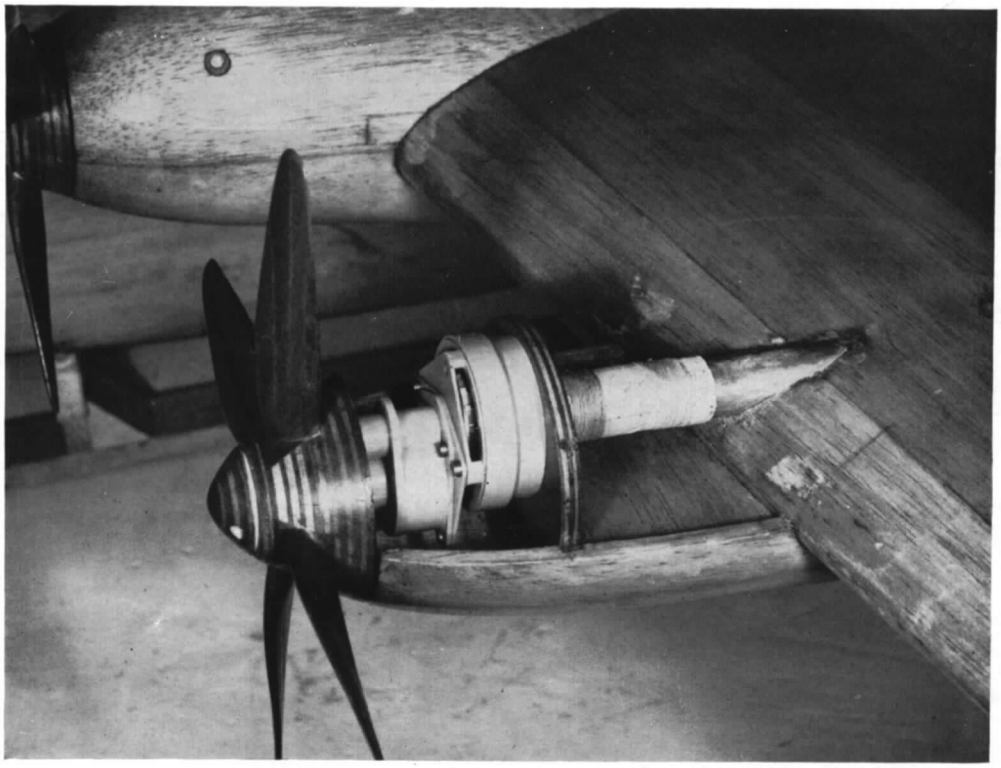

FIG. 13b.

FIGS. 13a and 13b. Dynamic models for longitudinal stability, trim and spray tests.

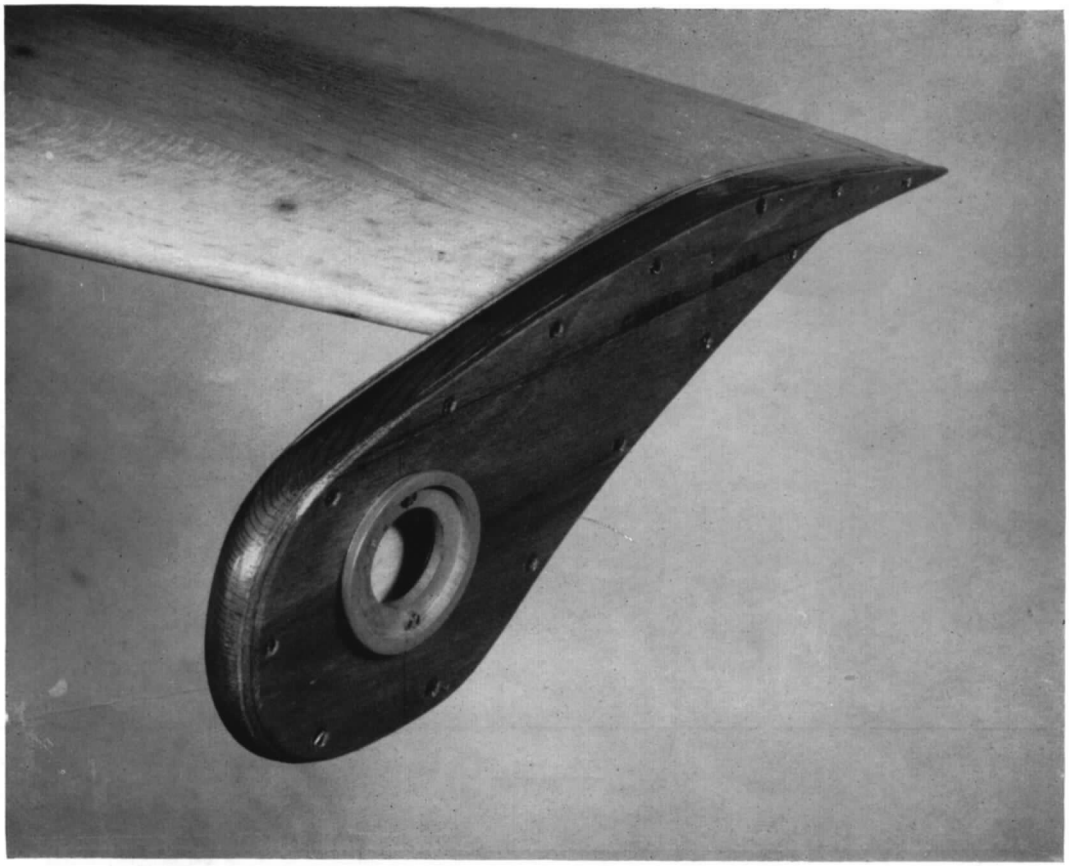

FIG. 14a.

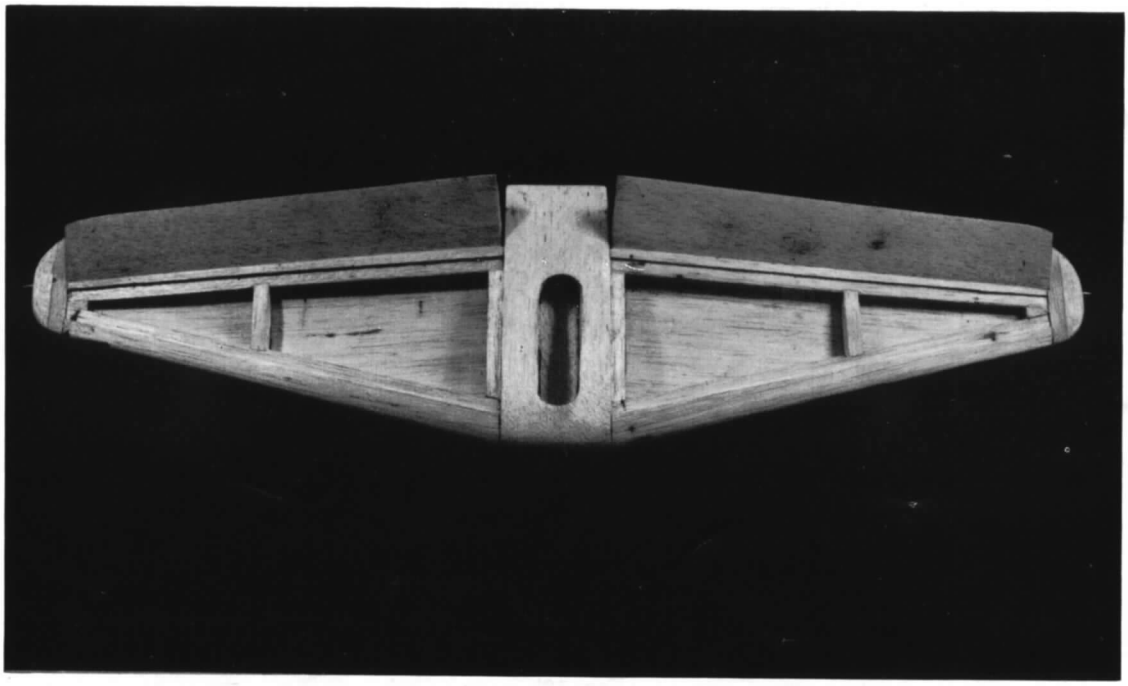

FIG. 14b.

FIGS. 14a and 14b. Dynamic models for longitudinal stability, trim and spray tests.

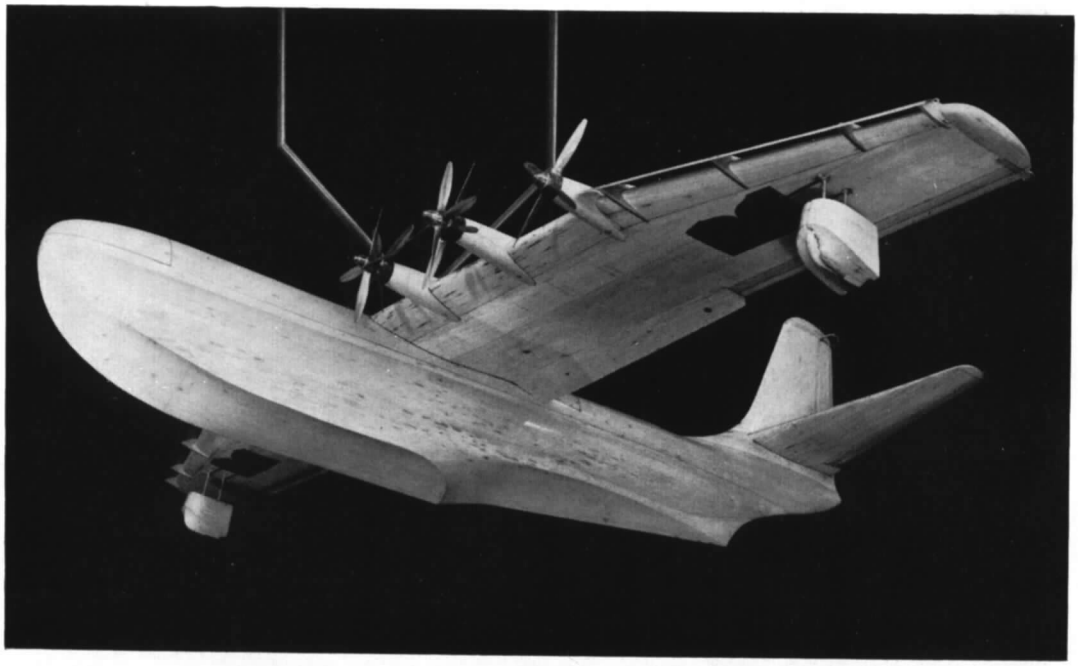

FIG. 15a.

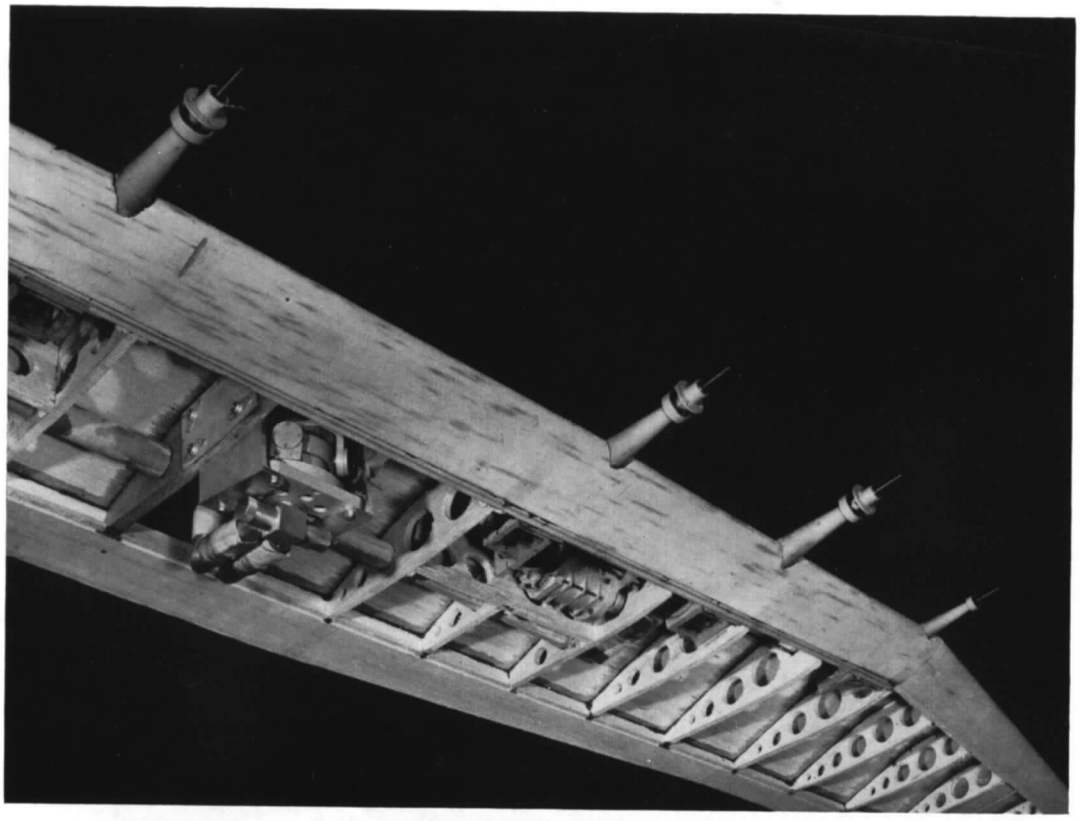

FIG. 15b.

FIGS. 15a and 15b. Dynamic model for directional stability tests.

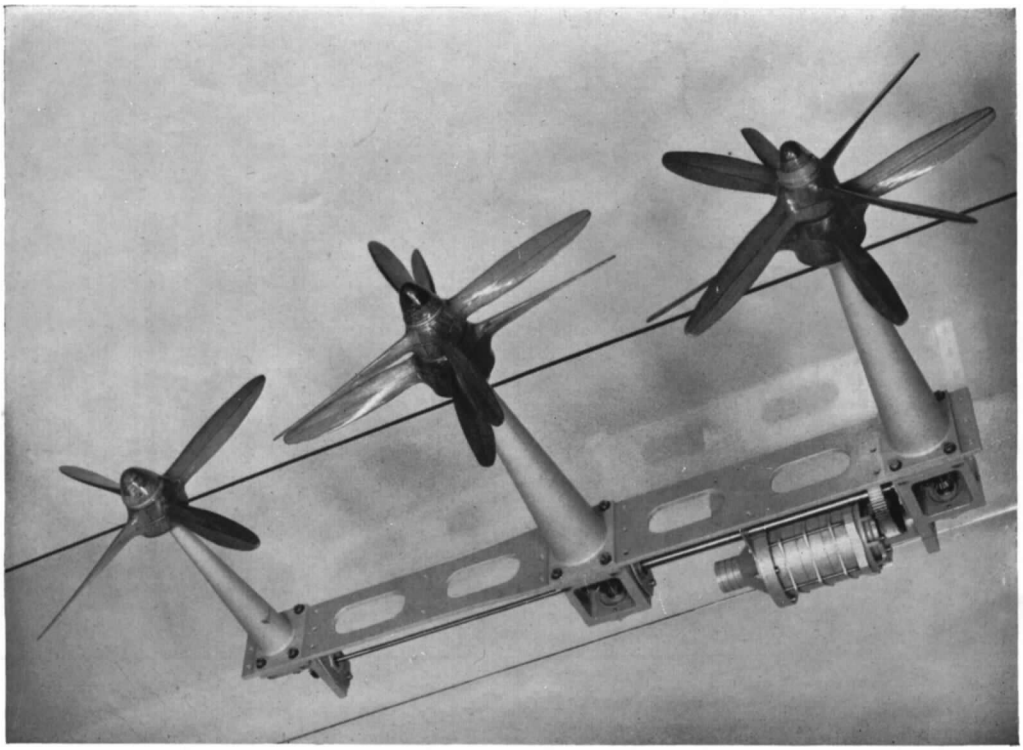

FIG. 16a.

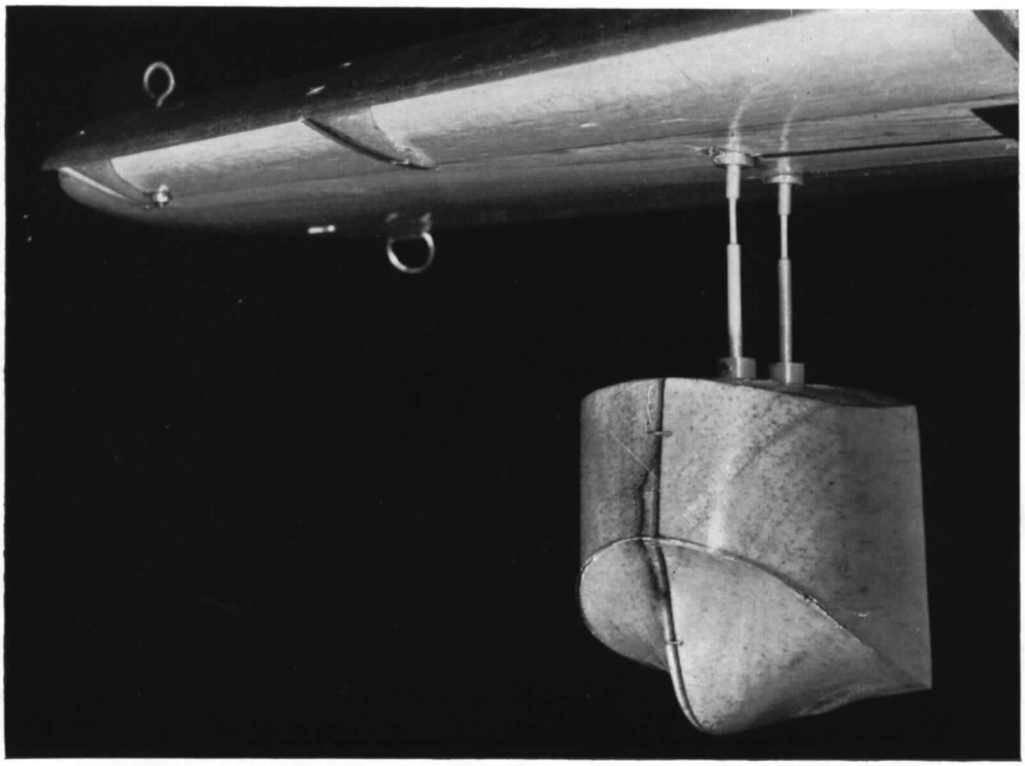

FIG. 16b.

FIGS. 16a and 16b. Dynamic model for directional stability tests.

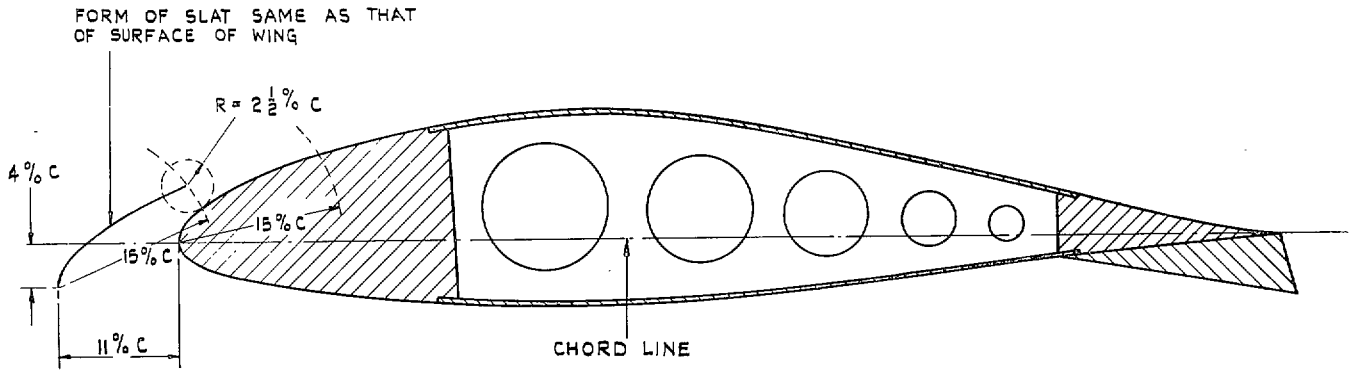

FIG. 17. Design of slat and flap for dynamic model.

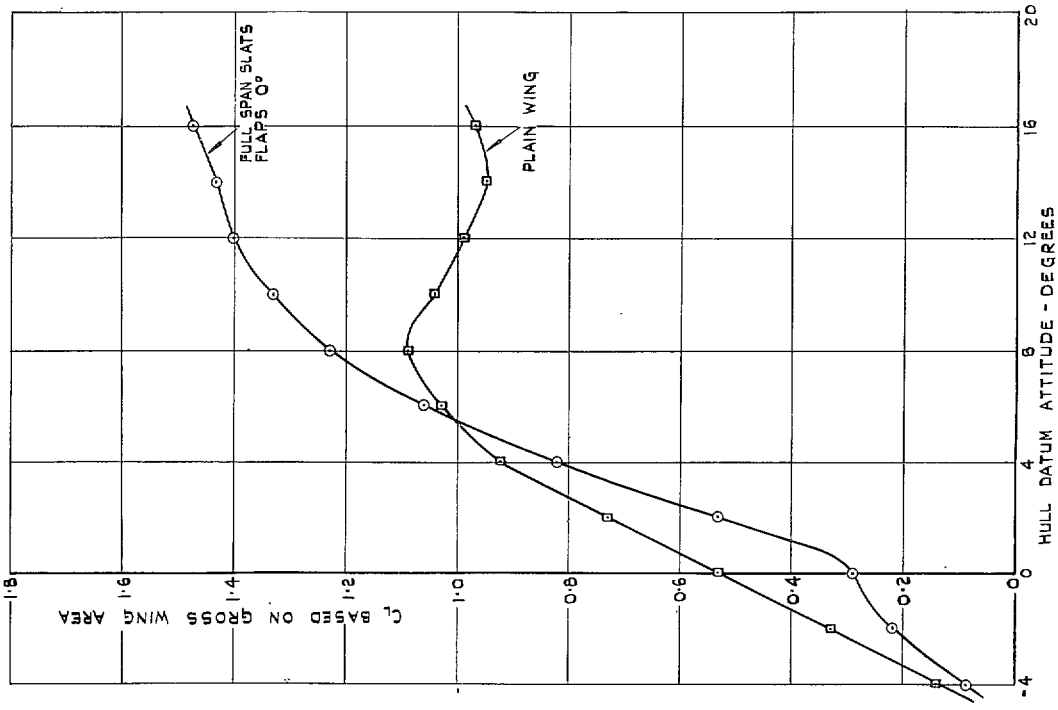

FIG. 18. Model lift characteristics. Complete model, no propellers.

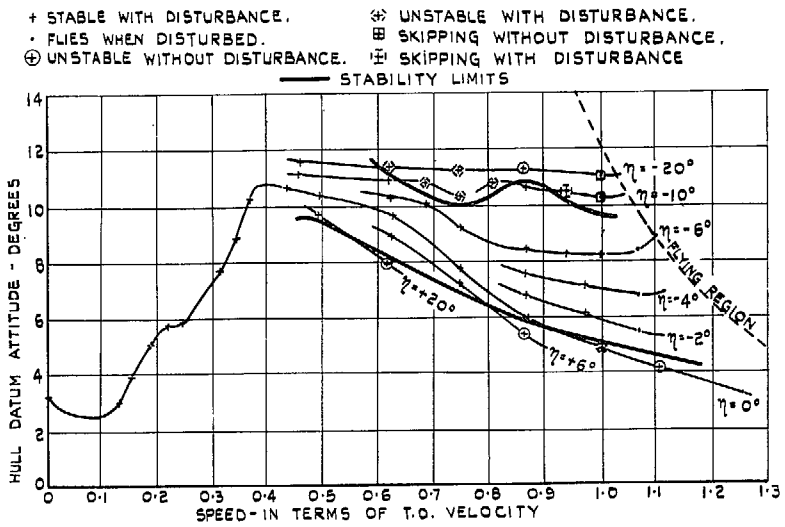

FIG. 19. Typical longitudinal stability and trim diagram at normal all-up weight. Hull length : beam ratio = 7.

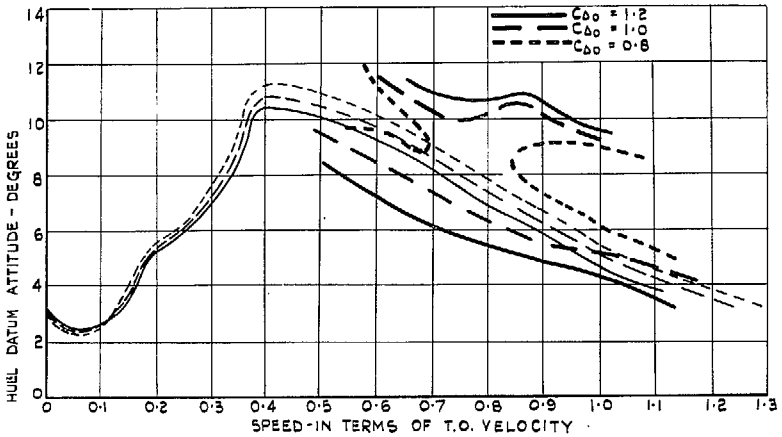

FIG. 20. Effect of weight on stability limits and trim. Trim lines $\eta = 0$ deg. Hull length : beam ratio = 7.

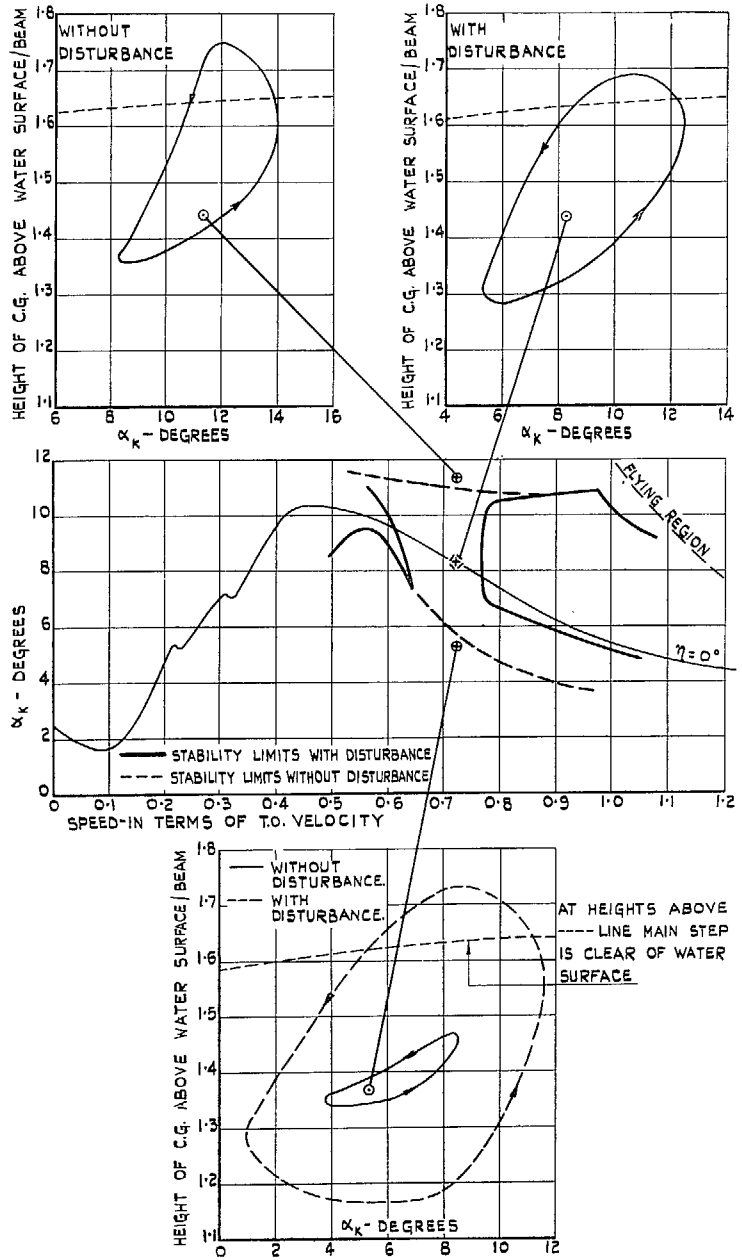

FIG. 21. Types of longitudinal instability. (Overload condition.)

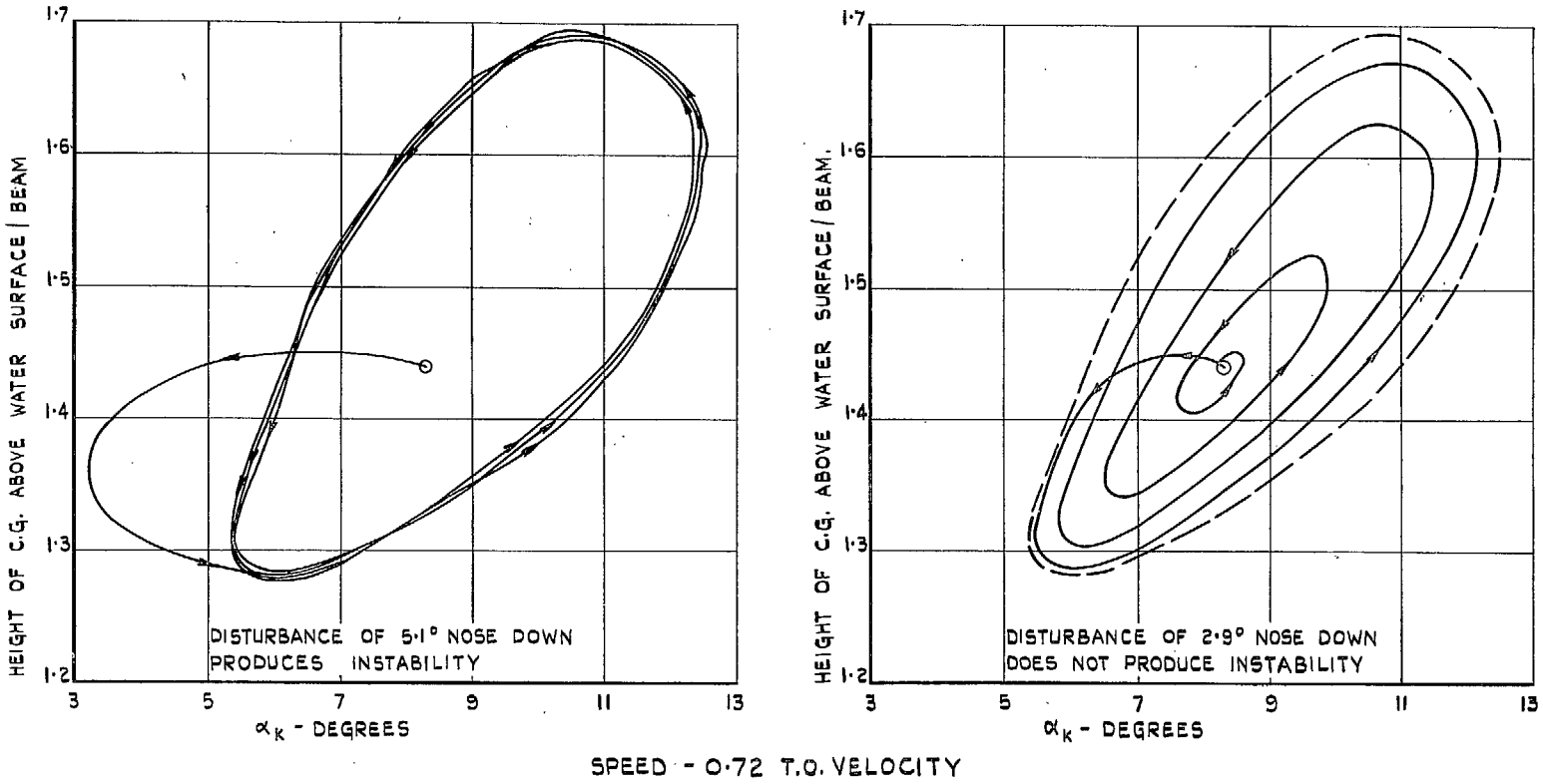

FIG. 22. Effect of magnitude of applied disturbance on mid-planing longitudinal instability (Appendix I).

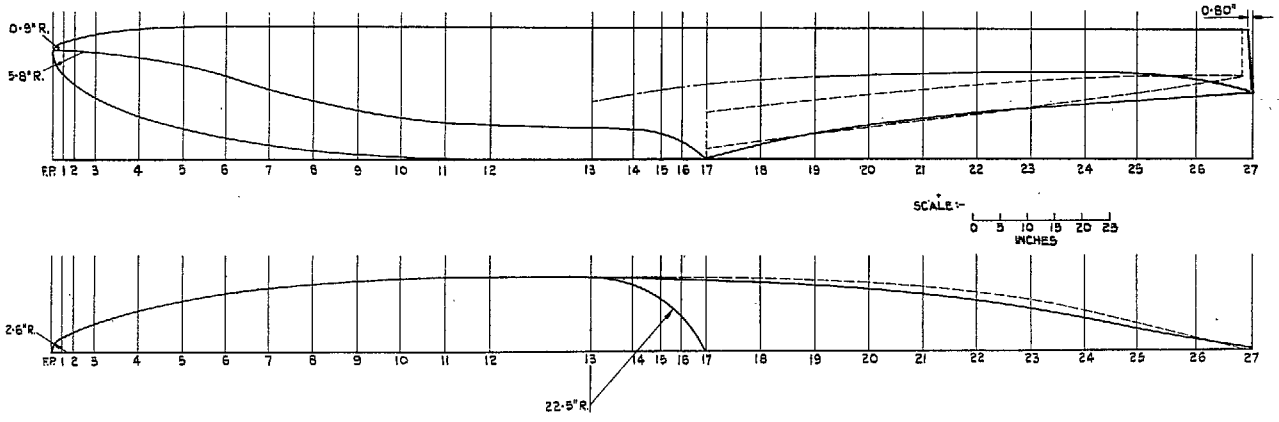

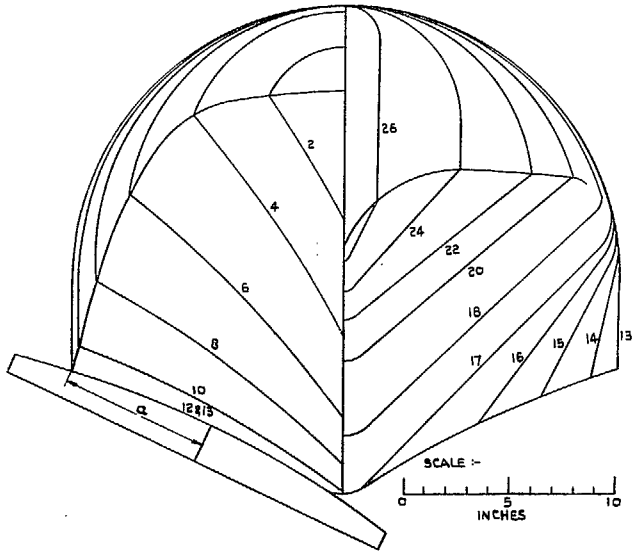

STATION No	F.P.	1	2	3	4	5	6	7	8	9	10	11	12	13	14	15	16	17	18	19	20	21	22	23	24	25	26	27
DISTANCE FROM F.P.	0·00	1·95	3·90	7·80	15·60	23·40	31·20	39·00	46·80	54·60	62·40	70·20	78·00	96·00	103·50	108·50	112·00	116·50	126·30	136·10	145·90	155·70	165·50	175·30	185·10	194·90	204·70	214·50
KEEL HEIGHT	19·15	14·85	13·05	12·65	7·45	5·25	3·55	2·25	1·25	0·55	0·05	0·00	→				0·00	2·70	4·85	6·20	7·30	8·20	8·90	9·60	10·30	11·00	11·70	
BODY CENTRE HEIGHT	19·15	17·75	17·15	16·40	15·10	13·95	12·80	11·95	11·30	10·80	10·50	10·25	10·20	→			10·20	10·25	10·50	11·10	11·95	13·00	14·25	15·90	17·70	19·60	21·55	23·20
BODY RADIUS	0·00	2·85	4·05	5·65	7·80	9·25	10·40	11·25	11·90	12·40	12·70	12·95	13·00	→			13·00	12·95	12·70	12·10	11·25	10·20	8·95	7·30	5·50	3·60	1·65	0·00
FOREBODY CHINE HEIGHT	19·15	19·05	18·95	18·75	18·05	16·65	14·45	12·25	10·15	8·45	7·00	6·15	5·85	5·65	5·45	4·62	3·31	0·00	—	—	—	—	—	—	—	—	—	—
AFTERBODY CHINE HEIGHT	—	—	—	—	—	—	—	—	—	—	—	—	—	** 10·20	** 11·25	** 11·90	** 12·50	** 12·80	** 13·90	14·65	15·00	15·10	15·20	15·30	15·40	15·20	14·10	11·70
FOREBODY CHINE HALF BREADTH	0·00	2·52	3·64	5·12	7·24	8·82	10·28	11·25	11·90	12·40	12·70	12·95	13·00	13·00	11·70	9·30	6·40	0·00	—	—	—	—	—	—	—	—	—	—
AFTERBODY CHINE HALF BREADTH	—	—	—	—	—	—	—	—	—	—	—	—	—	*** 13·00	*** 12·90	*** 12·80	*** 12·70	*** 12·60	*** 12·20	11·50	10·65	9·90	8·90	7·30	5·50	3·60	1·65	0·00
a*	0·00	1·55	3·60	4·95	6·65	7·35	7·60	7·55	7·50	7·40	7·25	7·25	7·25	7·25	a=7·25, MEASURED FROM CHINE PRODUCED TO HT. OF 5·65 & HALF BREADTH 13·00					—	—	—	—	—	—	—	—	—
KEEL RADIUS	—	—	—	—	—	—	—	—	—	—	—	1·25	1·80	→			1·80	1·75	1·60	1·40	1·20	1·00	0·80	0·60	0·40	0·20	0·00	
CHINE FAIRING RADIUS	—	—	—	—	—	—	—	—	—	—	—	—	*	2·60	2·60	2·40	2·00	1·75	0·70	0·00	—	—	—	—	—	—	—	—

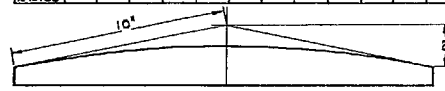

PARABOLIC TEMPLATE FOR FOREBODY BOTTOM

* DISTANCE FROM CHINE TO AXIS OF SYMMETRY OF PARABOLA.
** DISTANCE FROM DATUM LINE TO CENTRE OF CHINE FAIRING RADIUS.
*** DISTANCE FROM ℄ TO CHINE FAIRING RADIUS, MEASURED THROUGH C.F.R. CENTRE.

NOTE :- ALL DIMENSIONS IN INCHES

FIG. 23. Offsets for R.A.E. floats.

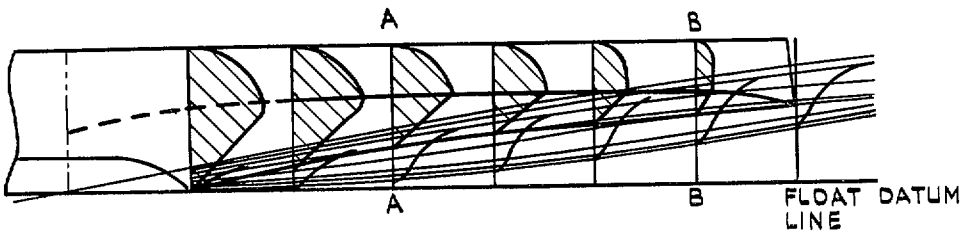

FIG. 24a. Wake shape at one speed and attitude.

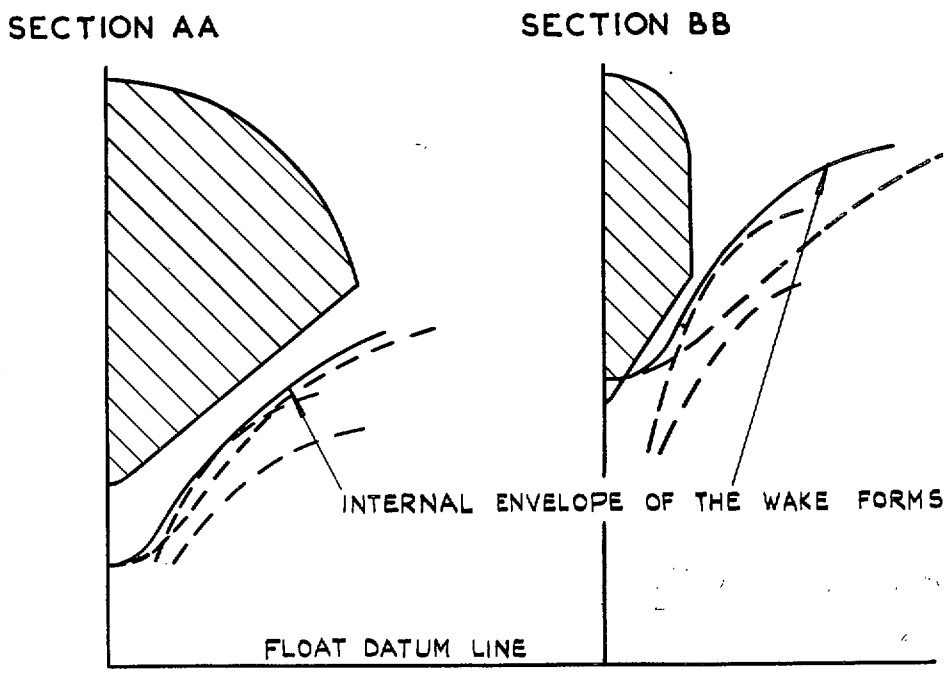

FIG. 24b. Internal envelopes of wake shapes at two afterbody stations.

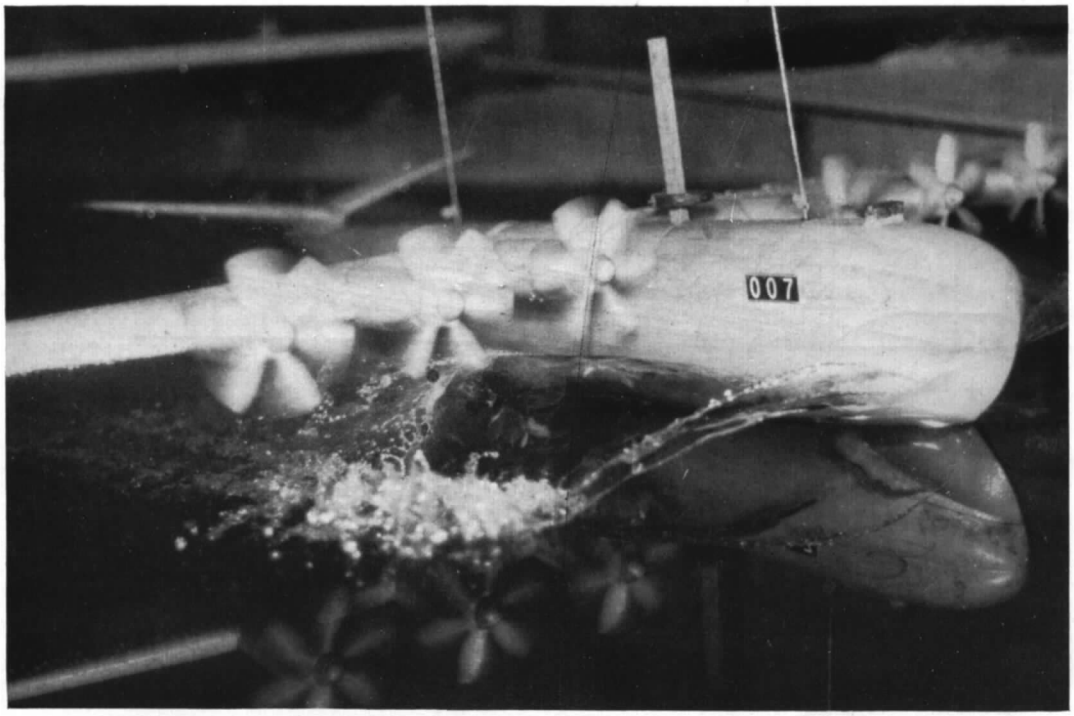

FIG. 25a. Electronic flash 1/3000th sec exposure.

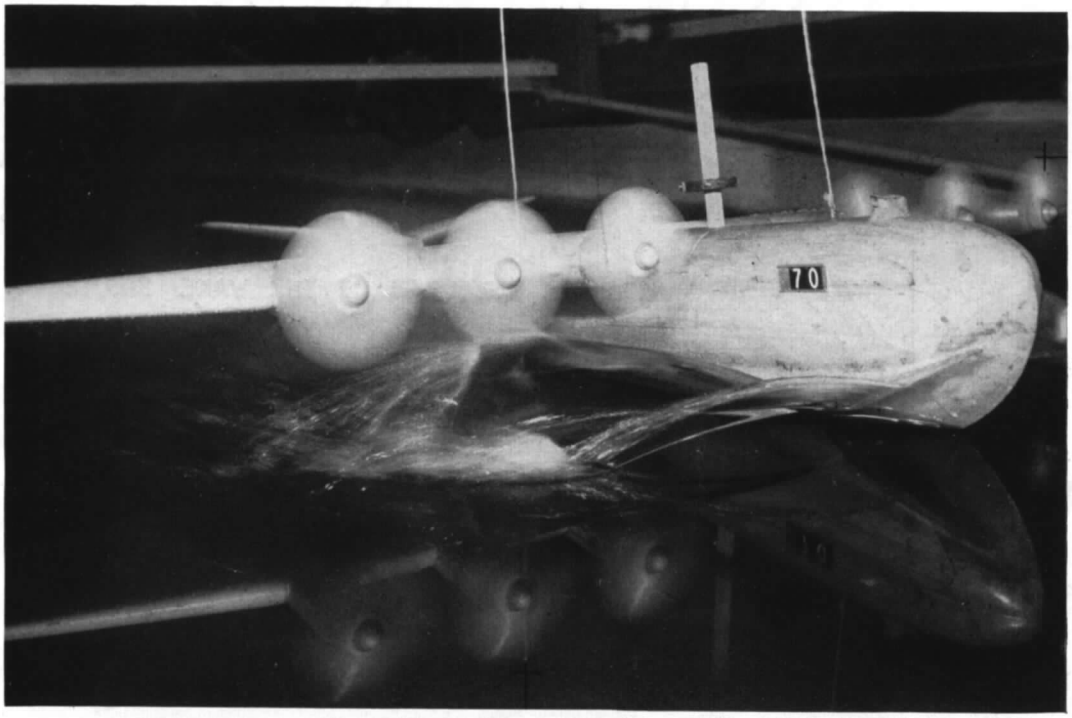

FIG. 25b. Flash bulb 1/30th sec exposure.

FIG. 25. Effect of exposure time on the appearance of spray formation. Aircraft speed = 0·2 take-off velocity.

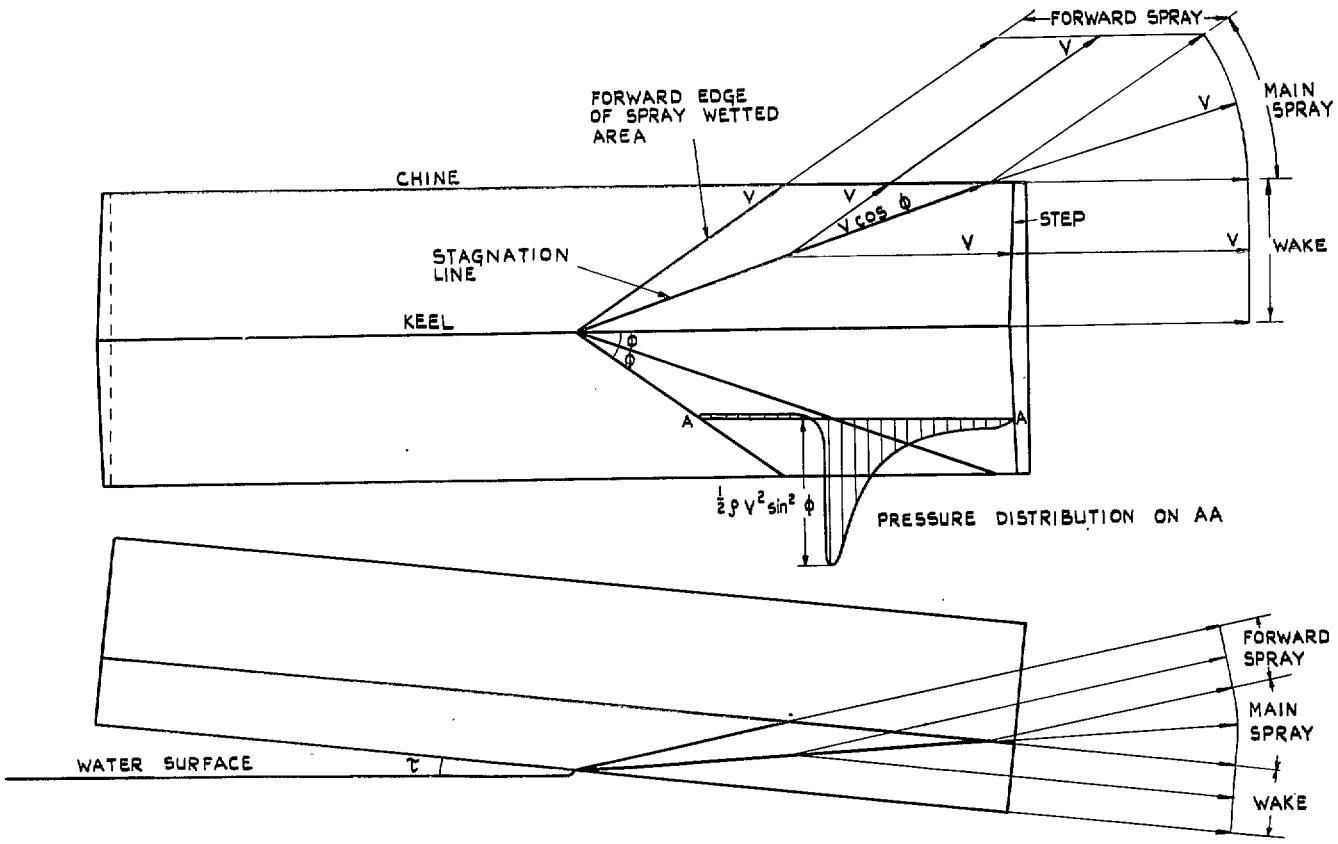

FIG. 26. Spray formation and wetted surfaces on a vee-bottomed planing surface.

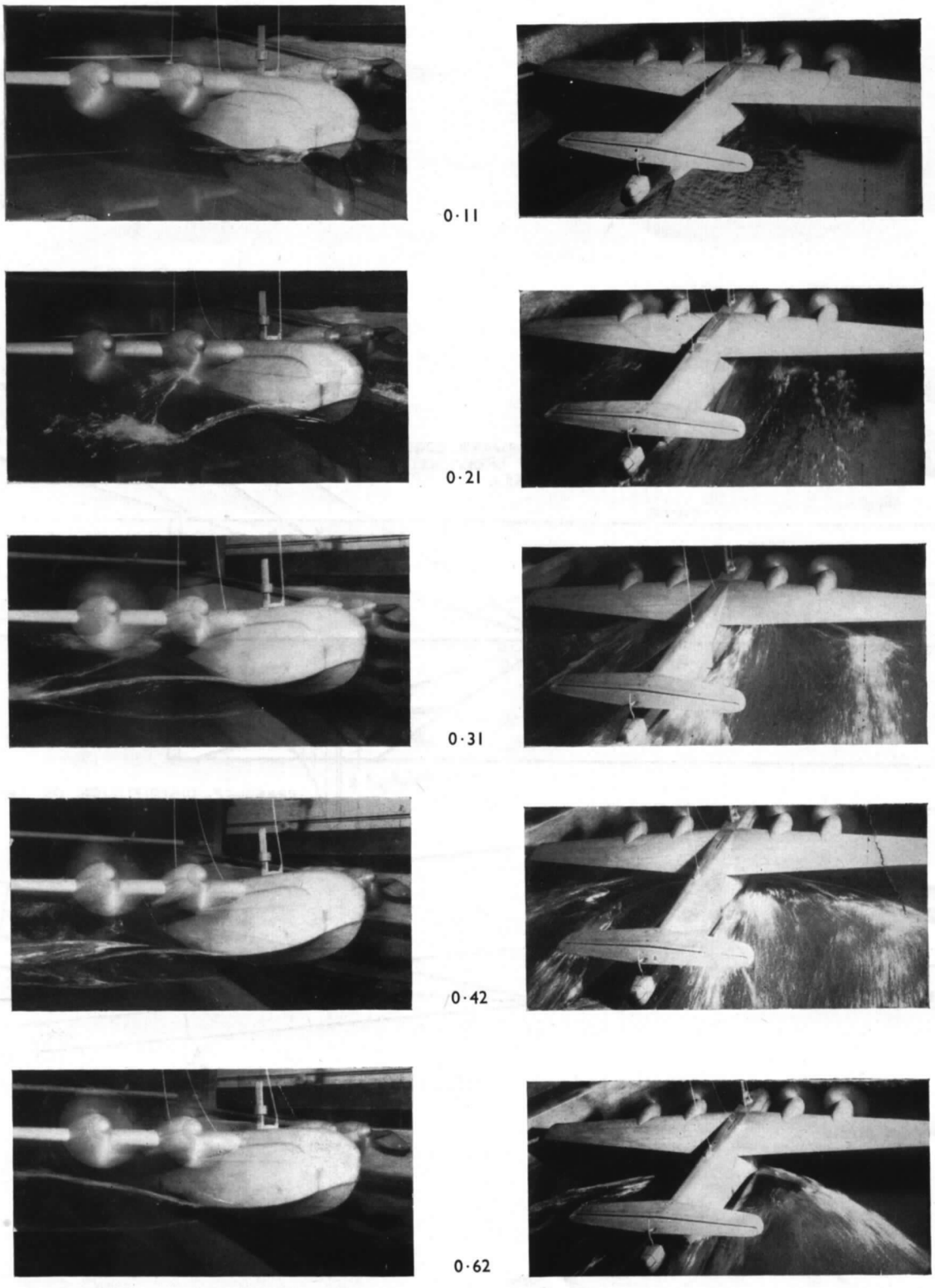

Speed—in terms of take-off velocity.

FIG. 27. Effect of speed on spray formation at overload.

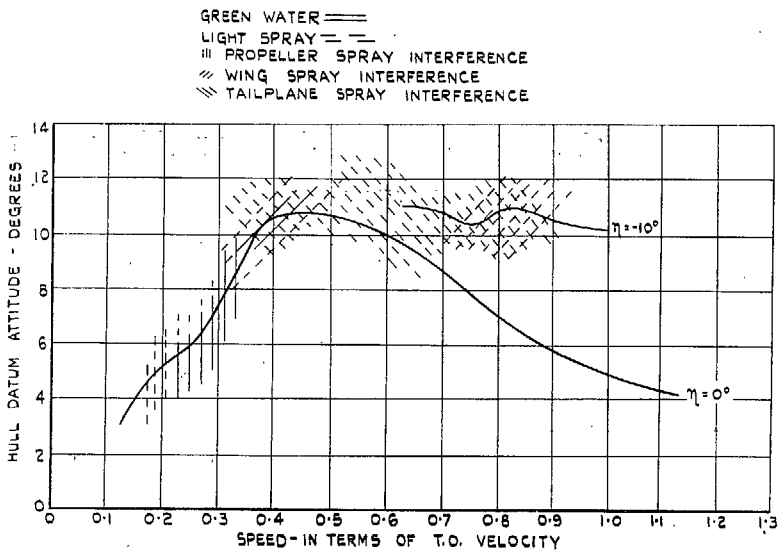

FIG. 28. Spray interference at normal all-up weight.

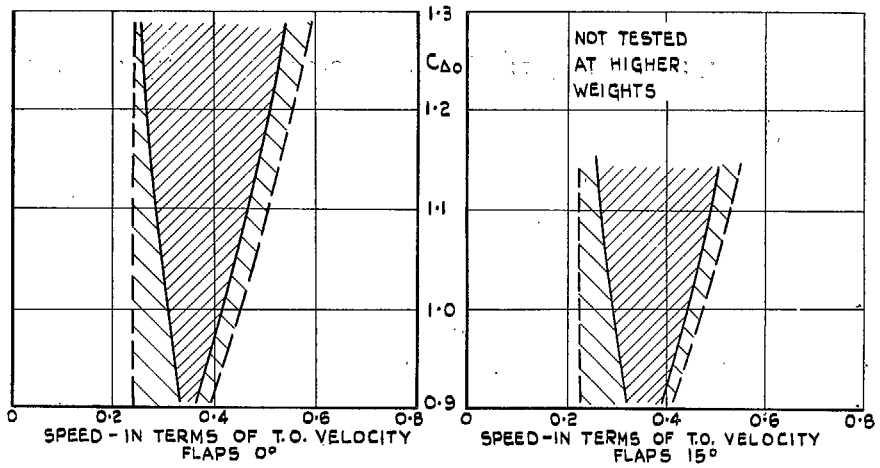

FIG. 29b. Wing interference.

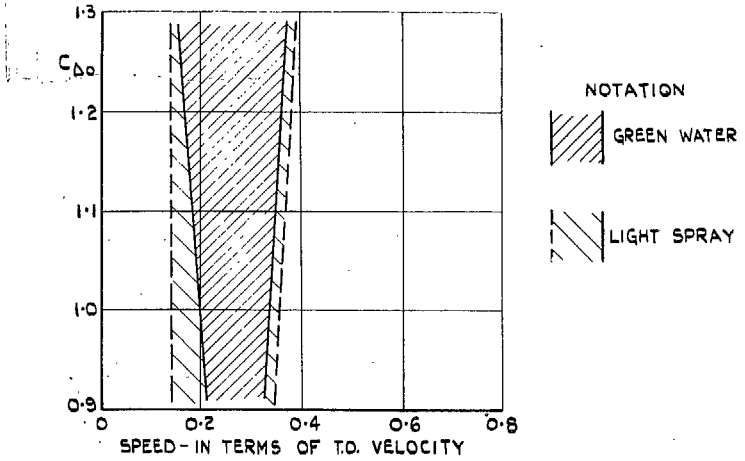

FIG. 29a. Propeller interference. Flaps 0 deg and 15 deg.

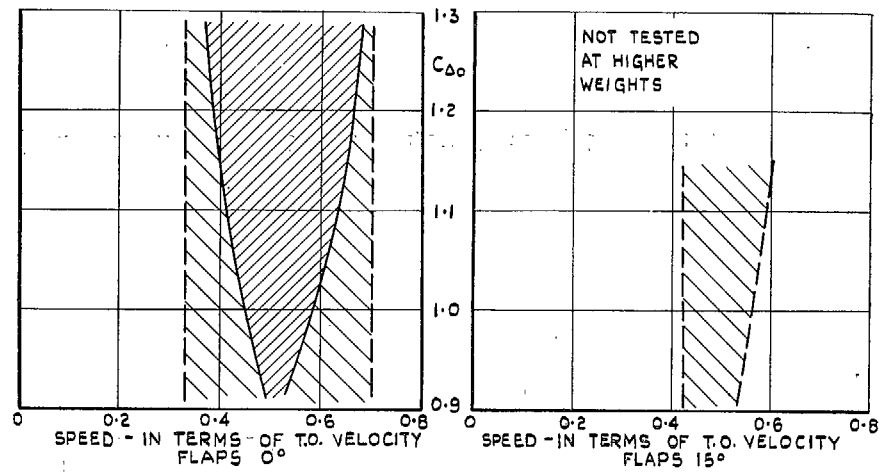

FIG. 29c. Tailplane interference.

FIGS. 29a, 29b and 29c. Effect of weight on spray interference.

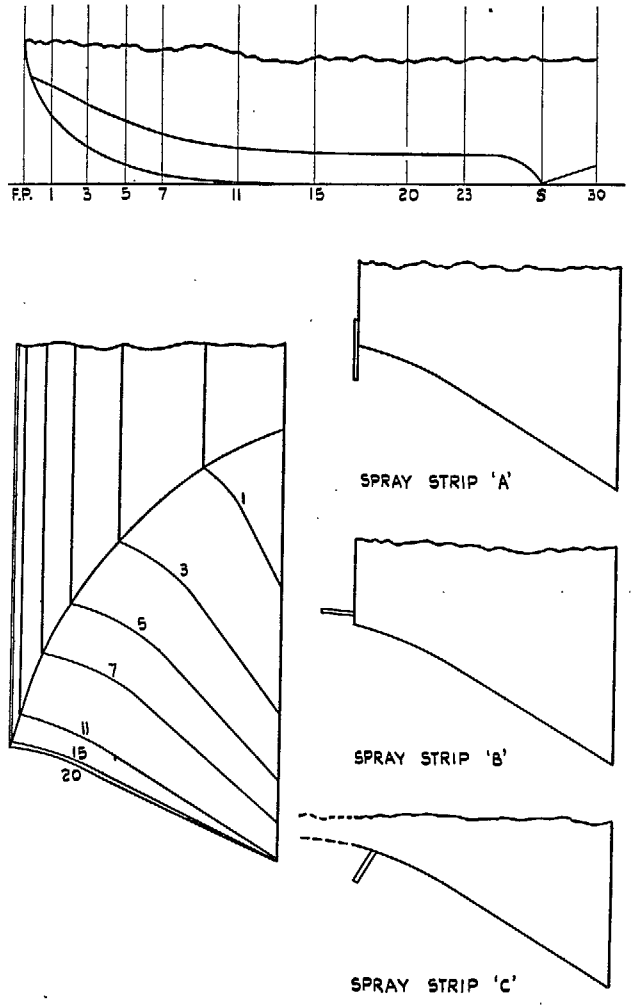

FIG. 30. Typical forebody and types of spray strip.

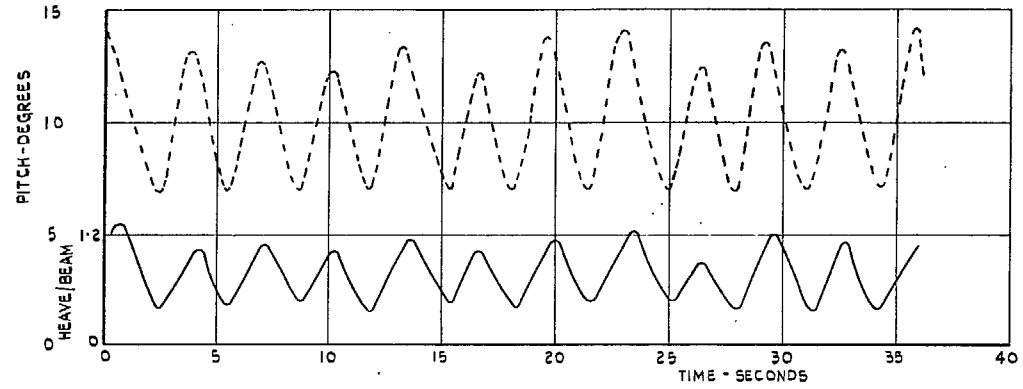

FIG. 31a. Wave height 0·3 beam, length : height = 160 : 1.

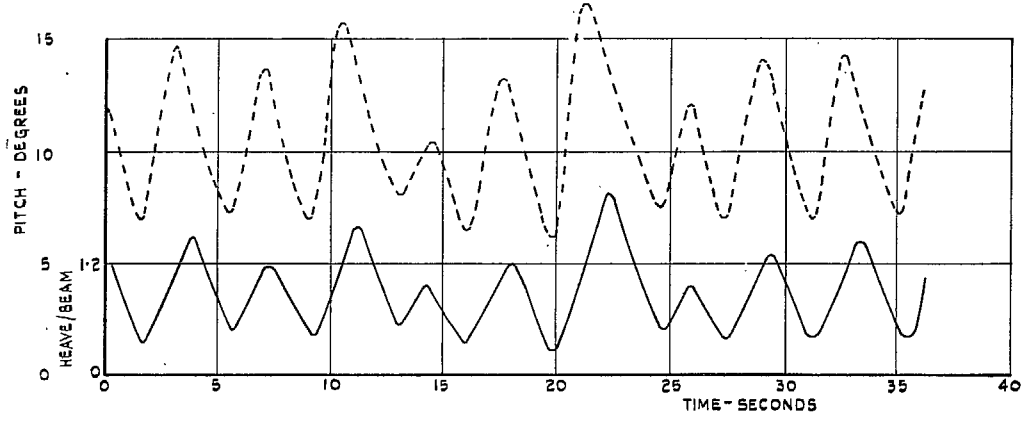

FIG. 31b. Wave height 0·3 beam, length : height = 180 : 1.

FIGS. 31a and 31b. Pitch and heave recordings of an aircraft running through steady wave trains at 0·6 unstick speed.

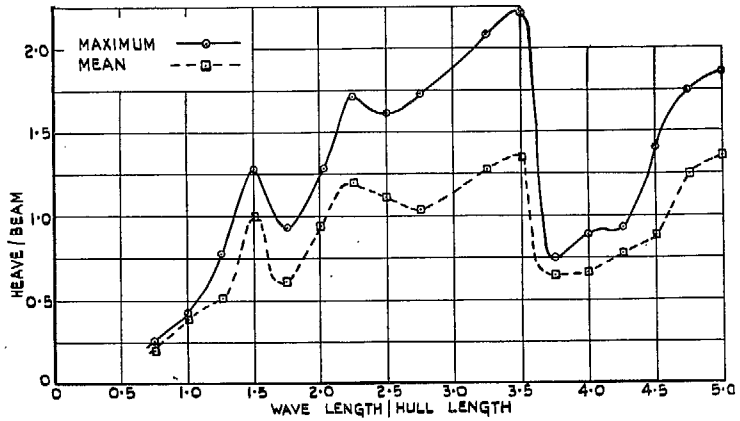

FIG. 32a.

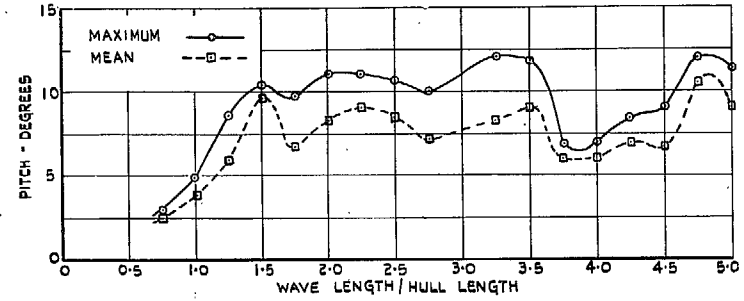

FIG. 32b.

FIGS. 32a and 32b. Effect of wave length on the response of an aircraft running through steady wave trains at 0·6 take-off speed.

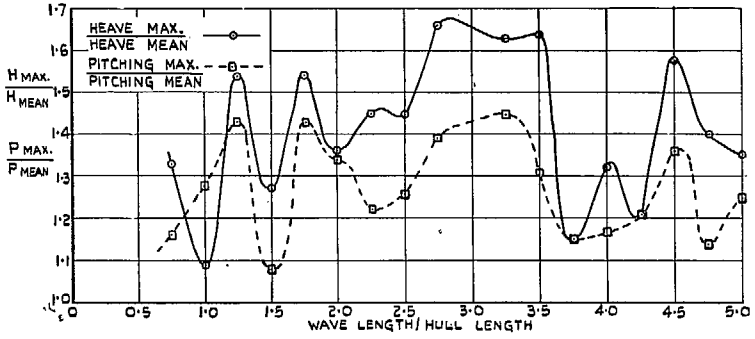

FIG. 33. Effect of wave length on the irregularity of the motion of an aircraft running through steady wave trains at 0·6 take-off speed.

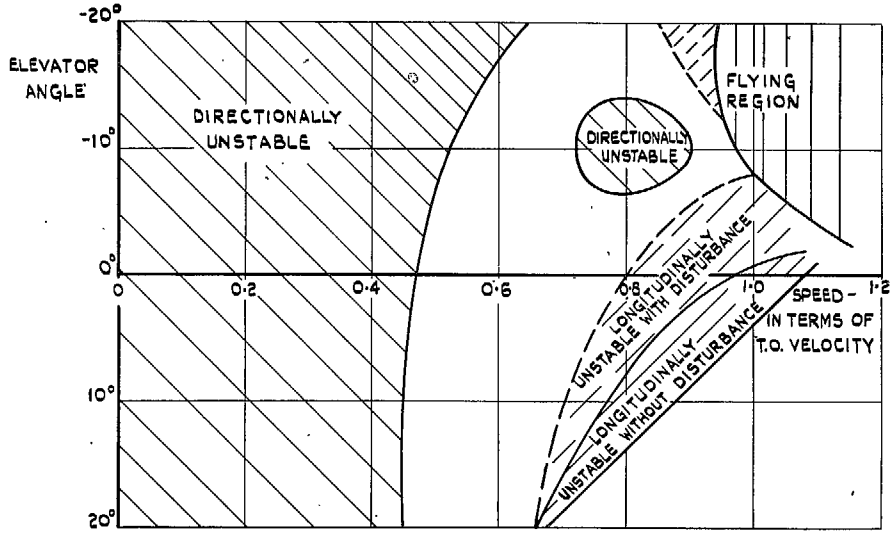

FIG. 34. Typical directional and longitudinal stability diagram.

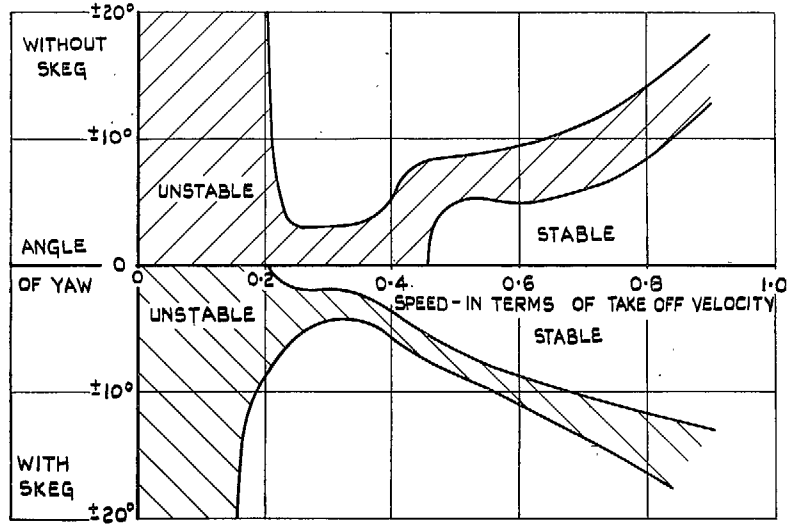

FIG. 35. Effect of skeg on directional stability at a typical elevator setting (about — 5 deg).

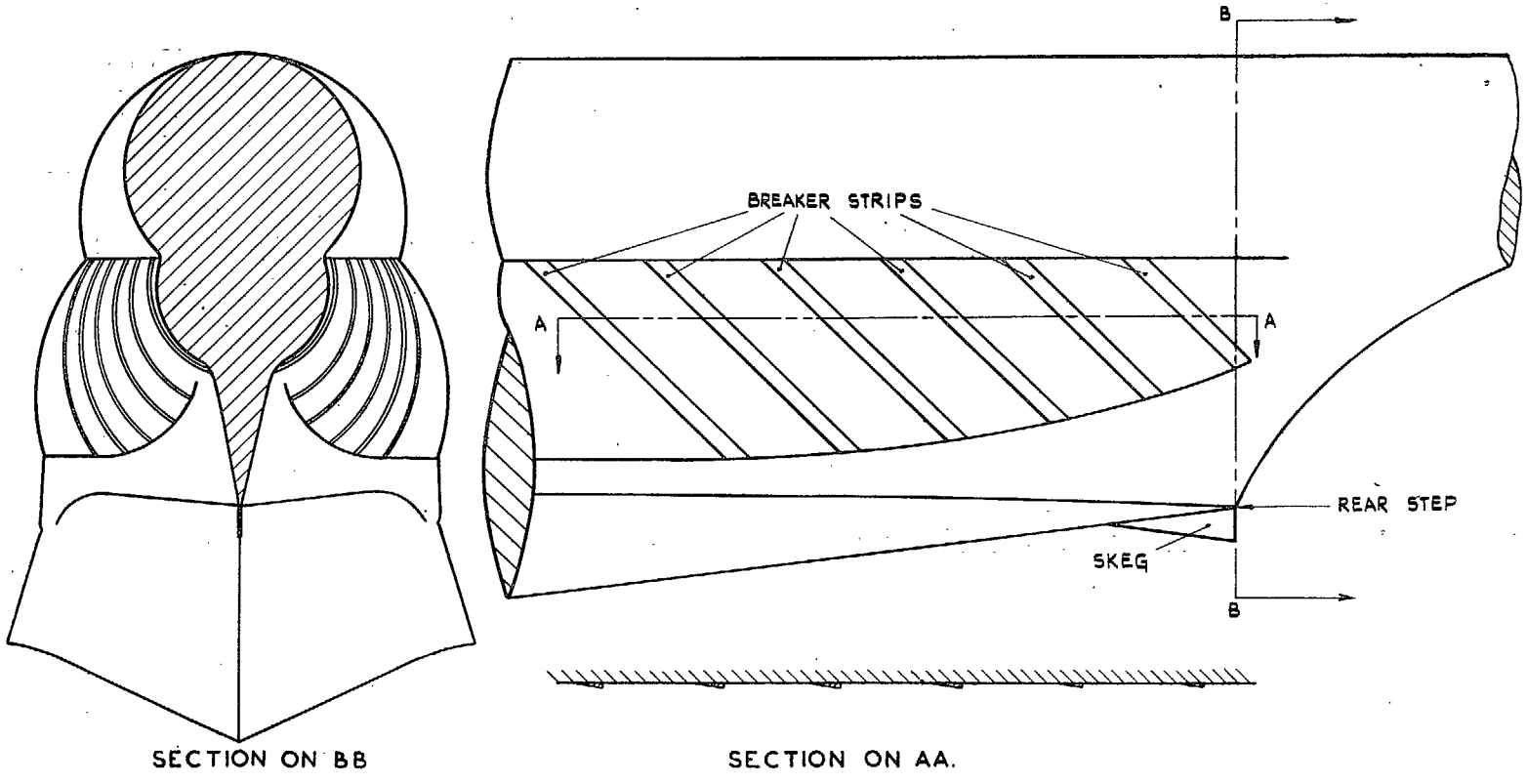

FIG. 36. Skeg and breaker strips on a flying-boat afterbody.

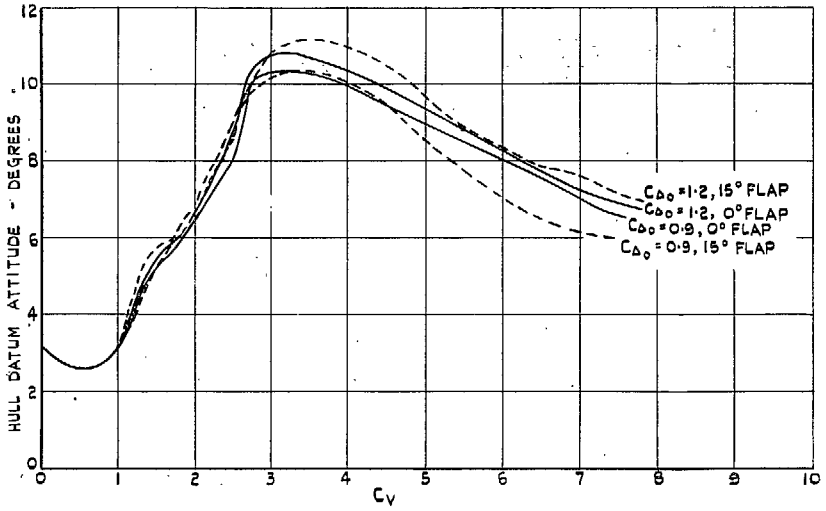

FIG. 37. Typical attitude variations during take-off at two weights and flap settings.

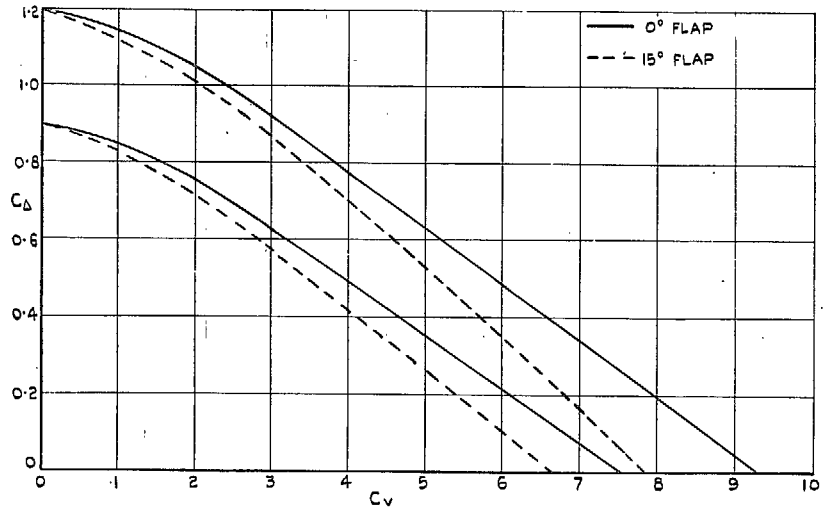

FIG. 38. Load on water variations during take-off for a typical aircraft at two weights and flap settings.

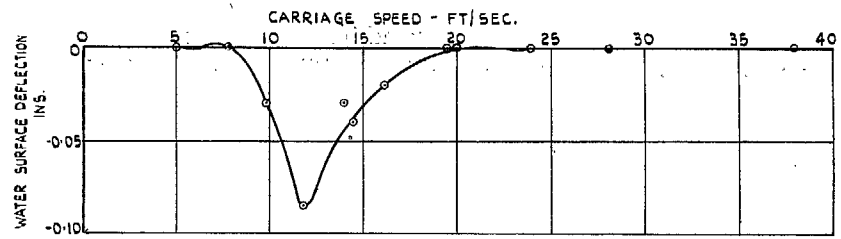

FIG. 39. Water surface deflection under No. 2 Carriage—airflow condition—measured 1·5 in. behind balance strut position.

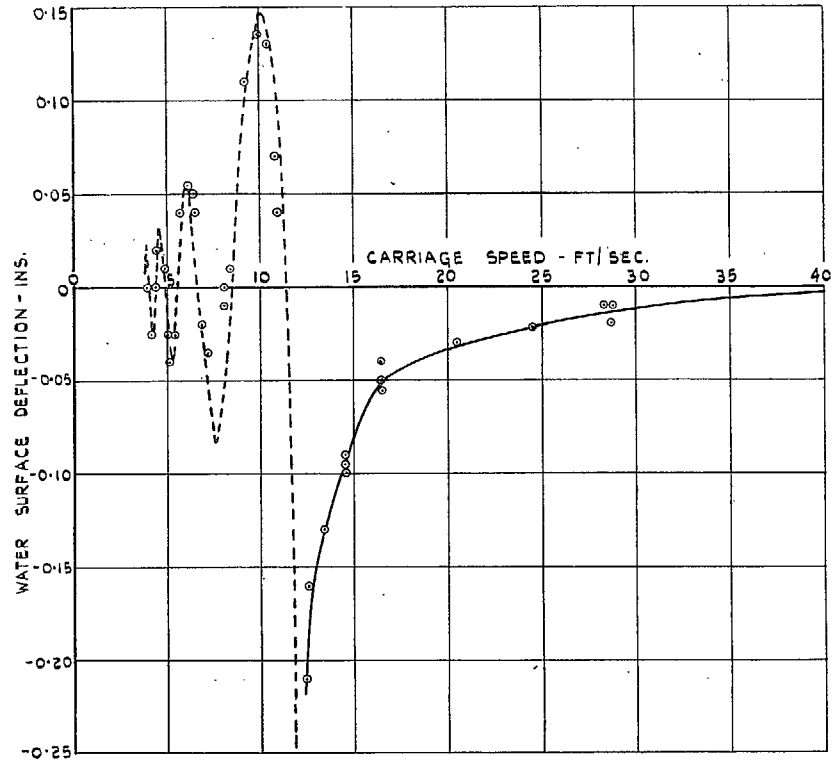

FIG. 40. Water surface deflection under No. 2 Carriage—screened condition—measured 1·5 in. behind balance strut position.

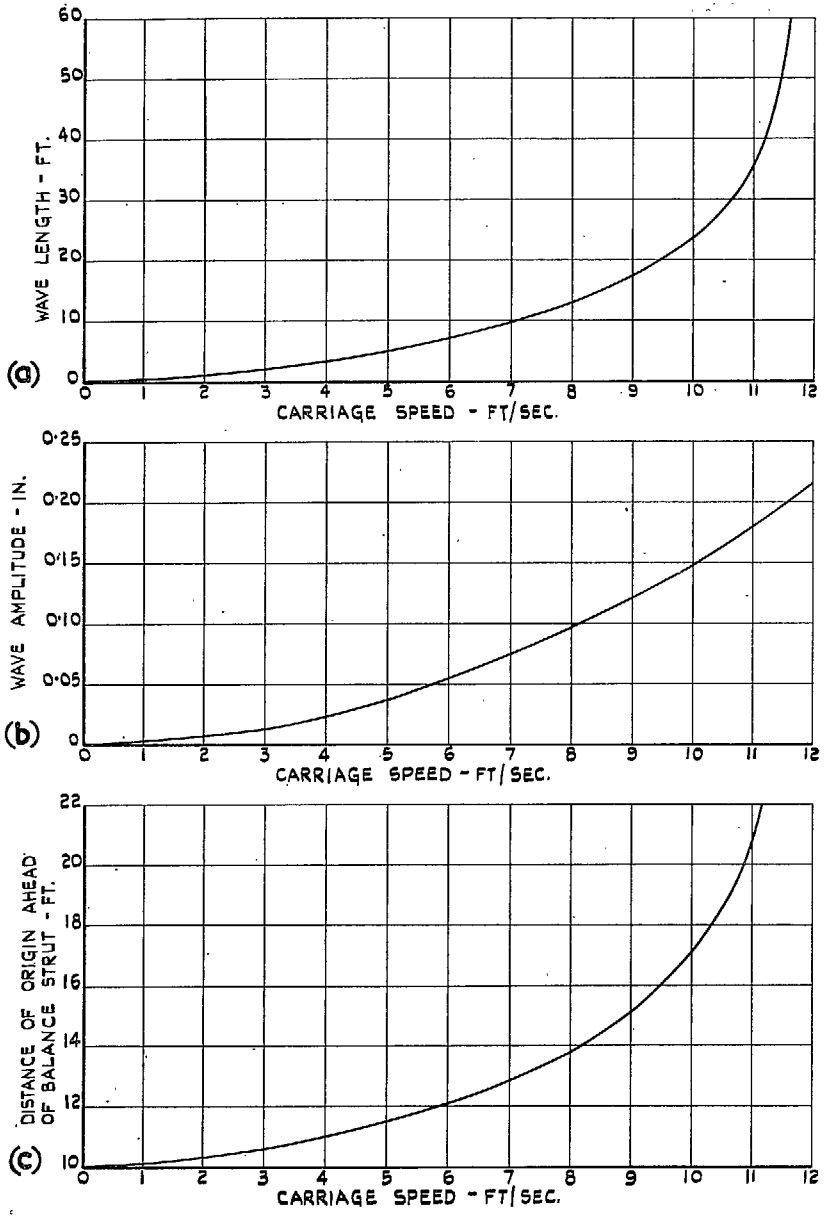

FIGS. 41a to 41c. Data for calculating water surface profile under No. 2 Carriage below 11 ft/sec. Screened condition.

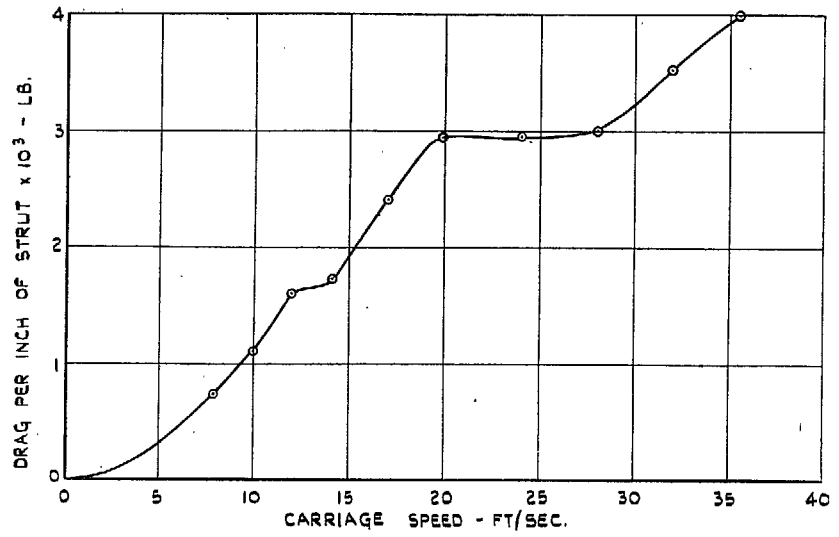

FIG. 42. Drag of balance strut No. 2 Carriage—airflow condition.

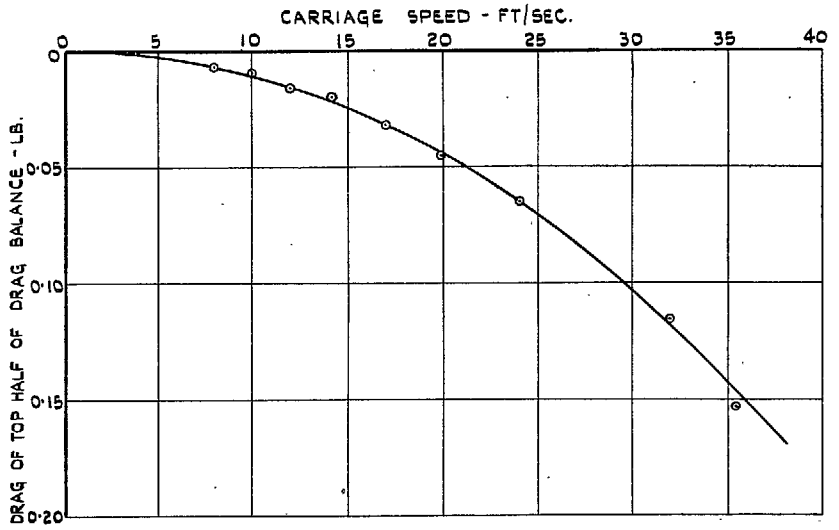

FIG. 43. Drag of top half of drag balance No. 2 Carriage—airflow condition—for one typical condition (section 4.4.1.2).

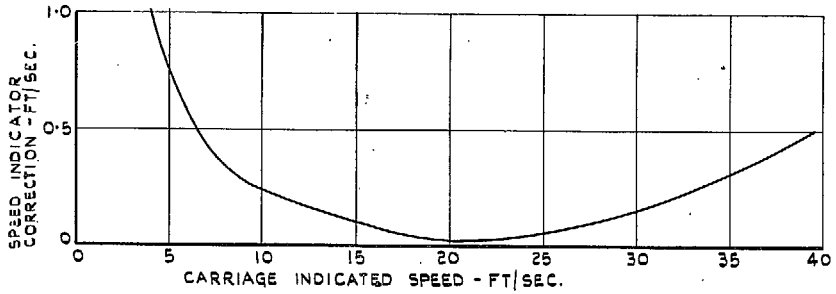

FIG. 44. No. 2 Carriage-speed indicator correction (April, 1950).

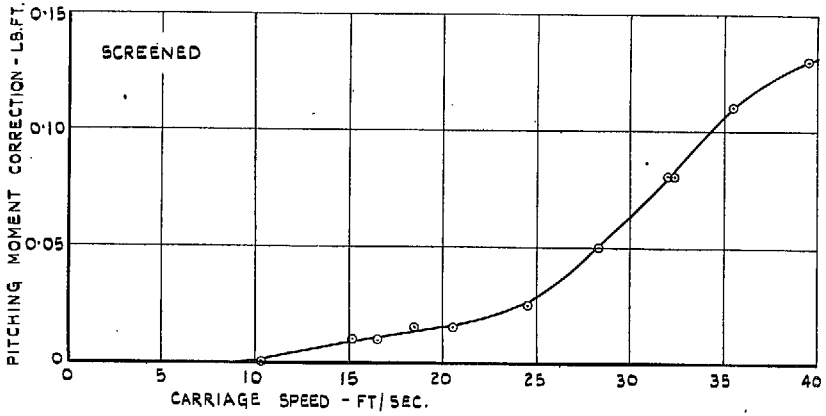

FIG. 45. Pitching-moment correction No. 2 Carriage—screened condition.

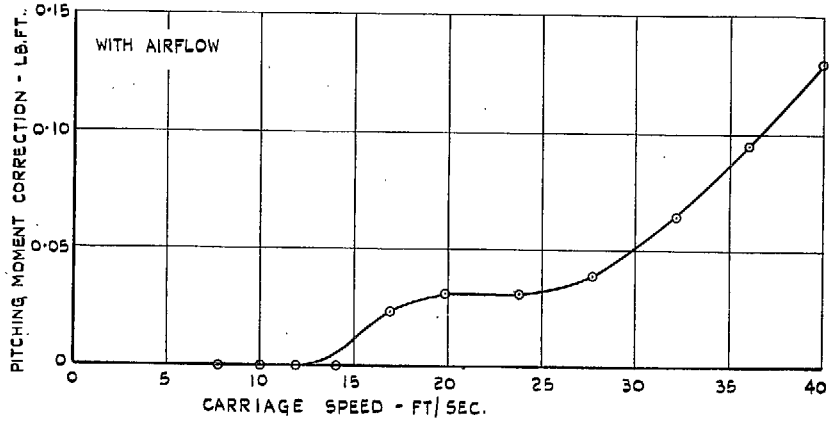

FIG. 46. Pitching-moment correction No. 2 Carriage—airflow condition.

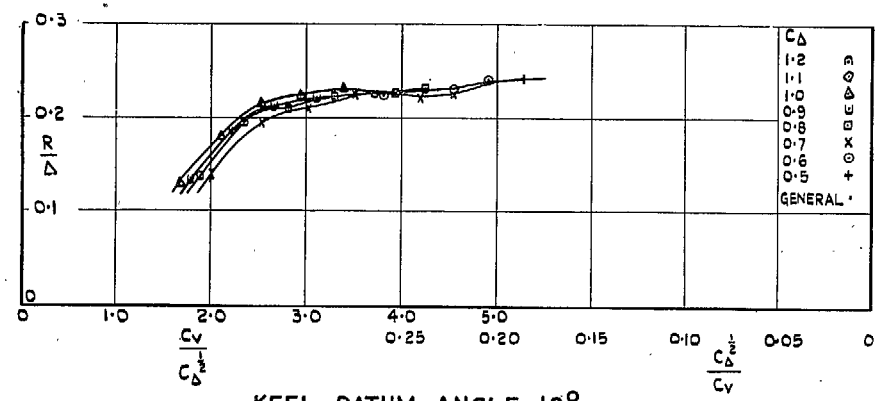

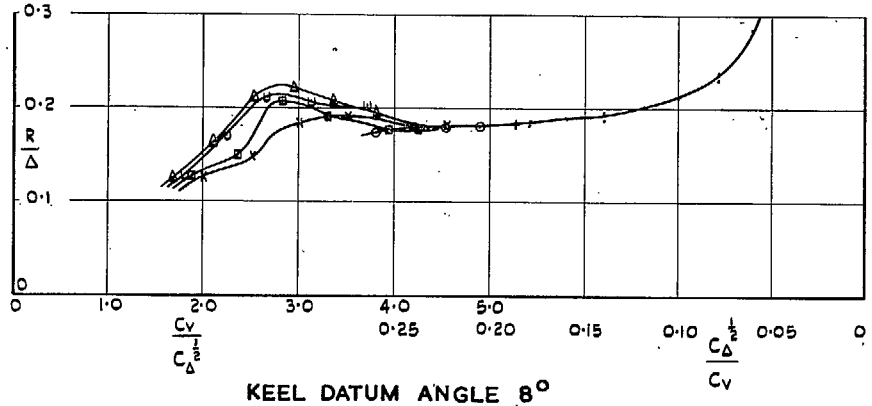

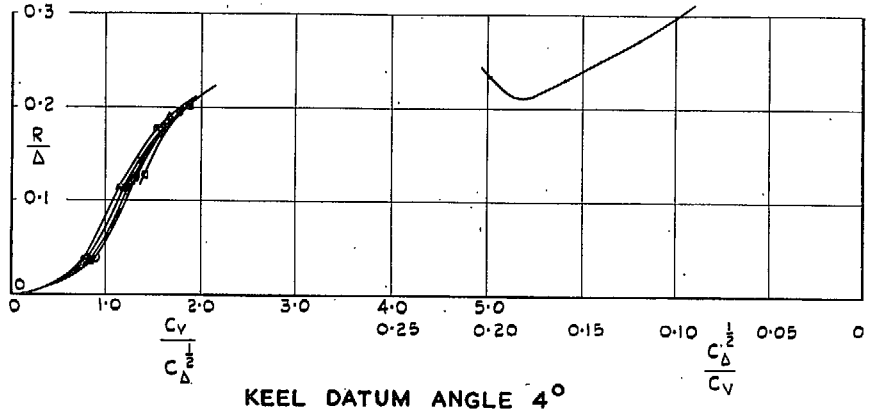

FIG. 47. Drag results on a typical hull model of length : beam ratio = 7.

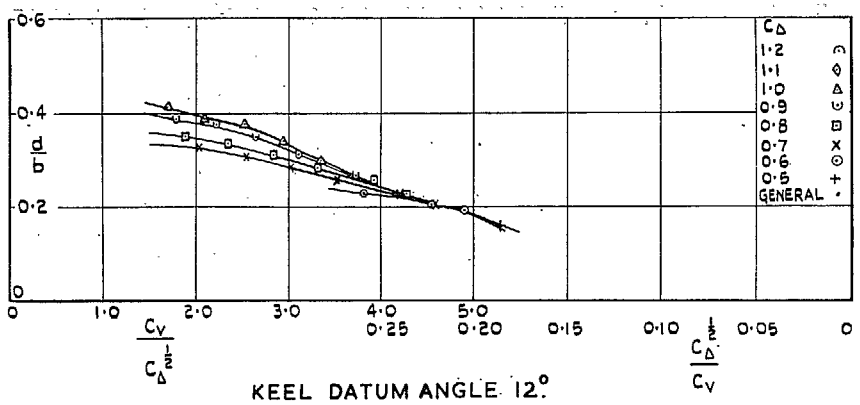

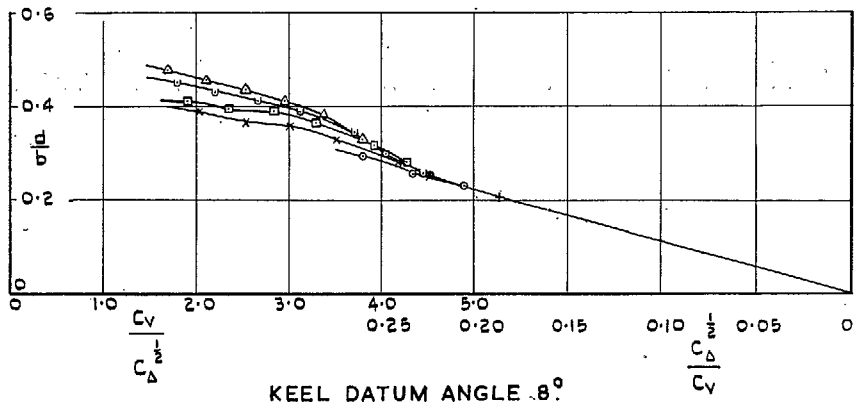

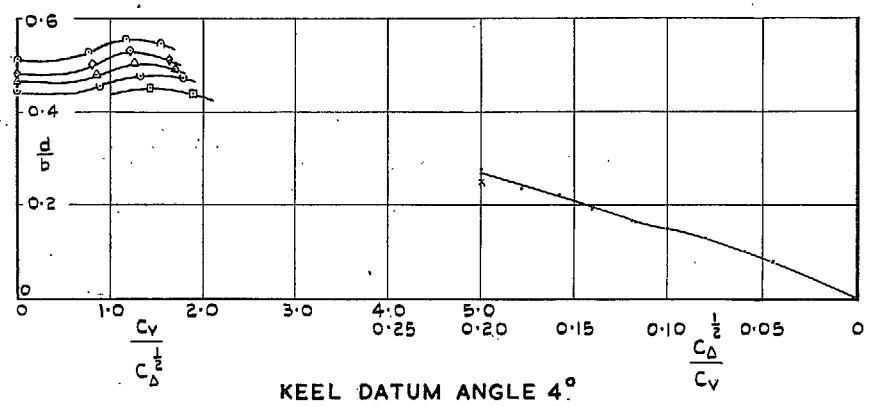

FIG. 48. Draft results on a typical hull model of length : beam ratio = 7.

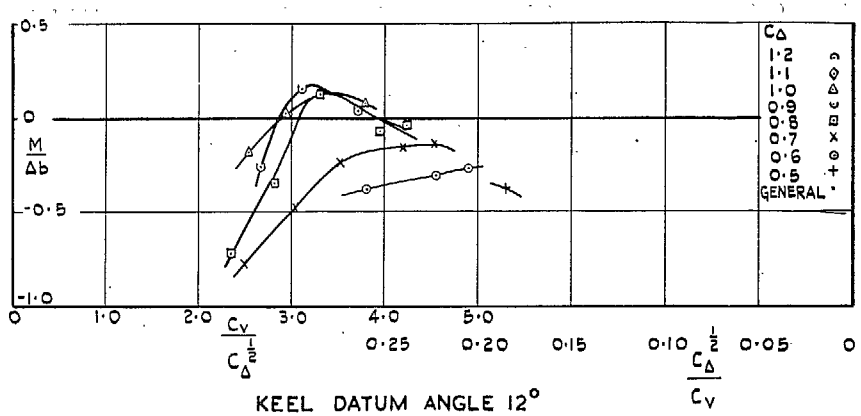

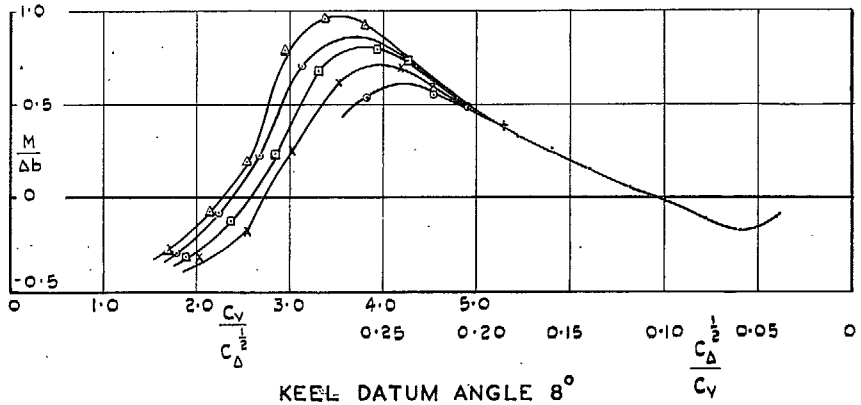

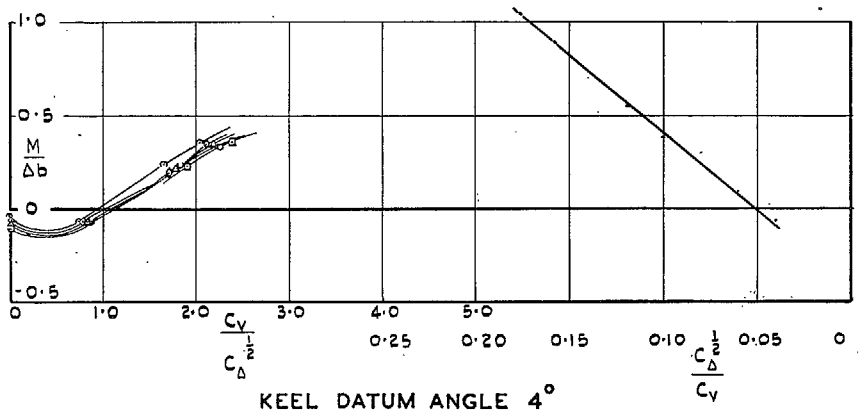

FIG. 49. Pitching-moment measurements on a typical hull model of length : beam ratio = 7.

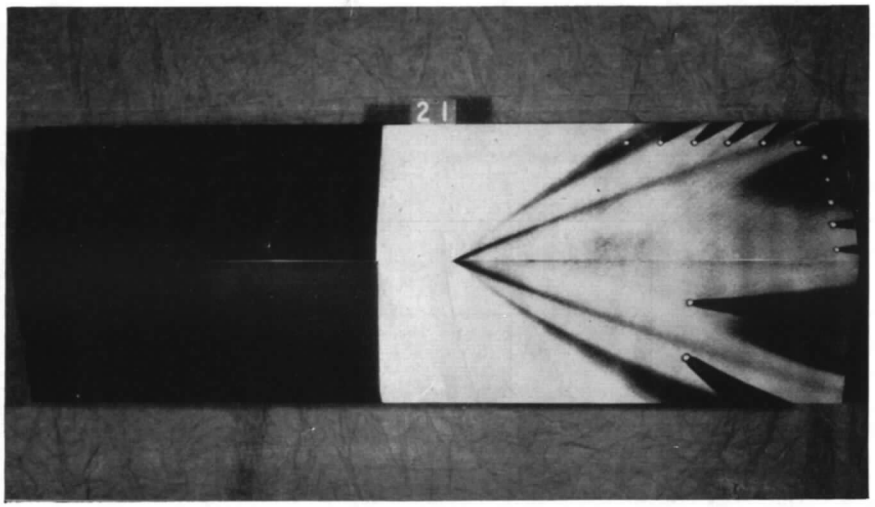

FIG. 50. Flow on a hull bottom.

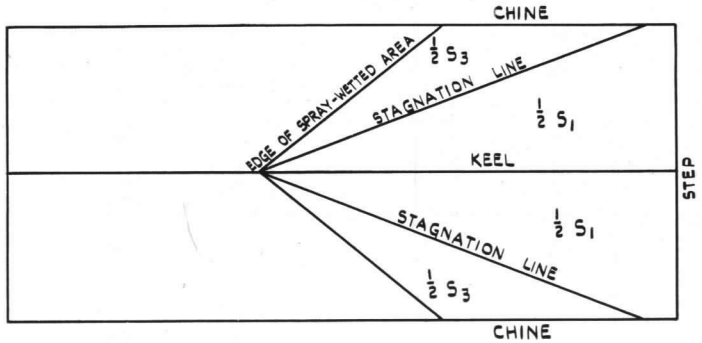

FIG. 51. Wetted areas on a hull bottom. S_1 is main wetted area. S_3 is spray wetted area.

Note : Areas are measured in their respective planes not projected on to a common plane.

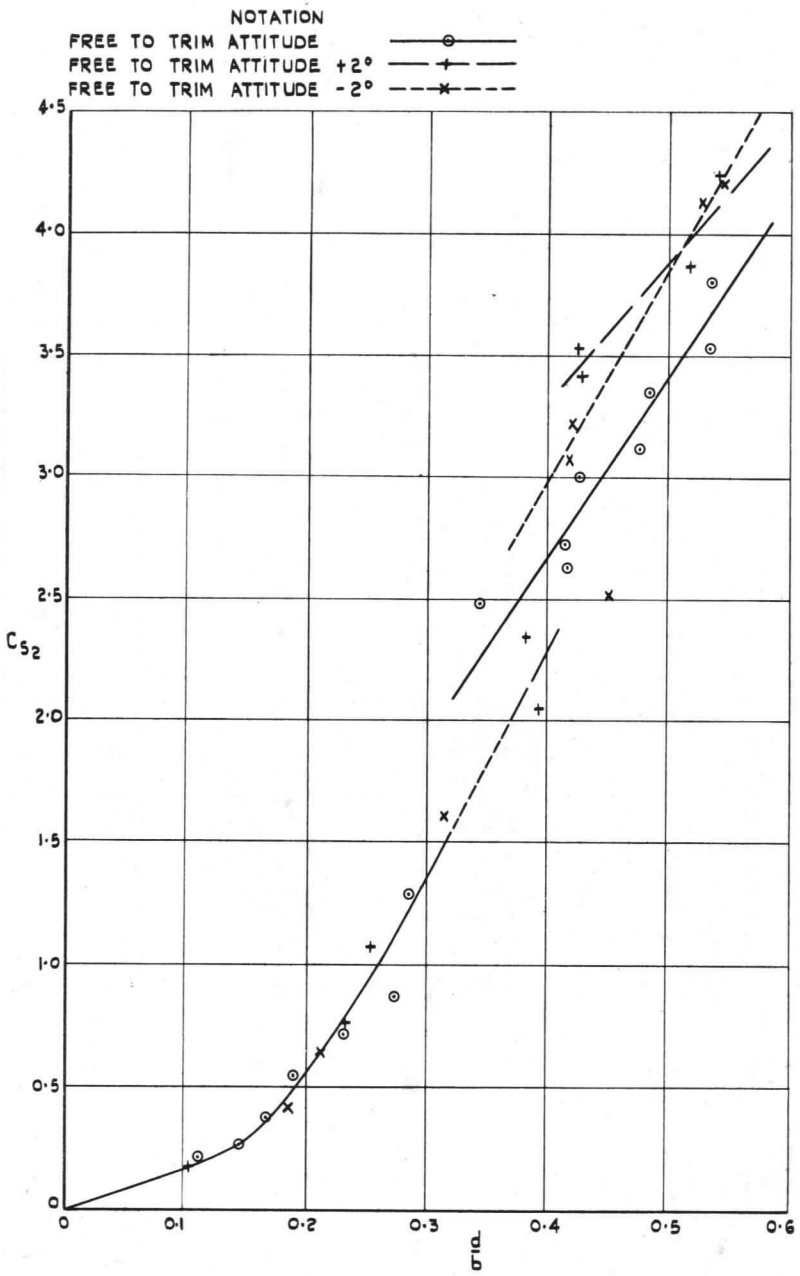

FIG. 52. Wetted area measurements on a typical hull of length : beam ratio = 7. Low-speed range.

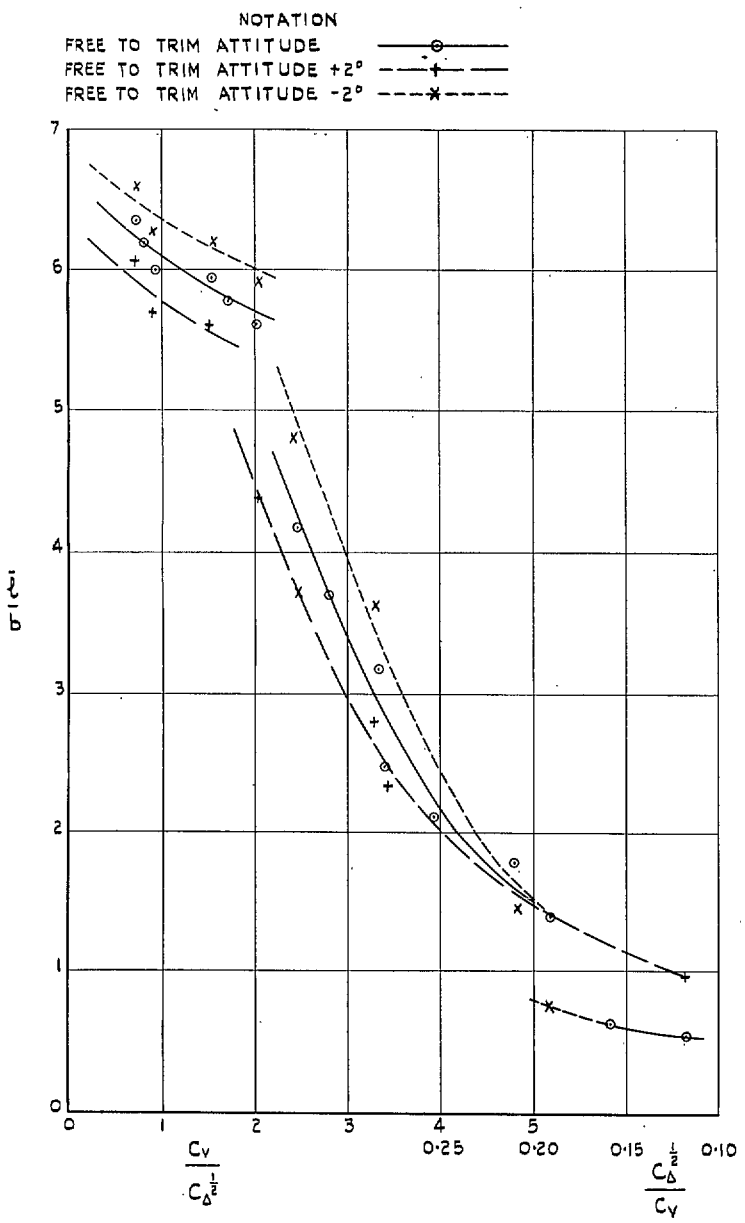

FIG. 53. Mean wetted lengths on a typical hull of length : beam ratio = 7. Low-speed range.

(3298) Wt. 19/8411 K.7 11/55 Hw.

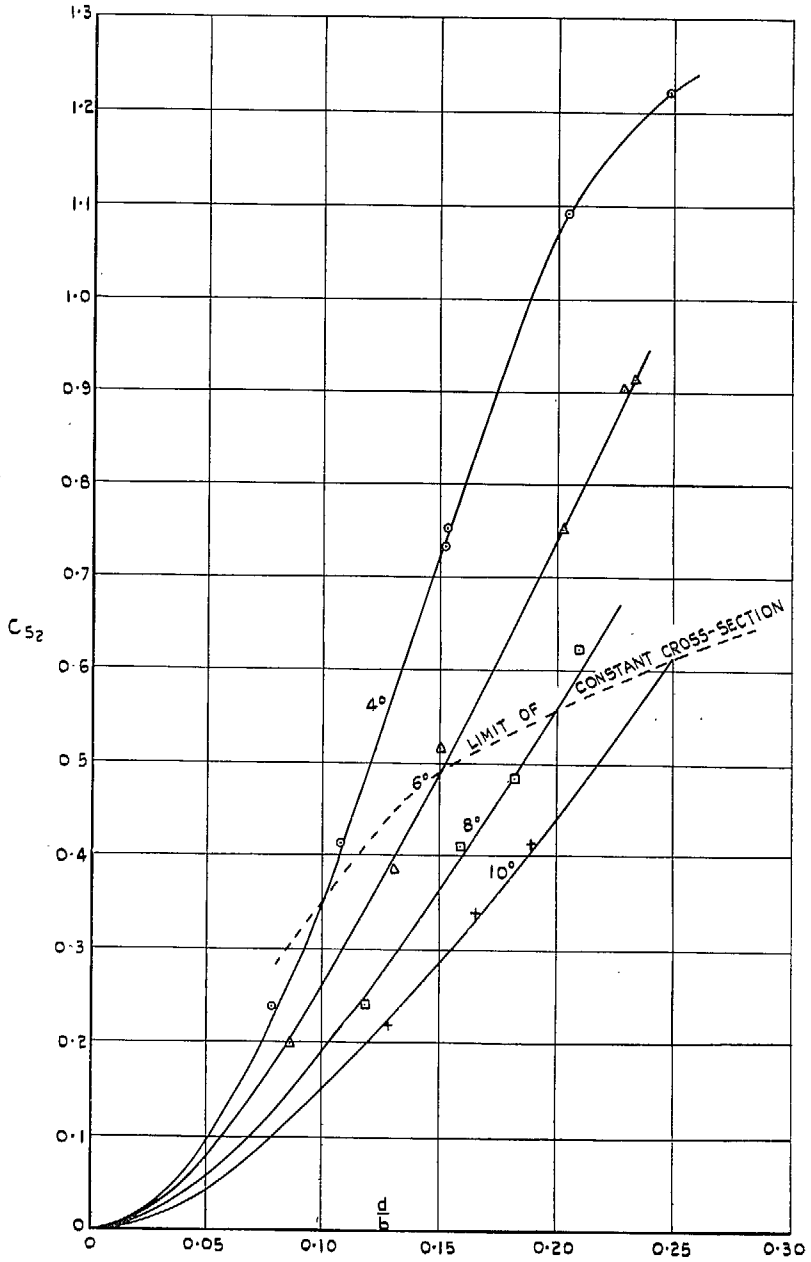

FIG. 54. Wetted area measurements on a typical hull of length : beam ratio = 7. Planing region.

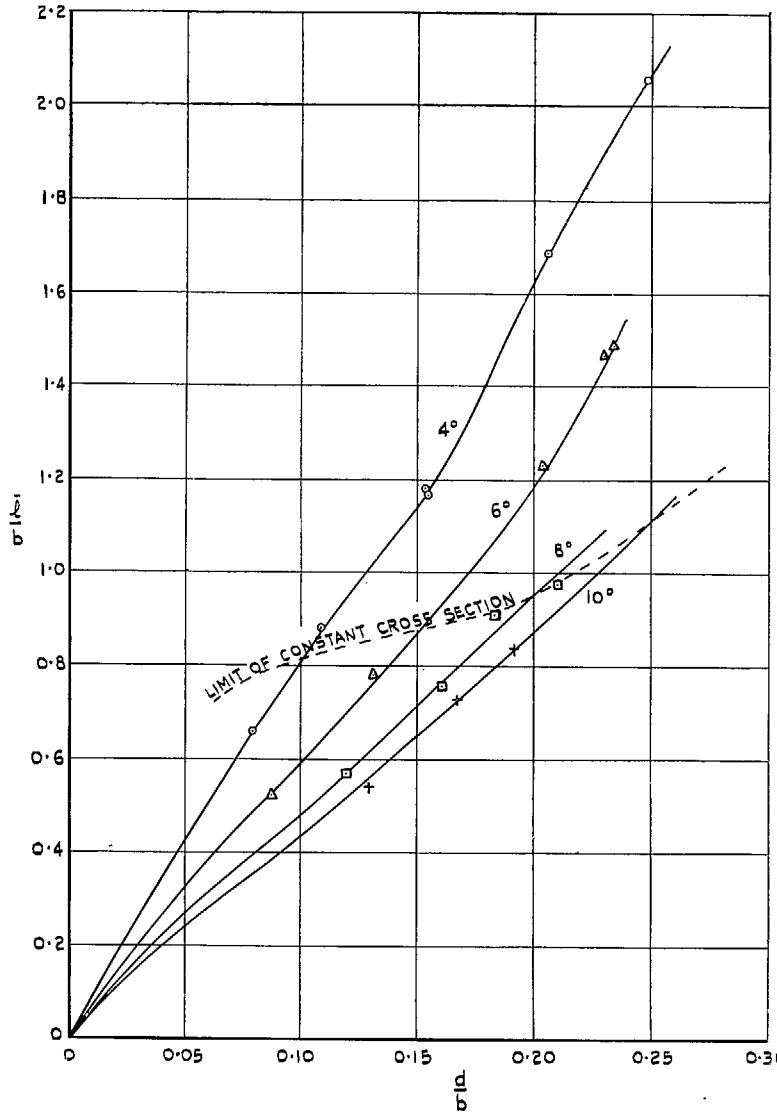

FIG. 55. Mean wetted lengths on a typical hull of length : beam ratio = 7. Planing region.

PRINTED IN GREAT BRITAIN

Publications of the Aeronautical Research Council

ANNUAL TECHNICAL REPORTS OF THE AERONAUTICAL RESEARCH COUNCIL (BOUND VOLUMES)

1936 Vol. I. Aerodynamics General, Performance, Airscrews, Flutter and Spinning. 40*s.* (41*s.* 1*d.*)
Vol. II. Stability and Control, Structures, Seaplanes, Engines, etc. 50*s.* (51*s.* 1*d.*)

1937 Vol. I. Aerodynamics General, Performance, Airscrews, Flutter and Spinning. 40*s.* (41*s.* 1*d.*)
Vol. II. Stability and Control, Structures, Seaplanes, Engines, etc. 60*s.* (61*s.* 1*d.*)

1938 Vol. I. Aerodynamics General, Performance, Airscrews. 50*s.* (51*s.* 1*d.*)
Vol. II. Stability and Control, Flutter, Structures, Seaplanes, Wind Tunnels, Materials. 30*s.* (31*s.* 1*d.*)

1939 Vol. I. Aerodynamics General, Performance, Airscrews, Engines. 50*s.* (51*s.* 1*d.*)
Vol. II. Stability and Control, Flutter and Vibration, Instruments, Structures, Seaplanes, etc. 63*s.* (64*s.* 2*d.*)

1940 Aero and Hydrodynamics, Aerofoils, Airscrews, Engines, Flutter, Icing, Stability and Control, Structures, and a miscellaneous section. 50*s.* (51*s.* 1*d.*)

1941 Aero and Hydrodynamics, Aerofoils, Airscrews, Engines, Flutter, Stability and Control, Structures. 63*s.* (64*s.* 2*d.*)

1942 Vol. I. Aero and Hydrodynamics, Aerofoils, Airscrews, Engines. 75*s.* (76*s.* 3*d.*)
Vol. II. Noise, Parachutes, Stability and Control, Structures, Vibration, Wind Tunnels. 47*s.* 6*d.* (48*s.* 7*d.*)

1943 Vol. I. Aerodynamics, Aerofoils, Airscrews. 80*s.* (81*s.* 4*d.*)
Vol. II. Engines, Flutter, Materials, Parachutes, Performance, Stability and Control, Structures. 90*s.* (91*s.* 6*d.*)

1944 Vol. I. Aero and Hydrodynamics, Aerofoils, Aircraft, Airscrews, Controls. 84*s.* (85*s.* 8*d.*)
Vol. II. Flutter and Vibration, Materials, Miscellaneous, Navigation, Parachutes, Performance, Plates and Panels, Stability, Structures, Test Equipment, Wind Tunnels. 84*s.* (85*s.* 8*d.*)

Annual Reports of the Aeronautical Research Council—

1933–34	1*s.* 6*d.* (1*s.* 8*d.*)	1937	2*s.* (2*s.* 2*d.*)
1934–35	1*s.* 6*d.* (1*s.* 8*d.*)	1938	1*s.* 6*d.* (1*s.* 8*d.*)
April 1, 1935 to Dec. 31, 1936	4*s.* (4*s.* 4*d.*)	1939–48	3*s.* (3*s.* 2*d.*)

Index to all Reports and Memoranda published in the Annual Technical Reports, and separately—

April, 1950 — R. & M. No. 2600. 2*s.* 6*d.* (2*s.* 7½*d.*)

Author Index to all Reports and Memoranda of the Aeronautical Research Council—

1909–January, 1954. — R. & M. No. 2570. 15*s.* (15*s.* 4*d.*)

Indexes to the Technical Reports of the Aeronautical Research Council—

December 1, 1936 — June 30, 1939	R. & M. No. 1850.	1*s.* 3*d.* (1*s.* 4½*d.*)
July 1, 1939 — June 30, 1945.	R. & M. No. 1950.	1*s.* (1*s.* 1½*d.*)
July 1, 1945 — June 30, 1946.	R. & M. No. 2050.	1*s.* (1*s.* 1½*d.*)
July 1, 1946 — December 31, 1946.	R. & M. No. 2150.	1*s.* 3*d.* (1*s.* 4½*d.*)
January 1, 1947 — June 30, 1947.	R. & M. No. 2250.	1*s.* 3*d.* (1*s.* 4½*d.*)
July, 1951.	R. & M. No. 2350.	1*s.* 9*d.* (1*s.* 10½*d.*)
January, 1954.	R. & M. No. 2450.	2*s.* (2*s.* 1½*d.*)
July, 1954.	R. & M. No. 2550.	2*s.* 6*d.* (2*s.* 7½*d.*)

Prices in brackets include postage.

Obtainable from

HER MAJESTY'S STATIONERY OFFICE

York House, Kingsway, London, W.C.2; 423 Oxford Street, London, W.1 (Post Orders: P.O. Box 569, London, S.E.1); 13a Castle Street, Edinburgh 2; 39 King Street, Manchester 2; 2 Edmund Street, Birmingham 3; 109 St. Mary Street, Cardiff; Tower Lane, Bristol, 1; 80 Chichester Street, Belfast, or through any bookseller

S.O. Code No. 23-2976